INTEGRATED ASSESSMENT OF BUILDINGS AND DISTRIBUTED ENERGY RESOURCES (DER) AT THE NEIGHBORHOOD SCALE

A Dissertation
Presented to
The Academic Faculty

by

Gustavo Antonio Carneiro

In Partial Fulfillment
of the Requirements for the Degree
Doctor of Philosophy in the
School of Architecture

Georgia Institute of Technology
December 2017

INTEGRATED ASSESSMENT OF BUILDINGS AND DISTRIBUTED ENERGY RESOURCES (DER) AT THE NEIGHBORHOOD SCALE

Approved by:

Prof. Godfried Augenbroe, Advisor
School of Architecture
Georgia Institute of Technology

Dr. Jason Brown
School of Architecture
Georgia Institute of Technology

Dr. Bert Bras
School of Mechanical Engineering
Georgia Institute of Technology

Dr. Roderick Jackson
Buildings Research
National Renewable Energy Laboratory

Dr. Santiago Carlos Grijalva
School of Electrical and Computer Engineering
Georgia Institute of Technology

Date Approved: October 06, 2017

To my wife and kids, for their affection, support and patience

ACKNOWLEDGEMENTS

I am very grateful for the support and trust deposited on me by my advisor, the faculty, colleagues, friends and family during my Ph.D. journey at Georgia Tech. They all helped me, in different ways, to push harder to achieve such a challenging accomplishment.

Professor Fried Augenbroe is a formidable professor and advisor, a role model, and a friend, who knows when to ask and when to give. I learned a lot from him, not only due to his profound academic knowledge, but also about strong human values, which I will carry throughout my life. His guidance during the development of this thesis was invaluable and helped me find the proper ways and methods to prove my point.

I have a lot to thank all the faculty of the College of Design at Georgia Tech and of other schools within the university, who made my experience in this Ph.D. program so productive and enriching. I would like to express my sincere appreciation to Professor Jason Brown for his dedication during classes, projects and competitions. I could testify how his support was fundamental to many accomplishments achieved by students of the High Performance Buildings program during my years in the Lab. I also would like to thank Professor Michael Gamble for the opportunities to work closely with his students and to contribute with the projects at his Zero Energy Design studio.

Special appreciation goes to Professor Bert Bras and the opportunity to work in the MEL microgrid project in collaboration with his advisee Jamie Kono at the Sustainable Design and Manufacturing Program. Bert's sharp observations, and our weekly multi-

disciplinary presentations contributed a lot to my own research and to my personal development.

I must acknowledge the contributions from Professor Santiago Grijalva, from the School of Electrical and Computer Engineering, and Roderick Jackson, from the Buildings Research Program at NREL, who provided valuable improvements to this dissertation.

The everyday burden as a full-time student and researcher in such a high-level educational institute was soothed by the camaraderie of the colleagues in the Ph.D. Lab: Mike, Qi, Yiyuan, Yuna, Ji-Hyun (Jeannie), Roya, Qinpeng, Yifu, Alya, Mohanned, Mayuri, Di (Ludy), Zhaoyun; as well as colleagues from the Master's program just across the corridor, and the dedicated visiting scholars. My gratitude also goes to Vikram, Ivana, René, and to all other members of the GT team that participated in the 2015 Race to Zero competition, for such an enjoyable time and successful project.

I am also very thankful to the friendship nurtured with Aster, Dalton, Gustavo, Silvia, Pranav, Sol, and many others, with whom I could chat, socialize, and find some time to escape the immersive work.

I would like to state my sincere gratitude to my wife and children, who embarked on this project with me, and gave me the necessary support and companionship to pursue this achievement.

Finally, I must thank CAPES (the Brazilian Coordination Agency for the Improvement of Higher Education Personnel), who financially supported this research.

TABLE OF CONTENTS

LIST OF TABLES

LIST OF FIGURES

LIST OF SYMBOLS AND ABBREVIATIONS

ADR	Active Demand Response
ARCH_*i*	Building ARCHetype – type *i*
BEM	Building Energy Model
BEST	Building Energy Software Tools
BSim	Building Simulation tool
Cal-ERDA	California – Energy Research Development Administration project
CEA	City Energy Analyst
CEN	European Committee for Standardization
CES	Community Energy Storage
CFD	Computational Fluid Dynamics
CHP	Combined Heat and Power
CitySim	EPFL CitySim software
COP	Coefficient Of Performance
CREST	Centre for Renewable Energy Systems Technology demand model
CTF	Conduction Transfer Function
DER	Distributed Energy Resources
DER-CAM	Distributed Energy Resources - Customer Adoption Model
DesignBuilder	DesignBuilder software
DHW	Domestic Hot Water
DOE	U.S. Department Of Energy
DR	Demand Response
EBC	Energy in Buildings and Communities programme
EE	Energy Efficiency
EIA	U.S. Energy Information Administration
EnergyPlus	EnergyPlus software
EPC	Energy Performance Coefficient
EPC (calculator)	Energy Performance Calculator
EPC_NHood	EPC building model for NeighborHood scale analysis
EPSCT	Energy Performance Standard Calculation Toolkit

eQUEST	QUick Energy Simulation Tool
ESP-r	ESRU building model
ETP	Equivalent Thermal Parameters
EV	Electric Vehicle
FCV	Finite Control Volume
FDM	Finite Difference Method
FEM	Finite Element Method
GA	Genetic Algorithm
GAMS	General Algebraic Modeling System
GIS	Geographic Information System
GridLAB-D	PNNL smart grid model
HAMBase	Heat, Air and Moisture model for Building and systems evaluation
HOMER	Hybrid Optimization Model for Multiple Energy Resources
HVAC	Heating, Ventilation, and Air Conditioning
IBPSA	International Building Performance Simulation Association
ICC	International Code Council
IDA-ICE	IDA Indoor Climate and Energy simulation tool
idf	Input data file
IEA	International Energy Agency
IECC	International Energy Conservation Code
IES-VE	Integrated Environmental Solutions building model
ISO	International Organization for Standardization
LBL	Lawrence Berkeley National Laboratory
LDC	Load Duration Curve
Matlab	MathWorks Matlab program
Modelica	Modelica modeling language
NARUC	U.S. National Association of Regulatory Utility Commissioners
NPC	Net Present Cost
NREL	National Renewable Energy Laboratory
ODEs	Ordinary Differential Equations
OpenStudio	OpenStudio cross-platform collection of software tools
PNNL	Pacific Northwest National Laboratory

PolySun	Vela Solaris PolySun simulation software
PV	PhotoVoltaic
PVWatts	NREL PVWatts calculator
RAM	Random Access Memory
RC-network	Resistances–Capacitance network
RES	Residential Energy Storage
SAM	System Advisory Model
SEER	Seasonal Energy Efficiency Ratio
SMUD	Sacramento Municipal Utility District
SynCity	Imperial College London SynCity tool kit
TMY3	Typical Meteorological Year – type 3
TRNSYS	TRaNsient SYStem simulation tool
umi	MIT Urban Modeling Interface
V2G	Vehicle-To-Grid
V2H	Vehicle-To-Home
VBA	Visual Basic Application
XML	eXtensible Markup Language
p-value	Probability value
PI_i	Performance Indicator *i*
$S\mu$	Scenario uncertainty
$P\mu$	Parameter uncertainty
$MF\mu$	Model Form uncertainty
A	Area
C	Thermal capacitance
º C	Degrees centigrade
GB	Gigabyte
GHz	Gigahertz
h	Heat transfer coefficient
H	Coupling transmittance
kW	kilowatts
kW_{DC}	Nameplate output (DC) capacity in kilowatts
kWh	kilowatt-hour

$\dot{m}$	Mass flow rate
MW	Megawatts
Q	Quantity of heat
R	Thermal resistance
SSE	Sum of squared errors
U	Thermal transmittance
W	Weight attributed to *SSE*
δ'	Total weighted error
δt	Time-step
η	System efficiency
θ	Nodal temperature
Λ_{at}	Dimensionless ratio between the internal surfaces area and the conditioned floor area
ρ	Density
Φ	Heat flow rate
ς	Factor that relates the building effective mass area with the building conditioned floor area

SUMMARY

In urban regions, traditionally a main electric grid fed by centralized power plants serves the growing energy demand of residential and commercial buildings. However, the advent of new technologies, such as distributed renewable energy generation, local energy storage, and smart controls, is transforming the way buildings interact and transact with the electric grid. When operating in coordination, several buildings or households can leverage their aggregate potential and use their energy flexibility and distributed resources to improve the operation of both the main grid and the pool of integrated and intelligent buildings. Much attention has been drawn to the potential benefits of these types of integration, especially the capabilities they can provide in terms of aggregate demand management and local power resilience. Nevertheless, building energy modeling at the urban level has not yet reached the necessary computational manageability and simulation robustness to assess these novel scenarios. To address this hiatus, the current thesis presents a computer-aided energy simulation method to model the integration of multiple buildings and distributed energy resources (DER) at the neighborhood scale. The proposed methodology uses a reduced order simulation approach to achieve a reliable and tractable dynamic modeling framework that can manage multiple transacting building energy models and DER models in a single platform.

To test the modeling approach, this study first carries out a virtual experiment of a small community in Miami, FL, where it is possible to compare the outcomes of community energy consumption from our reduced order model to the outcomes from a higher order simulation approach. When using the community energy model to evaluate

the performance of different DER options for community peak load shaving, we can observe that the influence of the model order reduction reveals to be very minor when compared to other uncertainties related to scenario variability and, especially, systems' efficiencies.

Secondly, we apply the reduced order modeling approach to an existing residential community in Rancho Cordova (Sacramento County), CA, with solar energy generation and battery energy storage. With this case study, we demonstrate the viability of our approach to construct and calibrate a reduced order model of fifteen households based only on limited and general data related to energy performance of the entire neighborhood. The developed reduced order model is used to evaluate the performance of different energy storage arrangements for reducing the occurrence of community super peak loads. In this virtual experiment, we can demonstrate how the model allows for uncertainty analyses over the influence of input parameters, as well as for more sophisticated optimization studies, including stochastic optimization, in a timely and transparent fashion.

Finally, the proposed reduced order simulation approach is used to construct and test relevant energy performance measures at the neighborhood scale. Using the model unique features of manageability, reliability and flexibility, we propose the foundations for quantifying and measuring "community energy resilience" for outage situations, based on concepts of number of sustained hours and respective energy end-use convenience levels. We also measure and monetize DER options for providing "community energy flexibility", aimed at shaping the load profile of a residential community to match the electric grid needs.

CHAPTER 1. INTRODUCTION

The electricity supply for buildings in urban spaces traditionally has been made with a main electric grid, fed by centralized power plants, with transmission and distribution power lines in a one-way energy flow direction. However, the advent of new technologies, such as distributed renewable energy generation, local energy storage, and smart controls, is transforming the way buildings interact and transact with the electric grid.

When operating in coordination, several buildings or households in a neighborhood can also leverage their aggregate potential and use their energy flexibility[1] and distributed resources to improve the operation of both the main grid and the pool of integrated and intelligent buildings.

Current efforts in the building energy modeling discipline fail to offer practical simulation solutions to capture these novel scenarios in a timely manner and under reasonable computational demand. This thesis addresses this issue by proposing an integrated and flexible modeling platform that provides a good balance between model fidelity and simulation practicality.

The model is formulated for the assessment of new energy performance measures at the neighborhood scale that are more relevant to the ever-growing presence of prosumers[2] in the transforming grid. The architecture of the model allows optimization

[1] We understand "energy flexibility" as the building's ability to temporarily modify its pattern of energy demand to meet specific targets by deploying different demand-side strategies and resources.
[2] Prosumers are entities that can both consume and produce energy in a transacting environment within the electric grid.

studies and risk analyses that are usually unfeasible to be performed in a comprehensive and truly dynamic manner by the existing modeling approaches.

1.1 Background

Energy supply, especially in the form of electricity, is essential for modern life in urban spaces. The twentieth century experienced great engineering achievements mainly led by the electrification of entire nations, with great advancement in the developed world. Electricity generation and electric power transmission and distribution formed the main infrastructure along with cities and their built environment were developed. Buildings traditionally have been great electricity consumers, providing space conditioning, lighting and the functioning of diverse electrical systems to support daily life activities.

Nowadays, electricity is even more crucial to many aspects of urban life, as many electronic devices and equipment are electric powered. Growing demands for electrified transportation also enhance the importance of the electric grid. In the United States, the residential buildings and the transportation sectors alone already account for roughly half of the country's energy use.

The conventional design of electric grids during this development process followed the usual format of a main electric grid fed by centralized power plants, which served the growing energy demands of cities and other human activities in a one-way energy flow. As the demand grew, more centralized power plants and additional transmission and distribution lines were connected to the grid. The oil crisis events in the 1970s put pressure

for the pursuit of more energy efficient buildings and systems to avoid shortages and even outages of electricity supply.

By the end of the twentieth century, environmental stresses and the realization of climate change threats posed additional pressure to the pursuit of energy efficiency in buildings as well as the necessity to develop cleaner and more efficient energy supply systems. The advent of new technologies, such as distributed renewable energy generation, local energy storage, and smart controls, started a transformation in the way buildings interact and transact with the electric grid. Bi-directional energy flows are now possible, creating "prosumers" that can both consume and produce the energy transacted within the grid.

More holistic and sustainable solutions are currently regarded by many as better options in comparison to the one-way electric grid operation with centralized generation. The need for reliable and resilient electricity supply is also becoming more relevant in the face of major storms and potential power outages in urban spaces.

Distributed energy resources and the various ways for their integration with buildings are thus considered important means for achieving optimized solutions for balancing energy needs with energy supply options.

At the neighborhood scale, a collection of buildings can potentially be orchestrated to leverage their aggregate potential and use their energy flexibility and distributed resources to improve the operation of both the main grid and the pool of integrated and intelligent buildings.

A better understanding of these schemes is necessary in order for designers and engineers to properly inform stakeholders and to support decision-making towards more sustainable solutions with lower costs and lower carbon emissions, as well as greater reliability and enhanced resilience.

In this context, the methodology developed in this thesis brings novel means on how to construct and simulate neighborhood energy models that can address part of such challenges.

1.2 Motivation

The necessity to better model and understand the energy use in the built environment in the presence of a transforming grid and of novel technologies has motivated this thesis.

Much attention has been drawn to the potential benefits of new types of energy integration between a collection of buildings and distributed energy resources, especially the capabilities they can provide in terms of aggregate demand management and local power resilience.

There is an abundance of materials and sources about this subject in the gray literature[3]. However, it is still hard to find adequate measures and robust evaluations of the applicability and the real benefits of such implementations in real life. Previous studies that

[3] Gray literature is regarded as the type of literature, often scientific or technical, that is produced by organizations of different levels, but which are not available through usual bibliographic sources (e.g. reports, working papers, and white papers).

took aggregate loads to mimic the dynamic grid operation cannot be used anymore as we have an ever-growing presence of prosumers in the grid. Building peer-to-peer interactions also necessitate a better understanding from the architectural and engineering perspectives.

The current reality is that building energy modeling at the urban level has not yet reached the necessary computational manageability and simulation robustness to assess these novel scenarios.

This thesis addresses this hiatus, by presenting a computer-aided energy simulation method that can be used with the necessary flexibility and reliability to model the integration of multiple buildings and distributed energy resources (DER) at the neighborhood scale. The model provides a fair combination of practicality, accuracy, and speed to help support decision-making in this area of expertise.

1.3 Research Questions and Objectives

The main purpose of the modeling approach developed in this thesis is to provide a transparent, reliable, and practical tool for assessing key measures of energy performance at the neighborhood scale related to aggregate energy production, storage, and consumption, such as aggregate peak load, energy flexibility, and energy resilience.

To achieve this aim, the following research questions are addressed throughout this thesis:

1. Are reduced order energy models appropriate to investigate those specific measures of energy performance and flexibility at the neighborhood scale?
2. How do they compare with higher order neighborhood energy models for supporting decision-making towards the selection of design and engineering parameters?
3. Can the proposed modeling approach be used to construct and test the means for quantifying those key measures of energy performance at the neighborhood scale?

Ultimately, the main objectives of this thesis are:

1. Propose and present a flexible and reliable modeling approach to be used in novel problem formulations regarding complex modes of energy consumption, generation, and storage between buildings and DER in connected neighborhoods.
2. Construct and test the sensitivity of relevant measures of energy performance at the neighborhood scale, such as "community energy resilience" and "community energy flexibility".

1.4 Contribution to the Field

The modeling methodology proposed in this thesis uses a reduced order simulation approach to achieve a reliable and tractable dynamic modeling framework that can manage multiple transacting building energy models and DER models in a single platform. This

unique co-simulation environment allows the modeler to virtually program any intervention in any building model or energy resource at any hourly time-step within the annual simulation interval.

The simulation framework can interconnect all sub-models at every simulation time-step in such a manner that the balances of energy and the related transactions can be seamlessly calculated at every hour. Complex control algorithms and decision-making support systems can be programmed in the neighborhood model as a practical way to mimic decisions and transacting operations between many parts.

This modeling flexibility allows the simulation of various types and combinations of complex DER strategies, including demand response, as well as microgrid interactions under many possible scenarios. With an hourly resolution, the model can be used to assess local peak shifting and peak shaving, as well as energy flexibility and increased resilience in connected communities. The model can also be used to perform robust optimization studies and risk analysis involving possible options for energy generation, consumption, and storage in connected neighborhoods.

Finally, this research paves the way for the definition and quantification of “community energy resilience” and “community energy flexibility” as key measures for assessing, designing, and optimizing DER solutions for energy security in future communities.

1.5 Thesis Outline

This first chapter introduces the context of the problem and demonstrates the importance of the proposed modeling methodology to address novel problem formulations regarding the integrated assessment of buildings and DER at the neighborhood scale.

The following chapter presents a review of the building energy modeling discipline, with special attention to the challenges for the integrated modeling of buildings and DER at the neighborhood scale. It concludes with the presentation of the proposed modeling approach with its unique features designed to address the limitations of previous modeling efforts.

In chapter three, a validation exercise is carried out by comparing the energy consumption data of the proposed reduced order community model, EPC_NHood, with the aggregated outputs from a collection of higher order models in a case study in Miami, FL. The relative importance of the discrepancies between the two approaches is tested along with other sources of building and parameter uncertainties in optimization studies aimed at finding tailored DER solutions for reducing the occurrence of electricity peak consumption in the neighborhood.

Chapter four tests the application of the proposed modeling approach to an existing solar powered community, in Rancho Cordova (Sacramento County), CA. Results of a full-scale physical experiment carried out in the locale are used as a basis for model calibration. The calibrated EPC_NHood model is then used to compare different energy storage arrangements for load-shaving in the community during critical days.

In chapter five, the EPC_NHood modeling framework is used to generate relevant measures of energy performance. Rational metrics are constructed to measure “community energy resilience” using the community energy model in Miami, FL as a test bed. This is followed by the definition and monetization of “community energy flexibility”, and its application to the Anatolia community model.

Closing remarks are presented in chapter six, followed by suggestions for future work in chapter seven.

CHAPTER 2. MODELING BUILDINGS AND DISTRIBUTED ENERGY RESOURCES AT THE NEIGHBORHOOD SCALE

The development and verification of adequate building energy modeling approaches that scale up to solve relevant questions at that neighborhood level is disregarded in current literature. In this chapter, we address this issue by presenting a comprehensive review of the efforts and methodologies used so far for this aim, after which we conclude with the proposition of an appropriate reduced order modeling approach to investigate specific measures of energy performance and flexibility at the neighborhood scale. This directly addresses the research question 1, as stated in section 1.3.

2.1 Introduction

Before defining the best model or modeling technique for a problem, we must understand the fundamental reason why we use models. In some sense, we may say that modeling is a natural function of our daily lives and we use models more often than we think. For the scope of this thesis, models are representations of natural phenomena that we formulate, mentally or computationally, to help us make decisions.

Therefore, models will always be a simplification of a complex problem that we cannot fully understand and/or cannot be completely replicated with all its complexities and finest details. The question lies on how much simplification is desirable or acceptable.

This question would likely yield an obvious answer in times before the advent of powerful computers: a simple and reliable model that could satisfactorily represent the phenomenon with a low demand for elaborate calculations. However, the advancement of computational tools in the recent decades distorted this notion, as software developers and researchers alike started pursuing ever more granularity in the architecture of their models.

In one hand, this trend supported the development of complex tools that revealed themselves extremely useful for solving problems in ways that we could have never imagined before. On the other hand, over-engineered models became a common feature in many disciplines, where the added model resolution implied extra effort and time without necessarily providing additional information or insights about the problem under investigation.

Parsimony, an important aspect of scientific method, becomes even more fundamental in this context. As stated by George Box in his seminal work about "science and statistics" a few decades ago, this concept could never be more precise today:

> "Since all models are wrong the scientist cannot obtain a "correct" one by excessive elaboration. On the contrary following William of Occam he should seek an economical description of natural phenomena. Just as the ability to devise simple but evocative models is the signature of the great scientist so overelaboration and overparameterization is often the mark of mediocrity." (Box, 1976)

With these aspects in mind, this chapter presents a review of the main categories of building energy models, the previous work on urban building energy modeling, the efforts to integrate BEMs with DER, and finally presents the ideal candidate modeling approach to be used to answer the questions posed by this research.

2.2 Review of Building Energy Models

Building energy models, also called BEM, are used mainly to estimate building performance, to forecast building energy consumption, to compare building designs, to audit buildings for code compliance, and to rate buildings according to pre-established certification criteria, among other potential applications.

Similar to any other modeling exercise, there is not a single BEM type that suits all applications and satisfies the whole range of problem-solving performance criteria. Input data management, ease of use, flexibility, running time, modeling granularity, time resolution, accuracy, and computational requirements are just a few examples of relevant aspects that one might consider when choosing an appropriate model for a specific task. The trade-offs between model representativeness and modeling effort are then inevitable.

A relatively wide list of methods, strategies, and computational packages for modeling energy consumption in buildings exist. The following sub-section navigates through the most comprehensive reviews on existing building energy models and describes the categorizations that are well accepted within the field. This sorting among model types helps with the understanding and the comparison of the modeling approaches that are addressed in the following chapter of this thesis.

2.2.1 Main Categories of Building Energy Models

Energy consumption in buildings is a result of a diverse mix of end-uses, including lighting, equipment, appliances, HVAC systems (heating, ventilation and air conditioning),

plug-loads, and other miscellaneous uses. Depending on the particular context and use of a building, some of these uses are relatively well known and can be estimated based on average schedules (e.g. times that lights are usually on, times when appliances are in operation). HVAC systems, on the contrary, depend on weather conditions and internal heat gains that fluctuate from day to day and within each day. Hence, understanding the thermal behavior of a building, with respect to cooling and heating thermal needs, and predicting the operational and physical aspects of the systems to meet those needs can be a challenging task for whole-building energy models. Furthermore, HVAC systems models embedded in building energy models usually only give us aggregated energy use rather than instantaneous power flow, i.e. voltage and current related values.

To develop a building energy model that is capable of simulating the whole-building thermal dynamics, one could rely on robust knowledge and a sound mathematical translation of the physics acting within and interacting with the building under investigation.

Conversely, with enough data one could develop a building energy model based entirely on statistical information, without requiring any heat transfer equation or any thermal or geometrical parameter of the building.

The combination of both approaches is also possible, where one could develop a hybrid model that is partly based on physics and partly driven by data.

These three different possibilities for building energy modeling are well established in the literature, although their definitions may vary slightly (Foucquier et al., 2013, Li and Wen, 2014, Coakley et al., 2014, Fumo, 2014, Harish and Kumar, 2016a,

Yildiz et al., 2017). The categorization presented below brings the essential definitions for these modeling approaches, and makes the connections between the diverse nomenclatures.

1. Physics-based models.
    - Alternative nomenclature for "physics-based" models: white-box, engineering, thermal, law-driven, deterministic, forward, classical.
    - Description: simulation tools that require information and parameters of building geometry and composition, occupancy patterns, energy systems, and outside weather conditions in order to calculate building energy consumption. These building models rely on physical knowledge regarding heat transfer and thermodynamic relationships with and within the building volume.
    - Advantages: Engineering models can be used to assess the performance of buildings and their systems virtually under any set of simulation variations or previously unobserved conditions (Coakley et al., 2014).
    - Disadvantages: Engineering models may require input parameters that are difficult to obtain or are not available. These models may also require expert work and time-consuming computational effort (Li and Wen, 2014).
2. Statistical models.
    - Alternative nomenclature for "statistical" models: black-box, surrogate, metamodel, model of the model, data-driven, empirical, inverse.

- Definition: models that do not require physical knowledge of the building thermodynamics. With an inverse approach, such models use building performance data to infer building properties.
- Advantages: These black-box models are designed to be computationally more efficient since they require a minimal set of inputs to describe the building behavior (Coakley et al., 2014, Cui, 2016).
- Disadvantages: Due to their data-driven approach, the development of these models require a large amount of training data, and the resulting models are bounded to the building operating conditions for which they were trained (Foucquier et al., 2013, Li and Wen, 2014).

3. Hybrid models.
    - Alternative nomenclature for "hybrid" models: gray-box, gray.
    - Definition: models designed from a combination of both physics-based and data-driven approaches. Such type of model holds a physics-based calculation structure, though the parameters of the building are indirectly defined from existing building performance data.
    - Advantages: Hybrid models can be both light and reliable (Viot et al., 2015), and they usually require reduced training data sets (Li and Wen, 2014).
    - Disadvantages: By borrowing from the two modeling approaches, the development of these types of model usually requires higher level of user

expertise both in modeling equations and in managing statistical data (Harish and Kumar, 2016a).

The literature contains sub-categorizations of these approaches, some of which are worth mentioning in this section. Firstly, mainly data-driven models, defined here as statistical, can be constructed from traditional statistical analyses such as regression analysis carried out between measured outputs (e.g. building energy consumption) and influential input parameters (e.g. building operation and weather data). For larger and more complex sets of data, the parameters of the statistical model can be derived using artificial intelligence techniques, such as genetic algorithms, artificial neural network, support vector machine, and regression trees (Foucquier et al., 2013, Yildiz at al., 2017).

Concerning physics-based models, they can be purely law-driven – forward – or can be fine-tuned or validated with measured data – calibrated (Coakley et al. 2014). However, if data is used to derive functions that would supplement parts of an incomplete physics-based model, then it becomes a gray-box, or hybrid model.

It is interesting to note that the identification of gray-models is not so obvious, in the sense that it is hard to tell when exactly they leave the purely white-box modeling realm. This grayness is related to the amount of data used to construct the model architecture in lieu of physics knowledge. It is a matter of a balance between **functional fidelity** – where the model can simulate the building behavior – and **physical fidelity** – where the model contains the building physical properties.

To illustrate this, one could think of a rigid process of calibrating a physics-based model of an existing building with available energy consumption data. By properly

adjusting the uncertain parameters of the building model to match its outputs with available energy data, one could achieve a very robust "calibrated" physics-based model that can still be considered a white-box model. On the other hand, in a very "loose" calibration process, where too many building parameters can be massaged to adjust the model outputs to existing performance data, one may generate a very useful prediction model although with very little physical resemblance with the original building. The latter case can arguably be considered a gray-box model even though its core was created from a white-box model structure.

Due to the subjective interpretation of gray-box models, this review does not intend to dive deep into this matter and is more interested in the dichotomy between the other two modeling approaches: engineering models (mainly physics-based); and black-box models (mainly data-driven).

The categorization depicted in Figure 1, as proposed by Fumo (2014), is in line with the segmentation presented in this section. According to this classification tree, the engineering type of building energy models is the one under major interests in this research. These models provide the necessary flexibility to simulate novel configurations, unobserved scenarios, or situations with very little available data, conditions which ultimately eliminate the possibility of using mainly data-driven approaches (e.g. purely statistical or hybrid).

A vast possibility of software packages and modeling techniques are available for physics-based models. Each option holds a particular balance between modeling

practicality and model resolution. The following section will address this range of possibilities and will situate the approach proposed in this thesis among them.

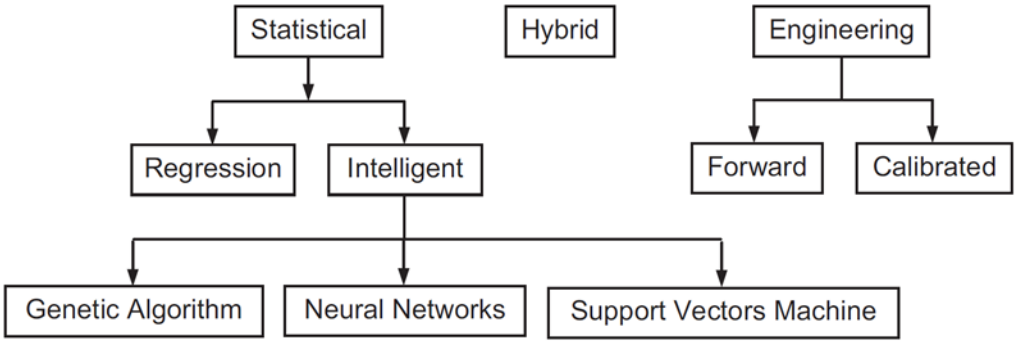

Figure 1 – Classification for energy estimation models (Fumo, 2014)

2.2.2 Physics-Based Models

Building energy models based on the physics-based approach are commonplace nowadays, and are broadly used in industry and academia. Their development as a robust discipline began a few decades ago, for the most part in response to the oil crisis of 1973. By that period, several energy conservation strategies were put in place, with special attention to energy consumption in buildings. Investments from the U.S. Department of Energy – DOE resulted in the creation of Cal-ERDA in 1977, a set of computer programs that were designed for "rapid and detailed analysis of energy consumption in buildings" (Graven and Hirsch, 1977). This initiative later evolved to the DOE-1 and DOE-2 simulation engines, and ultimately to EnergyPlus, which is currently the Department's staple open-source whole-building energy modeling software.

Around the same period, the International Energy Agency assembled what is today known as the Energy in Buildings and Communities Programme – IEA-EBC. The Programme's first initiative, later labeled EBC Annex 1: Load/Energy Determination of Buildings, was developed between 1977-1980. The project compared the ability of different computer models to simulate the thermal load and energy requirements of commercial buildings (IEA, 1980). Since then, IEA-EBC has carried out several other projects that resulted in new software or in improvements to existing software or to modeling techniques. As of March 2017, IEA-EBC has launched 75 projects or "Annexes" (IEA, 2017a).

These initiatives along with efforts from several expert groups resulted in a broad palette of options for building energy modeling. The Building Energy Software Tools (BEST) directory, currently hosted online by the United States regional affiliate of the International Building Performance Simulation Association – IBPSA-USA, lists 152 software packages in its web directory. Within this listing, 55 are identified as "whole-building energy simulation" tools, which fall under the physics-based type (IBPSA, 2017).

Included among these are well established tools for detailed building energy modeling, both proprietary and open source, such as eQUEST, EnergyPlus, IDA-ICE, IES-VE, ESP-r, TRNSYS, and Modelica Building Library (Wetter, 2009).

Although all these models simulate physical phenomena related to building hygrothermal processes, and ultimately the related whole-building energy consumption, their ways of representing a building and the underlying calculations may vary significantly. The variation in the granularity of the building representation can be related

to internal air volumes, envelope masses, building systems, and temporal resolution. Advanced numerical methods are often necessary to simulate very-finely grained physical representations of buildings, with additional computational burden.

Woloszyn and Rode (2008) define three major types of numerical methods that are employed in building energy modeling:

- Finite Difference Method (FDM) / Finite Control Volume (FCV) methods;
- Finite Element Method (FEM);
- Response Factor / Transfer Function methods.

Normally, the underlying numerical method of a model will limit the granularity of the physical representation of a building. This is the case of internal volumes, where the whole building can be represented as one single zone (coarse-grained representation) up to thousands of zones (very-finely grained representation) (Woloszyn and Rode, 2008). This aspect is illustrated in Figure 2, which shows four different levels of granularity, as described by Berger et al. (2016), that can be carried out by building models to simulate the physical processes related to heat and moisture behavior in the indoor air.

In the Computational Fluid Dynamics – CFD approach, every room inside a building is subdivided into several control volumes, or cells, in a very detailed representation of the flow field. The method allows for higher accuracy in modeling thermal gradients within a room (Berger et al., 2016). Nevertheless, this approach is usually limited to very specific applications, such as particle transport or natural ventilation across large spaces, since it implies computational overhead and the necessary coupling of

different software packages to perform a whole-building energy simulation (Foucquier et al., 2013).

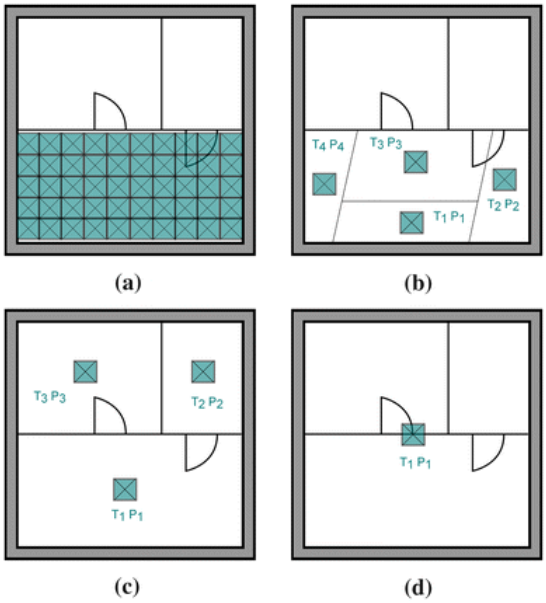

Figure 2 – Different approaches for the description of the internal building zones. (a) CFD, (b) sub-zonal, (c) multi-zone, and (d) single-zone (Berger et al. 2016)

Sub-zonal[4] models are used as a simplified alternative for CFD models, where internal spaces are subdivided into sub-zones in a much coarser mesh. This simplification alleviates the computational load associated with CFD models, but comes with drawbacks. Due to the heuristic aspect of the subdivision of rooms into sub-zones, pre-calculation is necessary to better inform the sub-zonal representation of the flow structure (Song et al., 2103). Even then, a validation of the sub-zonal model with a full-scale CFD analysis is often needed (Bonvini and Leva, 2011). These characteristics make sub-zonal models

[4] Berger et al. (2016) originally called this category as simply "zonal". However, to avoid confusion with the multi-zone and single-zone approaches that are commonly used in whole-building energy models, we will refer to this unconventional approach as "sub-zonal".

possible solutions for providing complex real-time management of building thermal performance for which CFD models cannot deliver the necessary simulation speed. However, this approach should not be used for forecasting whole-building energy consumption, since the sub-zoning assumptions have a good chance of not being physically sound.

In the multi-zone representation, each room or each group of rooms with similar characteristics is modeled as a separate zone. Also called the nodal method, it considers each building zone as a homogeneous volume, perfectly mixed, and thus approximated to a node where the state variables are lumped. The mainstream detailed energy models use the multi-zone approach, which allow them to perform a more granular simulation of the behavior of a multiple zone building with a small computation time when compared to CFD (Foucquier et al., 2013).

Finally, in the single-zone model for air volume the whole building is represented as one perfectly mixed zone, or node. On one hand, this approach eliminates the ability to simulate different states occurring within the building volume at the same time, while on the other hand it greatly eliminates computational complexity. In neighborhood scale analyses, usually the scope of investigation does not involve an inward monitoring of the granular internal building behavior, but is about simulating the whole building as one energy consuming entity. Therefore, it is worth investigating the adequacy of single-zone building representations in neighborhood energy models.

Apart from different treatment of internal building zones, physics-based models also differ with regards to the envelope representation. A higher granularity approach is

made possible with 1D finite volume, finite element, or finite difference methods, with typical size of meshes that can go from a few millimeters to several centimeters (Woloszyn and Rode, 2008). The most popular detailed building energy software packages offer a finely grained method for modeling envelopes as default. The exception applies to EnergyPlus and TRNSYS, which use the simplified Conduction Transfer Function – CTF as the automatic method for calculating heat transfer in the facades (Loonen et al., 2017). Nonetheless, the modeler has the option to bypass the CTF approach in TRNSYS by coupling the building model (Type 56) with finite element or finite difference modules such as Type 260 or Type 399 (Kośny, 2015). Also, EnergyPlus recently added the capability of simulating the envelope with a finite difference scheme for conduction, although the effects of this scheme on computation time and accuracy has been greatly underexplored in the literature (Loonen et al., 2017).

It should be noted that such numerical methods for the envelope representation notably increase the computational load. Once again, the option for a reduced order approach, such as simplified transfer functions, may provide the necessary balance between accuracy and computational effort for neighborhood scale analyses. This aspect of model reduction is also examined in this thesis.

Other aspects that differentiate engineering models are the representation of the building systems and the related temporal scale for simulation. Systems can be represented as packages within a library of standard options or can be customized to imitate non-standard HVAC or domestic hot water systems, for example. The finer resolution of such systems usually comes bundled with an interest for smaller simulation time-steps. This combination allows for better understanding of the performance of systems and an

enhanced observation of the fluctuation of state variables in the model. The mainstream detailed energy simulation tools use hourly or sub-hourly calculation steps (Coakley et al., 2014). Software packages as TRNSYS and Modelica can handle very detailed representations of building systems, with extremely fine time resolutions that can get down to 0.1 second in TRNSYS (Solar Energy Laboratory, 2017) and to milliseconds in Modelica (Otter and Elmqvist, 2001).

Matlab is also a common simulation platform that is used by many researchers to develop in-house building energy models with varied levels of granularity. HAMBase (Heat, Air and Moisture model for Building And Systems Evaluation) is an example of a realization of a whole-building model in Matlab (Shijndel, 2007; de Wit, 2006). Harish and Kumar (2016a) report several other studies that developed building energy models in Matlab. Nevertheless, such in-house products are usually constrained to academic hubs, as they require high-level expertise and great computational effort.

It is important to note that these highly detailed representations of building components or systems are of particular interest in specific inward investigations of building behavior. For neighborhood scale assessments, where the whole building is approximated to a single node, such high-end methods and complex software programs could produce over-engineered implementations. For that reason, this thesis also investigates the adequacy of model reduction with aspects to temporal and systems resolutions.

Going to the other end of the palette of physics-based models we find non-dynamic approaches, or more specifically steady-state or quasi-steady-state models. Such models

are used in simulations with larger time-steps, usually equal or greater than 1 day (Fumo, 2014). The ISO-CEN Standard for Energy Performance of Building – ISO 13790:2008 establishes a fully prescribed monthly quasi-steady-state calculation for the assessment of the energy use for space heating and cooling of buildings (ISO, 2008). This approach with monthly resolution has been used with great reliability for quick normative building performance assessment, building energy rating, and energy-efficient building design among other applications (Lee et al., 2014, Lee et al., 2015). Nonetheless, it lacks the ability to track peak loads or agent-based behavior such as thermostat setbacks, which is fundamental to the types of investigations pursued in this research.

Fortunately, there is a dynamic modeling method described in the same ISO 13790:2008, which is a simple dynamic hourly calculation method for energy performance of buildings. This approach embraces both the reductionist strategies advocated here and the temporal resolution necessary to carry out flexible and robust assessment of energy consumption at the neighborhood scale. With such qualities, this reduced order modeling method will be explored in more detail in the following section, as a practical alternative to high-resolution models that are potentially over-engineered.

2.2.3 Detailed and Reduced Order Building Energy Models

It was elaborated above that there is a wide range of tools and methods for building energy simulation under the engineering approach. From one extreme end, highly detailed models and finely grained resolutions are deemed impractical for most simulations at the neighborhood scale. These types of models were originally designed for more inward

looking assessments, which require excessive input data and significant computational effort. Such features can potentially render these models over-engineered for simulations at larger scale. On the other extreme end, overly simplified engineering models with non-dynamic characteristics, such as those with monthly time-step calculations, are not suitable for the type of problems under investigation in this research, since they cannot capture transient states within the simulation hours. This filtering, though, still leaves us with a myriad of modeling strategies in the middle range. In order to make a simpler distinction among the remaining options, those are labeled into two main groups: (1) detailed; and (2) reduced order building models.

According to Woloszyn and Rode (2008), most whole-building energy models fall under those two classes, which the authors call intermediate-grained and coarse-grained models respectively. As depicted in Figure 3, left, the detailed – or intermediate-grained – tools usually employ multi-zone models for air volumes, and 1D numerical models for the envelope (e.g. control volume or finite element techniques).

The reduced order – or coarse-grained – tools use the single-zone approach for internal air volumes, and transfer function models as the conduction solution method for the envelope. As illustrated in Figure 3, right, the whole-building in this case is represented as a homogeneous zone, and the simulation of heat (and possibility mass) transfer through the building enclosure does not allow the investigation of state variables within the envelope elements.

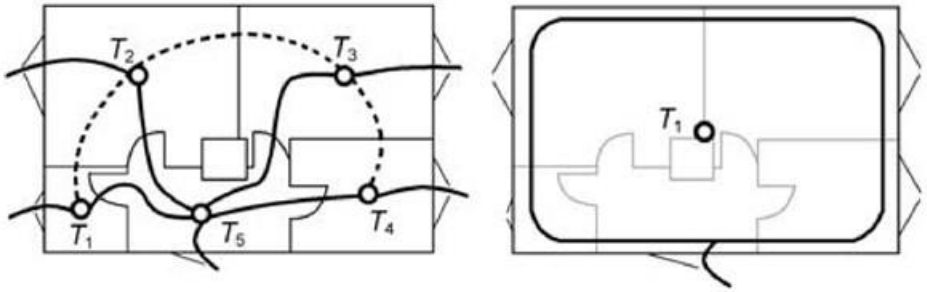

Figure 3 – Levels of granularity for room air (Woloszyn and Rode, 2008)

EnergyPlus, IDA-ICE, IES-VE, and ESP-r are among the most popular detailed models for whole-building energy simulation. It is important to note that packages such as TRNSYS, Matlab, and the Modelica Buildings Library are not considered in this same class, as they may be used in the creation of building models with deep granularity, especially considering aspects of temporal resolution and systems representation.

In this research, EnergyPlus is used as the reference detailed model to be contrasted with the reduced order modeling approach. EnergyPlus is a continually updated free software provided by the U.S. Department of Energy – DOE. It handles detailed building physics for air, moisture, and heat transfer, and supports flexible component-level configuration of HVAC, plant, and refrigeration systems for sub-hourly calculations (DOE, 2017a).

Figure 4 gives an overview of the modeling structure of EnergyPlus, which comprises a collection of specific modules that work together in the calculation of the whole-building energy demand for heating and cooling considering various systems and energy sources (DOE, 2016a).

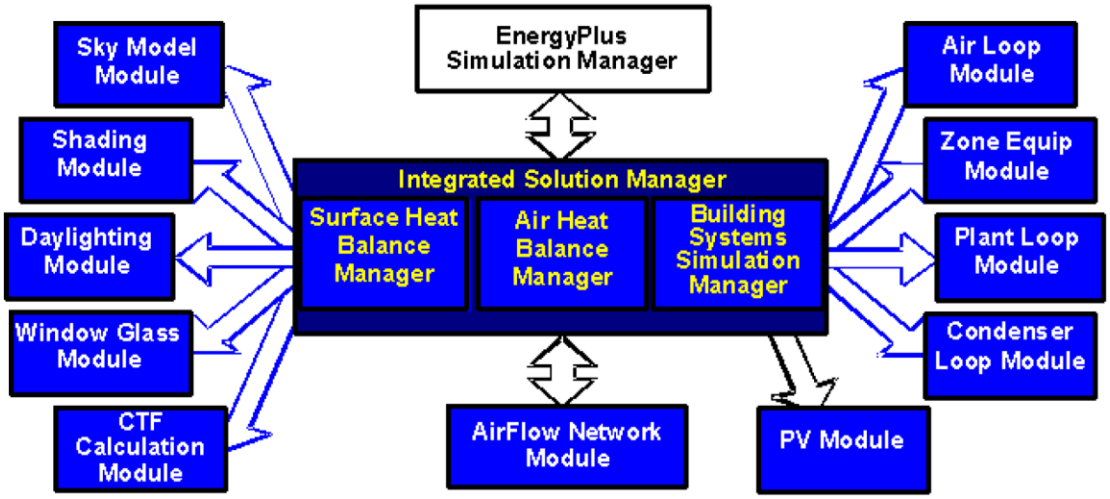

Figure 4 – EnergyPlus Program Schematic (DOE, 2016a)

Although it is a very powerful engine for building energy modeling, EnergyPlus lacks a graphical user interface. The software is usually called within the routine of other simulation software packages, or it relies on the development of front-end tools especially designed to use EnergyPlus as the simulation engine, such as OpenStudio and DesignBuilder (Lee at al., 2015, Harish and Kumar, 2016a).

For the reduced order approach, there are not many software packages readily available, but one technique has been used with fair popularity (Harish and Kumar, 2016b). It is the RC-network model, which relies on the electrical network analogy. In this type of technique, resistances – R and capacitances – C are used in a network representation of heat transfer in building elements. The connecting nodes represent the lumped elements' temperatures, where the more capacitances in the model the higher its order (Kramer et al. 2012).

RC-networks are also called lumped capacitance models, lumped parameter models, and thermal network models (Lauster et al., 2014, Harish and Kumar, 2016b, Panão et al., 2016). Figure 5 shows a schematic representation of a simplified 3R1C network model.

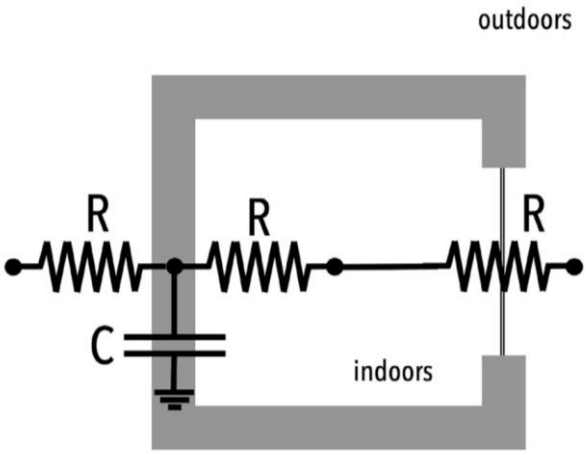

Figure 5 – Schematic example of a simplified RC-network model with 1 capacitance and 3 resistances (Panão et al., 2016)

The order of the simplified model and the number of resistances are subject of constant debate. The literature contains many studies that have utilized RC-networks with different reduction orders for diverse applications with satisfactory accuracy.

Del Barrio et al. (2000) used model size reduction techniques to test the applicability of building energy modeling with several degrees of reductions. The simplified RC-network models were compared against a reference detailed model of a multi-zone residential building. The authors concluded that even the lowest order model allowed suitable predictions of the total energy consumption.

Nielsen (2005) developed a simplified building simulation tool to evaluate energy demand and thermal indoor environment in the early stages of building design. Using a very simplified RC-network, the author could find reliable results compared to a detailed tool (i.e. BSim).

Bacher and Madsen (2011) employed RC-network models, ranging from 1R1C to 6R5C, in the simulation of a multi-zone one-story building. The performance of the models was compared against a set of 5-minute measurements over 6 days. The 4R4C model was selected as the most suitable to give reliable estimates, which were found consistent with reality and were statistically validated.

Lauster et al. (2014) tested three low order models with three capacitances and different number of resistances each, and compared their performance for urban scale applications using the detailed model IDA-ICE as reference. The authors concluded that improved low order models (with more resistances) could lead to well-balanced options regarding computational effort and simulation accuracy.

Berthou et al. (2014) tried four simplified RC-network models, ranging from 4R2C to 7R3C, to assess the thermal performance of occupied office buildings. The models were compared against the results of a detailed multi-zone model (i.e. TRNSYS). They found the 6R2C-model version well suited to predict the building thermal behavior.

Harish and Kumar (2016b) applied an optimization routine to estimate the appropriate values of resistances and capacitances of a 3R2C model used to simulate building construction elements. The optimized model was compared with a finely grained

finite-element representation of the building elements and the results showed close approximation of the step responses.

The international standard EN ISO 13790:2008 employed a 5R1C thermal network for the calculation of building energy demand (ISO, 2008). The use of this standard is relatively widespread and it was adopted in many European countries as a reference methodology for energy assessments in buildings (Panão et al., 2016). The standard defines the building model with many normative stipulations, as the model was used to standardize the calculation of an energy performance coefficient (EPC) across functionally equivalent buildings, which was then used for benchmarking proposed building designs. The ISO 13790 presents two different methods for building energy calculation according to the required temporal resolution:

- a quasi-steady-state method: calculates the heat balance over a sufficiently long period (a month or a whole season), and uses empirically determined gain and/or loss utilization factors to take dynamic effects into account;

- a simple dynamic method: calculates the heat balance with hourly time-steps, and takes into consideration the heat stored in and released from the building mass.

This thesis uses the hourly dynamic method described in ISO 13790 as the core calculation technique for building energy consumption under the reduced order modeling approach. The equivalent resistance-capacitance scheme used in this method is presented in section 3.2.1.2, with a brief description of the nodes, equivalent resistances and capacitance, and heat flows.

For the implementation of such dynamic RC-network calculation method, this study uses an adapted version of the hourly Energy Performance Calculator (EPC Calculator) (Augenbroe et al., 2017). The EPC calculator, originally developed as the EPSCT toolkit, is an energy performance assessment tool developed according to the calculation methods defined in ISO 13790. In the tool, all normative stipulations were removed so the model formulation can be used to calculate the expected energy consumption of a specific building using any set of building inputs or simulation scenarios (Lee, 2012, Zhao, 2012). Besides the thermal energy demand for heating and cooling, the building total energy consumption calculated in the EPC tool also considers the required energy for ventilation, lighting, pumps, domestic hot water, and miscellaneous loads. Figure 6 shows the overall scheme of inputs, calculations modules, and outputs in the EPC calculator. With a small set of input data, the modeler can define the building geometry, envelope properties, systems specifications, and occupancy behavior.

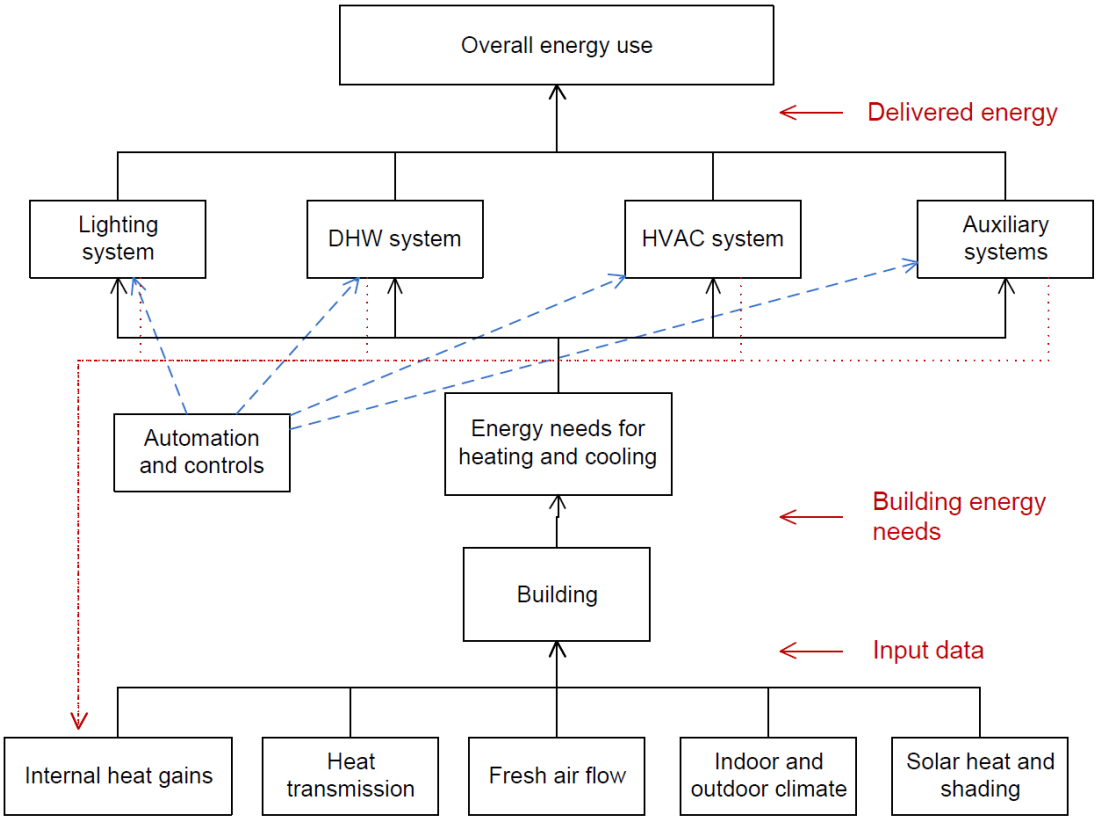

Figure 6 – EPC Calculator Schematic (Lee, 2012)

The EPC tool is programmed in a multiple spreadsheet environment with embedded Visual Basic applications for weather data conversion, model calibration, and building performance optimization. Due to its architecture, the EPC building model can be easily connected to other software packages for more advanced studies, such as uncertainty analysis and risk assessment. The adapted version used in this thesis allows the simultaneous simulations of multiple EPC building models, including peer-to-peer interaction. This modeling flexibility, which allows virtually unlimited interventions or controls at every time-step, brings an immense advantage to the application of this tool in the complex modeling scenarios that are explored in this research.

In order to have a clear distinction of the two modeling approaches (and reference modeling tools) presented in this section, Figure 7 illustrates the overall level of representation of both cases. The reduced order model has lumped representations of building elements, air volumes, and heat flows, as well as simplified representations of building systems and efficiencies. The detailed model has a more granular representation of building spaces, envelope elements, heat flows, with detailed representation of building systems operations. These differences are more specifically described in Table 1, and a better description of these two models is presented in section 3.2.

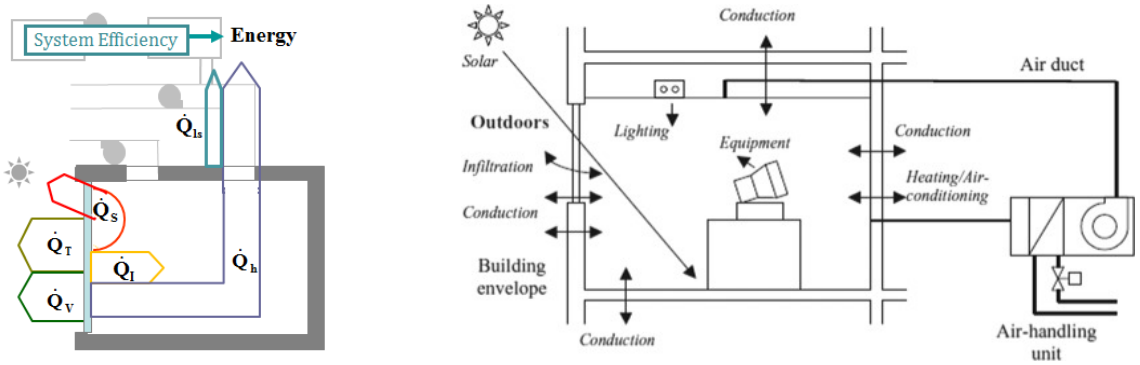

(a) Reduced-order model

(b) Detailed model

Figure 7 – Levels of overall building representation: (a) Reduced order model (Yeonsook, 2011), (b) Detailed model (Harish and Kumar, 2016a)

Table 1 – Comparison of the levels of representation between the detailed and the reduced order building energy models.

Levels of representation in the selected tool	Detailed Building Model	Reduced Order Building Model
	EnergyPlus	**EPC Calculator (hourly)**
Internal air volume	Multi-zone	Single-zone
Envelope heat transmission	Conduction Transfer Function – CTF*	Resistance-Capacitance – RC
Building systems	Detailed systems representation with built-in controls	Model simplifications, applied to the hourly energy balance with simplified controls
Occupancy	Schedules with hourly variation	Schedules with hourly variation
Simulation time-step	15 min	60 min

*The Finite Difference method can be used for better dynamic response of the envelope

2.3 Urban Building Energy Models

The modeling of energy consumption in urban developments comprised of many buildings has gained attention since the beginning of the new millennium (Robinson et al., 2011). This movement was greatly influenced by the need to provide policy makers and city planners with toolsets that could analyze the impacts of different measures for reducing energy consumption and associated greenhouse gases emissions in building stocks (Reinhart and Davila, 2016).

Energy models of building stocks can be grouped in two broad categories:

1. Top-down models; and
2. Bottom-up models.

The top-down approach uses aggregate data (e.g. typical time series of energy consumption) of a building sector (e.g. residential) to estimate the impacts of macroeconomic indicators or technological trends on the energy consumption of the investigated sector (Kavgic et al., 2010). These models are used to examine long-term changes or transitions within the sector, and cannot breakdown energy consumption into end-use types (Swan and Ugursal, 2009).

Bottom-up models, on the contrary, use data from disaggregated components – or individual building models – that are combined to form the urban level energy model (Kavgic et al., 2010).

Figure 8 illustrates different types of approaches for modeling energy consumption of building stocks. Although originally designed for the residential sector by Swan and Ugursal (2009), this classification can be used to any other sector and is in line with the model categorization adopted in this thesis. The left branch represents the top-down approach, which can be divided into econometric (based on macroeconomic indicators, such as gross domestic product or price indices) or technological (based on technological trends, such appliance acquisition preferences).

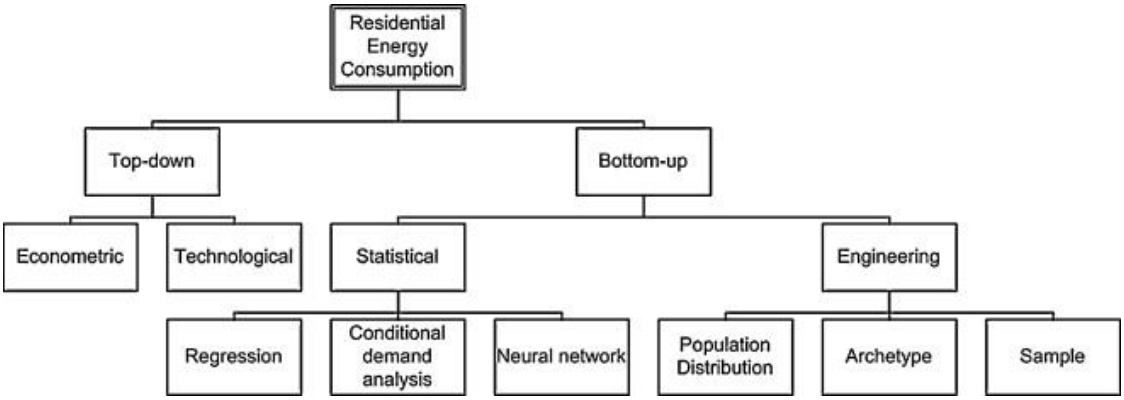

Figure 8 – Top-down and bottom-up modeling techniques for estimating the regional or national residential energy consumption (Swan and Ugursal, 2009)

Due to the limited applications of the top-down approach, as explained above, this type of urban energy model is not of interest in this thesis. Furthermore, as highlighted by Reinhart and Davila (2016), such models are ill-suited for investigating more integrated energy supply-demand scenarios or for analyzing specific neighborhoods.

Therefore, our focus is on the right branch of Figure 8, which represents the bottom-up models. Under this perspective, we are specifically interested in the engineering models, because they can provide the necessary simulation flexibility and reliability for assessing novel and complex scenarios about which there is no available data to enable purely data-driven assessments. However, it is interesting to note that Swan and Ugursal (2009) divide the types of engineering models in Figure 8 in a different way from the general classification for individual building models proposed by Fumo (2014), as depicted earlier in Figure 1. In the case of building stocks, the engineering models are sub-classified as "population distribution", "archetype", and "sample", which relate to different strategies for using individual building models to represent a large group of buildings. These

strategies are intrinsic to urban building energy models and are discussed in more detail later in this section.

Considering that bottom-up urban engineering models are formed by the aggregation of individual building models, the modeler has to choose from a palette of physics-based options to use. Following the same reasoning defended in the last section, this thesis considers the two major groups of physics-based models – detailed and reduced order – as possible approaches to be used in the urban building energy models.

Figure 9 illustrates similar applications of the bottom-up approach using reduced order or detailed energy models. The image shows how simplifications are made as we move from “closer look” to “distant look” representations. The left-hand side of the diagram presents building systems and components, which can be modeled with very fine granularity in terms of space and time. Special tools that are designed to model these types of elements, nonetheless, require great amount of knowledge of the particular building under investigation, as well as significant computational time.

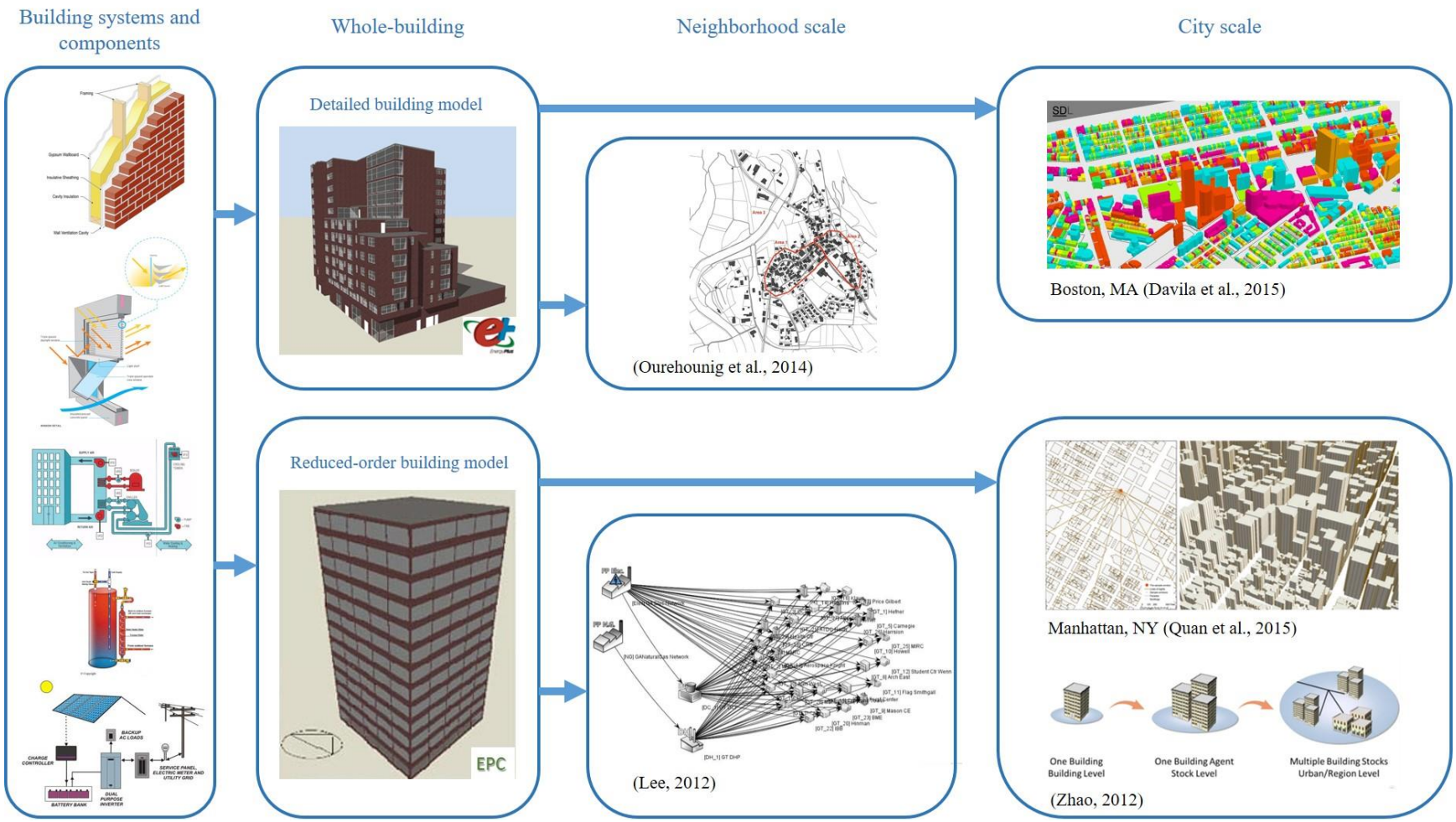

Figure 9 – Representation of urban energy simulation with detailed and reduced order building energy models

Therefore, the first necessary simplification in Figure 9 comes with the whole-building representation, where all building components and systems are modeled in a single simulation tool. When reduced order building models are used for this step, there is significant simplification of such components and systems, which limits the capabilities of the resulting urban model, especially for simulating short-term transient behavior (with time-steps smaller than 1 hour). Detailed whole-building models, on the other hand, can represent such components and systems with more granularity. However, the necessary data to thoroughly inform such detailed models are likely to be incomplete, inaccessible, or impractical to handle when dealing with a large collection of buildings.

To be consistent with the previous section, the studies composing the right-hand side of Figure 9 present EnergyPlus as the reference building energy simulation engine for the detailed approach, and EPC for the reduced order approach. While Orehounig et al. (2014) used EnergyPlus at the neighborhood level, Davila et al. (2016) used the same simulation tool to develop a citywide model. Despite using detailed models, both studies had to rely on simplification strategies for computing and for handling large and incomplete datasets.

Orehounig et al. (2014) clustered approximately 300 buildings of the investigated village into six different categories, and generated only one representative model in EnergyPlus for each category. The results of the heating demand of the representative models were extrapolated to the entire neighborhood according to the net heating floor areas of all buildings.

In their city scale study, Davila et al. (2016) generated one model in EnergyPlus for each one of the more than 80,000 buildings investigated. The authors also went through a cumbersome process to map and assign a 2.5-D geometrical representation of every building model according to the available GIS database of the city. However, due to limitations in data access and management, the non-geometric characteristics of all buildings were based on only 52 archetypes that were assigned according to "use type" and "year of construction".

With a reduced order approach, Lee (2012) used EPC as the core engine in a network model constructed to assess energy performance at a campus level. In that study, one EPC model was generated for each one of the buildings investigated. Information from the 30 existing buildings was used for the definition of their model properties, and standardized data were used to define the buildings operation and internal activities.

Zhao (2012) used EPC to create building prototypes for the simulation of large stocks of commercial buildings within the same climate zone and with the same vintage. The author compared the prototypical representation of commercial building stock with the massive modeling approach (one EPC model for each building), and concluded that the prototype-based building stock model is accurate and scalable to perform large-scale intervention analysis.

In the city scale study carried out by Quan et al. (2015), the EPC tool was used to generate one building model for each one of more than 45,000 buildings in an urban patch. Because of the simplified input requirements of EPC, the authors could explore the available data and retrieve several levels of information to better represent each model

individually. The study utilized available GIS-based urban data to define building geometry and properties, locally averaged shading aspects, and rudimentary microclimate differentiations within the investigated area. In order to run the simulations, the necessary but missing input data were completed with the utilization of a dataset of reference buildings for the locale. The results showed a good balance between model accuracy and modeling simplicity.

From the discussion above, it is evident that analyses at larger scales require inevitable simplifications in the modeling effort, mainly due to data access and availability, manageability, and computational burden. Looking from this perspective, it may seem even contradictory to use detailed tools to simulate building behavior in an urban context. This conflict is illustrated in Figure 10, where the closer we look at or into a building, the finer should be its understanding, hence its representation. In the opposite direction, as we look to the aggregation of more and more buildings, the coarser becomes the representation of each building in the whole picture.

Nonetheless, it is common to observe a mismatch between the model scale and the building representation granularity in many studies, in the sense that researchers often use intermediate-grained building model engines to simulate large collections of buildings. This may be due to the convenience of using sophisticated modeling software that allow the simulation of complex controls as well as detailed occupant behavior for demand side assessments. However, these capabilities do not come without computational overhead. Another possible reason is the idea that such detailed models will reveal additional information that reduced order models fail to do. For these assumptions, this thesis aims to prove that the proposed reduced order methodology can also be satisfactorily used to

address specific aspects of energy performance at the neighborhood scale with the right balance between simulation accuracy and modeling practicality.

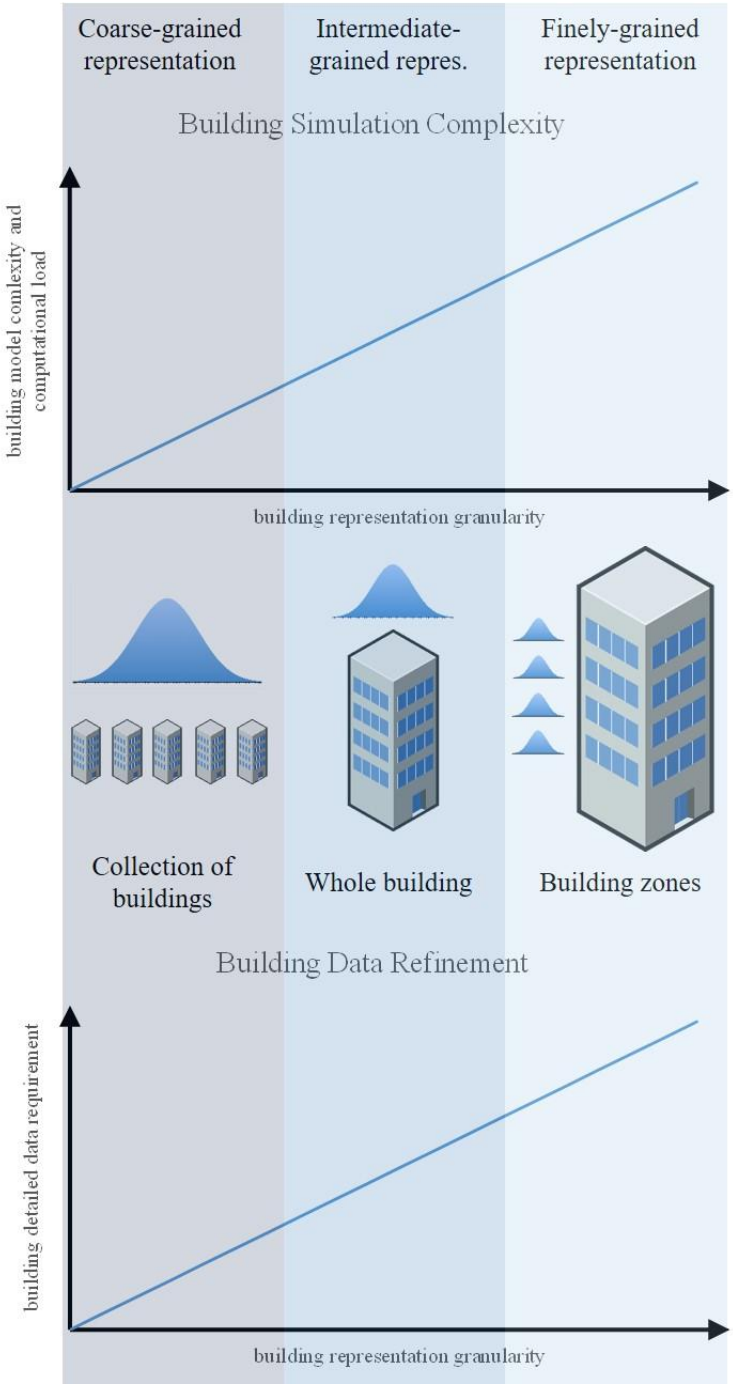

Figure 10 – Building energy modeling at different scales: granularity vs simulation complexity and data requirement

Furthermore, many urban models apply clustering techniques with representative buildings, or match missing data in the modeled buildings with information from libraries of building archetypes or building prototypes (Davila et al., 2016, Orehounig et al., 2016, Quan et al., 2015). The impact of this significant simplification is often understated in many cases. When using such techniques, the follow-up simulation with a detailed building model is likely to result in unnecessary computational load that cannot overcome the loss in information granularity. The trade-offs between the necessity to invent missing data in higher order modes and the convenience of using simplified models for scarce or unmanageable data need further investigation.

This aspect is illustrated in Figure 11, which shows a schematic comparison between detailed and reduced order modeling approaches when using representative building models. Under these conditions, the representation of the characteristics and properties of the building models usually boils down to four layers of information coarsely represented: envelope thermal transmission properties, systems efficiencies, occupancy schedules, and thermostat settings. As observed in the studies mentioned above, the first two groups of information are normally derived from building vintage, while the latter data sets are estimated base on building function typology.

In the detailed urban model with representative BEMs, the information granularity is lost, while the computational complexity is preserved. However, in the reduced order approach, the simplified input parameter and the computational efficiency is maintained throughout the process.

Perhaps a more important aspect when using representative buildings is not the greater accuracy of the building simulation tool, but the right variability in the distribution of representative buildings within the network of buildings. Although this aspect is out of the scope of this thesis, it is worth mentioning the work of Wilson et al. (2016), which present a robust proposition for an adequate balance between the representativeness of the distribution of building stock profile and the required number of building simulations.

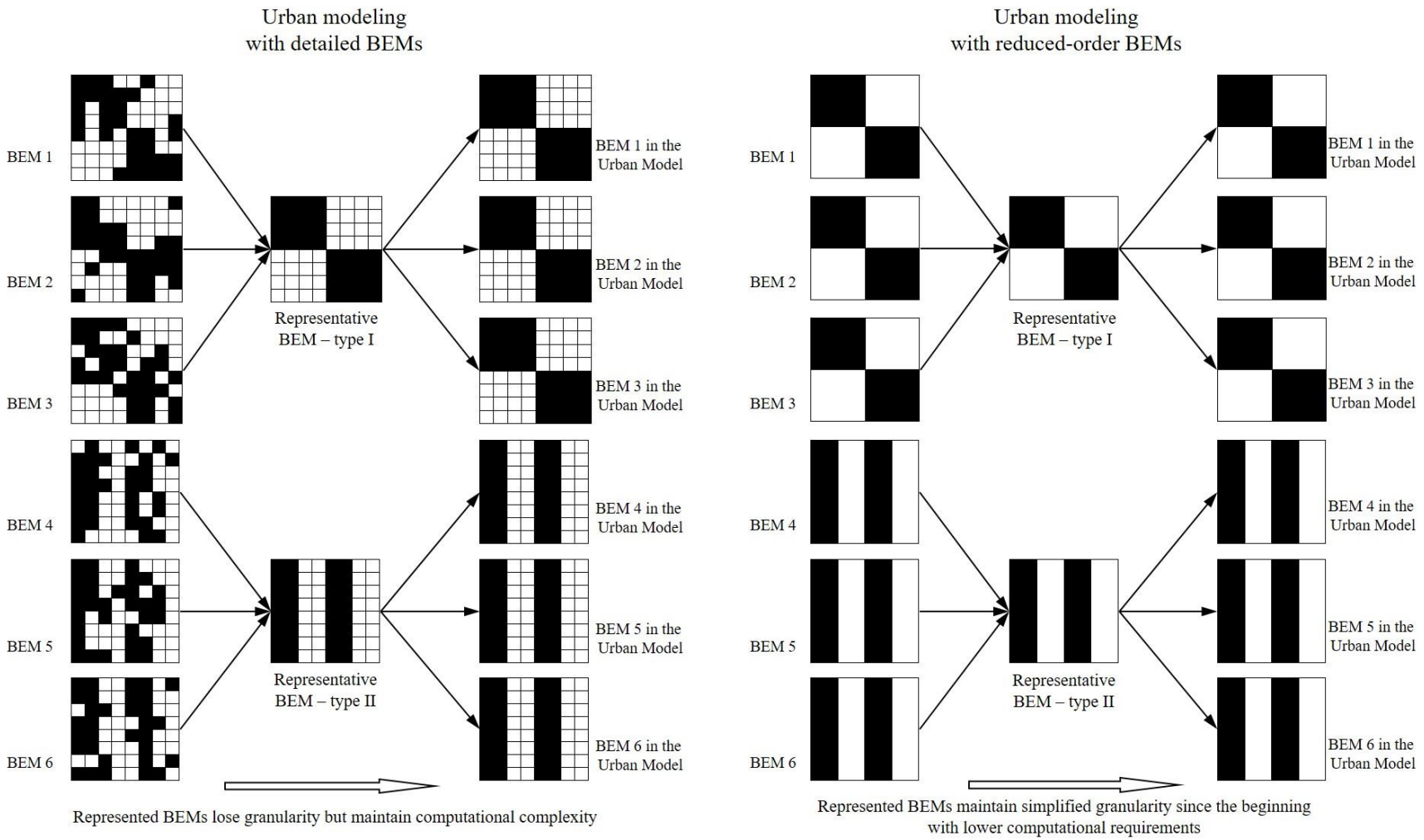

Figure 11 – Schematic representation of urban energy models using building archetypes: left – detailed BEMs; right – reduced order BEMs

2.4 Distributed Energy Resources (DER)

The definition of distributed energy resources (DER) is still loose in the gray and academic literatures. There are common classifications, but diverse interpretations of the fitness of specific technologies may occur. In this thesis, we adopt the definitions described in the recent Manual prepared by the U.S. National Association of Regulatory Utility Commissioners – NARUC, which addresses the complexities of rate design and compensation policies as they apply to the increasing presence of distributed energy resources in the electric grid (NARUC, 2016). In the absence of an official definition of DER, NARUC's manual provides guidance to utilities, customers, and other stakeholders regarding what constitutes DER. It builds upon definitions already made by relevant sources, such as the U.S. Department of Energy, the Lawrence Berkeley National Laboratory, industry specialists, and commissions of utility public services of relevant states in the U.S.

The definition provided by the manual is presented below:

> "A DER is a resource sited close to customers that can provide all or some of their immediate electric and power needs and can also be used by the system to either reduce demand (such as energy efficiency) or provide supply to satisfy the energy, capacity, or ancillary service needs of the distribution grid. The resources, if providing electricity or thermal energy, are small in scale, connected to the distribution system, and close to load. Examples of different types of DER include solar photovoltaic (PV), wind, combined heat and power (CHP), energy storage, demand response (DR), electric vehicles (EVs), microgrids, and energy efficiency (EE)." (NARUC, 2016)

Following this definition, the next sub-sections describe each cited example of DER in more detail, trying to show their relevance to the types of neighborhood energy flows and interactions investigated in this thesis.

2.4.1 Solar PV Systems

Solar PV systems use photovoltaic – simply named PV – cells to convert solar energy from sunlight into electricity. A comprehensive comparison chart of PV cell types and related conversion efficiency values over time is presented in NREL (2017). According to the chart, the cell types are classified as multijunction, single-junction, crystalline, thin-film and other emerging PV technologies. It is interesting to note that NREL (2017) reports conversion efficiencies as high as 46%, as the case of the Franhofer ISE/Soitec technology, although this type of solution is still constrained to high-level laboratory environments. Realistic efficiency values for market-available PV systems are usually under 20% (Dobos, 2014).

PV systems can be ground-mounted or located on rooftops of buildings and households. They are installed in modules that can be added to form arrays of varied sizes, including single-building, community, and utility scales. Technological advances, falling PV panel prices, and favorable policies made PV systems the fastest-growing type of DER (NARUC, 2017).

The increasing penetration of distributed PV systems in the electric grid imposes many operational and regulatory challenges, especially regarding the transaction of excess

energy generation (when the building becomes an energy producer to the grid) and voltage regulation issues.

PV systems are handled in the proposed modeling approach as an independent calculation module that can seamlessly integrate the values of energy production with the other flows of energy in the neighborhood at every time-step. The embedded calculator can support any value of cell efficiency and can be calibrated, if needed, using more sophisticated tools such as the System Advisory Model – SAM (Gilman, 2015) and PVWatts (Dobos, 2014).

2.4.2 Combined Heat and Power

Combined Heat and Power (CHP) systems, also known as cogeneration systems, can provide both electric power and heat from the same source (NARUC, 2017). These systems can capture the thermal energy of the power generation process, which would otherwise be released as waste heat, and use it for many other applications, such as hot water and space heating needs in buildings. Five main CHP technologies made up almost 99 percent of the total CHP electric capacity in the U.S. in 2015 (EPA, 2015): (i) reciprocating engine; (ii) gas turbine; (iii) boiler/steam turbine; (iv) microturbine; and (v) fuel cell.

CHP systems can be operated with diverse fuels, including natural gas, biomass, coal, and process wastes, achieving efficiencies of over 80 percent, which is significantly higher when compared with a usual value of approximately 50 percent for conventional

technologies. In addition, some CHP systems can be used for islanding or for providing black start services during outages when allowed (NARUC, 2017).

Although very relevant for neighbourhood applications, CHP solutions are not part of the scope of this study and are not be investigated in this thesis. Nevertheless, it is worth mentioning that our proposed modelling approach can be used to hold CHP technologies in the hourly calculations, as long as an additional calculation module for such systems is developed. The resulting CHP outputs for generated electricity or heat could then be easily integrated into the hourly thermal and electrical energy balances at every time-step.

2.4.3 Wind

In wind energy systems, turbines convert wind's kinetic energy into mechanical power that is ultimately converted into electricity via generator. The U.S. wind power capacity has grown significantly over the past years, with a surge in 2015 (over 8,500 MW of new added capacity) and a projected continued and rapid growth in the coming few years (DOE, 2016b).

Wind energy systems can vary in size due to the number and type of turbines, ranging from a single small turbine system (below 100 kilowatts) to large utility-scale systems with several megawatts. In the U.S., the adoption of wind energy systems varies greatly by state due to local wind conditions, policies, and regulations, where Texas leads the installed capacity (EIA, 2017). When distributed, these systems can be connected to

buildings in residential, agricultural, commercial, industrial, and community sites (NARUC, 2017).

The case studies of this thesis do not consider wind energy systems in their problem formulation. However, the proposed integrated simulation approach already incorporates a module for wind energy generation that can be used with the same flexibility of the PV calculator module.

2.4.4 Energy Storage

As a resource, energy storage can be used to add stability, control, and reliability to the electric grid (NARUC, 2017). Energy storage types vary according to the energy conversion type and application size (ESA, 2017). Pumped hydro is an option for large-scale energy storage, but it is limited to very specific aspects of environmental and economic suitability.

Thermal storage can be achieved by using water as the storage mean, usually in water tanks, or even in the form of ice tanks specifically designed for coolth storage. In buildings, the thermal capacity of solid-state materials present in the envelope or in the building slabs or internal elements can also be used to store thermal energy. This thesis does not investigate the first options of thermal storage technologies in separate devices, but does consider the implications of the building thermal mass in providing thermal inertia against temperature fluctuations in its reduced order building energy calculator.

Alternatively, chemical storage is possible with solid state and flow batteries that can store electrical energy in the form of chemical energy, which can be converted back into electricity when needed. Battery storage have not been widely used historically, because of cost issues and technological limitations. However, the recent decline in costs and improvements in technological solutions have made batteries more competitive in the realm of energy resources (NARUC, 2017). The use of batteries becomes even more relevant when they are coupled with PV or wind systems to compensate their intermittency and thus boost their full generation potential.

The simulation approach of this thesis integrates calculation modules for batteries that can simulate the state of charge and perform smart decisions regarding charging and discharging strategies at every time-step. These battery modules can represent devices that operate at a single building level or as a shared resource.

2.4.5 Microgrids

A microgrid is a localized small network of electricity consumers and sources that is usually connected to the main grid at one point of common coupling, but can be islanded and operate independently if needed or desired. Several benefits are advocated for the use of microgrids, such as: (i) adding resilience to the grid infrastructure; (ii) meeting the end-user needs by ensuring uninterrupted power supply for critical loads; (iii) enabling grid modernization and interoperability; (iv) enhancing the integration of distributed and renewable energy resources (SANDIA, 2014).

The simulation platform developed in this thesis can model microgrids as interconnected and intelligent buildings and energy resources, thus calculating the integrated energy balances and flows at every time-step. With this modeling environment, the microgrid can be subject of optimization studies regarding several performance aspects, such as peak load management, carbon emission reduction, or simply electricity cost minimization.

2.4.6 Demand Response

In this thesis, demand response (DR) is defined as the building capability of responding to a request from the grid (either the main grid or the microgrid) to reduce or reshape its energy demand during critical days or intervals. This is made by allowing the reduction of space conditioning needs with thermostat setbacks, the reduction of lighting usage wherever possible, and/or the rescheduling of major appliances operation to non-peak hours.

NARUC (2017) highlights that although traditionally viewed as a peak reduction resource, DR can also be used to relocate specific modes of consumption to hours of excess generation, thus enhancing the efficiency of the grid.

This thesis considers DR strategies in a case study as an impacting option that can be synergistically integrated with other DER alternatives in the neighborhood with microgrid settings to provide improved energy flexibility. The simulation platform allows the programming of controls that enable DR actions in every participating building, which

automatically adjusts the thermostat setting and the involved end-uses during the critical hours of a DR event.

2.4.7 Electric Vehicles

Electric Vehicles (EVs) are relevant to the palette of energy resources in the modern urban environments as they carry batteries that can usually store as much energy as an average U.S. residence consumes in a day (Nelder et al., 2016). If such storage devices are charged at the preferable times of off-peak demand, both the householder and the grid operator can find benefit in terms of electricity bills and grid efficiency respectively. In addition, as a pooled resource connected to the grid in a vehicle-to-grid (V2G) interaction mode, EVs can potentially function as grid supply during times of high demand (Nelder et al., 2016). When connected to a microgrid, EVs can also provide mobile backup power during and outage or emergency situation (NARUC, 2017).

These DER capabilities of electric vehicles are investigated in the proposed simulation platform by using calculation modules similar to the ones used for stationary batteries. The aspects of mobility, driving habits and related energy use are considered in the calculations as to represent realistic profiles of state-of-charge and battery availability for V2G operation.

2.4.8 Energy Efficiency

Energy efficiency is considered as a distributed energy resource[5] since it can effectively compete with other alternatives for reducing, shifting or shaving loads. Energy efficiency measures might not be as flexible or as easily implemented as other distributed options, but they are still regarded as the most cost-effective energy resource option. Molina (2014) collected data for 20 U.S. states from 2009 to 2012 and found that electricity efficiency programs are one half to one third the cost of alternative new electricity resource options.

In buildings, energy efficiency can be pursued by investing in better insulation of envelopes, in more efficient HVAC systems, lightbulbs and appliances, as well as in more intelligent controls.

The proposed modelling approach supports the simulation of various alternatives for energy efficiency in buildings by allowing the manipulation of the parameters of the underlying building energy models.

2.5 Modeling the Integration of Buildings and DER

In section 2.3, there was already a discussion on the challenges for modeling a collection of buildings with a good balance between model fidelity and simulation practicality. Adding distributed energy resources to the mix makes such task even more

[5] This consideration follows a broader understanding of DER, as adopted by the U.S. National Association of Regulatory Utility Commissioners – NARUC.

complex. The present section discusses previous modeling efforts for the integration of several buildings and DER for different performance assessments. Then it describes the modeling approach proposed in this thesis, and contrasts its capabilities with those from the previous studies.

2.5.1 Previous Work

With the dissemination of DER, many modeling packages have been developed for assessing urban energy systems with such energy resources (Allegrini et al., 2015). Figure 12 shows a matrix with a recent review of software tools and packages for the simulation of district-scale energy systems. From the matrix, only CitySim, PolySun, and SynCity carry simplified building thermal models with occupant and operator behavior simulation capability and allow their integration with several options of DER. Nevertheless, these tools still lack some characteristics that are fundamental to the analyses that are required to meet the research objectives in this thesis.

CitySim uses Java and C++ languages, and employs an XML file format to allow data exchange between simulating modules. However, it still carries rather complex implementation effort (Robinson et al., 2009; Walter and Kampf, 2015).

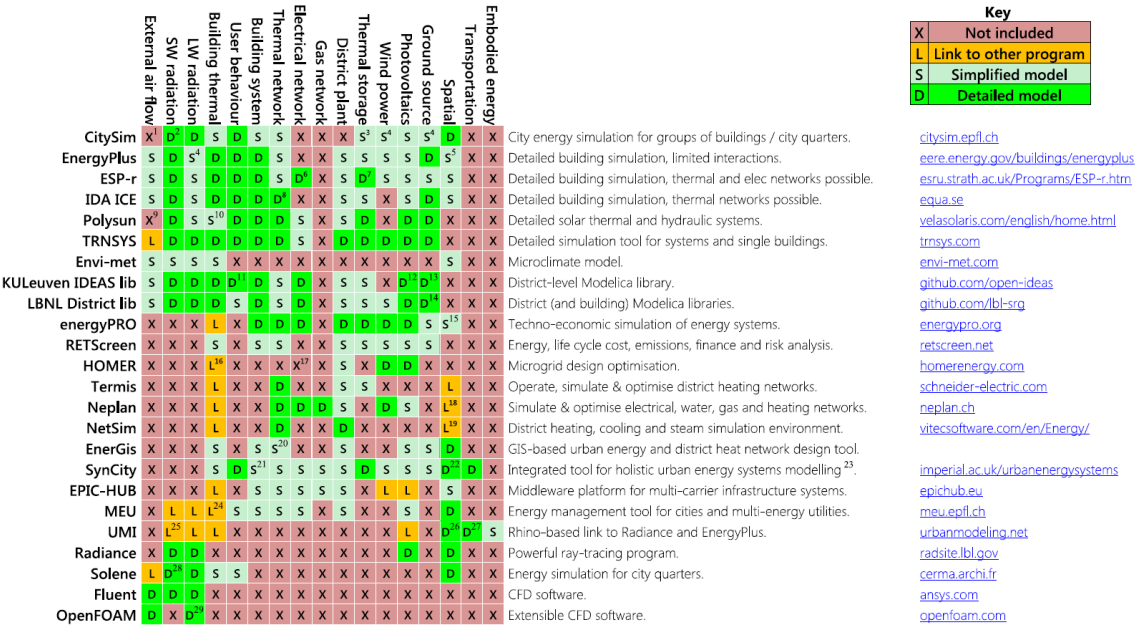

Figure 12 – Matrix indicating the capabilities of a selection of software tools and packages (Allegrini et al., 2015)

PolySun is not building oriented and it is a proprietary software (Vela-Solaris, 2017). Its packaging makes it very limited for modeling customizations and for addressing specific research problems.

SynCity uses Java language and an overly simplified building representation. Furthermore, the proposed layouts and technologies of resource supplies and demands are assumed static in the model (Keirstead et al., 2009).

Other tools or modeling approaches that are more focused on the grid performance, such as DER-CAM and HOMER are being increasingly used in research and evaluation assessments. However, these models do not allow the adequate exploration and examination of the building thermal model, which is ultimately reduced to a function or is substituted by a set of building load data. Thus, they lack the necessary resolution from the

building perspective to allow for agent-based modeling and the quantification of key energy performance measures based on building simulations at the neighborhood scale. In these cases, the building energy demand is usually given or preprocessed with a building simulation tool. This detached simulation approach renders the dynamic investigation of the interaction between buildings and DER in different scenarios impractical.

The Distributed Energy Resources Customer Adoption Model (DER-CAM) was developed by the Lawrence Berkeley National Laboratory – LBL to minimize the combined cost of local energy generation and CHP systems (LBL, 2017). Koirala et al. (2016) used DER-CAM to assess integrated community energy systems. The authors used hourly-metered data for both gas and electricity as the building demand inputs.

The Hybrid Optimization Model for Multiple Energy Resources (HOMER) is a tool for optimizing microgrid design. It was originally developed at the National Renewable Energy Laboratory – NREL , and later improved and distributed commercially by HOMER Energy (HOMER Energy, 2017). Best et al. (2015) used an in-house energy supply model to optimize the mix of energy supplies for urban districts. The authors used HOMER to validate the modeled representation of the community. In the study, the buildings' load profile was previously generated by EnergyPlus.

GridLAB-D software was developed by the Pacific Northwest National Laboratory – PNNL to simulate the power distribution system (GridLAB-D, 2017). It applies the equivalent thermal parameters (ETP) approach, which employs a simplified RC-network analogy method to model building thermal response (Chassin et al. 2014). It is important to note that GridLAB-D was designed from the grid operation perspective, and thus it treats

buildings and its end-loads as external “signals” (Taylor et al, 2008). Williams et al. (2013) used GridLAB-D to simulate a self-regulating distribution system for a smart-grid with DER. The authors coupled GridLAB-D with Matlab for data exchange and post-processing capabilities. Though dynamically flexible, such integrated modeling approach is limited with respect to changing building input data and to the representation of diverse end-uses in the buildings.

Several researchers have also developed modeling approaches using engineering building models as the underling simulation engines coupled with other tools or scripts to allow them to be scaled up to urban levels. However, many faced issues with achieving an appropriate level of integration of building models with DER, inevitably posing the risk of over-engineering the model.

Reinhart et al. (2013) developed an urban modeling design tool called “umi”, which integrated multiple performance aspects, such as operational energy, daylighting and walkability. The tool used the detailed simulation engines EnergyPlus and Radiance/Daysim coupled with scripts in Grasshopper and Python to carry out assessments of complete neighborhoods. The tool, however, was not designed for the integration of buildings with DER, since the Umi-Energy module is based on the simulation of EnergyPlus models for each building, considering simplified inputs and general assumptions. The authors acknowledged the relevant challenges for setting up an operational umi model.

He et al. (2015) developed a neighborhood model to predict hourly thermal demand for a group of dwellings. Although not as detailed and not as comprehensive in terms of

performance aspects as the approach developed by Reinhart et al. (2013), this study was innovative in the way it used a stochastic occupancy model to yield more realistic and representative hourly thermal demand profiles. However, in order to generate the building energy demands, He et al. (2015) also used EnergyPlus as the underlying simulation engine. The authors used a parametric tool to manage several building simulation runs and to extract their outputs, as well as Python scripts for post-processing and for output visualization.

Orehounig et al. (2014) proposed the integration of decentralized energy systems in a neighborhood using a concept of "energy hub". In the case study, the authors modeled a village by using representative building models for each building category (considering type and vintage), which were simulated in EnergyPlus. The modeling approach showed enough flexibility for optimizing the management of energy supply systems based on preprocessed hourly energy demand values. Similar to the other studies above mentioned, the use of EnergyPlus for the prior quantification of energy demand limits the applicability of the model for interventions within the buildings during the simulation run.

To overcome the complexities and lack of flexibility of urban models with high-end building simulation engines such as EnergyPlus, many modelers have opted to use reduced order models instead. The usual approach in these cases is the RC-network model. The intention is to achieve a good compromise between model accuracy, computational overhead, and data availability (Robinson et al., 2009).

Nevertheless, the integration of these simplified building models with DER in urban studies still faces various difficulties and limitations.

Robinson et al. (2009) conceived the software CitySim that enables the simulation of flows of energy, water, and waste in neighborhoods. The proposed software uses an RC-network model that is flexible enough to simulate both single-zone and multi-zone building models. However, the authors recognize that there remains significant work to render the model more comprehensive for urban resource flow studies, as well as suitable for optimization studies. In addition, CitySim lacks the capability to model possible synergetic exchanges of energy between buildings.

Lee (2012) and Zhao (2012) used the EPC calculator with the embedded RC-network representation as the building thermal model. While Lee (2012) developed an assessment at a campus level with local energy resources, Zhao (2012) used the EPC tool to create building prototypes for the simulation of large stocks of commercial buildings under demand response scenarios.

Quan et al. (2015) applied the EPC calculator for a city-scale energy use estimation. The study experimented with the diversification of input data in each building model with respect to microclimate, and building type and vintage.

Patteeuw et al. (2015) used a reduced order building model with a thermal RC-network representation (Patteeuw et al., 2014) to develop an integrated neighborhood model that takes into account the dynamics and constraints on both the supply and demand side of the electric power system. The authors used the model to assess the use of Active Demand Response (ADR) strategies with high quality results at a low computational cost. The proposed integrated model is applied to an optimization problem targeting the minimization of the overall operational cost of the electricity consumed in the collection

of buildings, subject to techno-economic and comfort constraints of both the supply and demand sides. The supply side consisted of a combination of 26 power plants of different types and size, while the demand side consisted of 25 identical buildings with different behavior and with thermal energy storage capability via building shells and hot water storage tanks. Very integrative and robust, the model was implemented in Matlab, coupled with the optimization software GAMS. However, it seems to have limited flexibility and practicality for modeling diverse integrations of multiple buildings and various forms of DER.

Berthou et al. (2015) developed the tool Smart-E for the simulation of thermal and electrical uses of energy in dwellings and commercial buildings. The tool was used to model an existing medium sized city with short time Demand Response (DR) strategies. In a case study, Berthou et al. (2015) investigated and compared the impacts of two DR strategies on occupant comfort and aggregate electric load curve over one winter day. A single-zone RC-network model (Berthou et al., 2014) with only 10 input parameters is used by Smart-E for simulating the building heating needs. The other energy uses in the buildings such as domestic hot water, lighting and appliances are calculated independently in sub-models that are based on existing databases. For these data-driven sub-models, Smart-E prioritizes the use of high detailed information at the building level, and when not available, the tool uses probabilistic functions or average values to fill up the necessary input data. The whole-building energy consumption is ultimately calibrated with existing energy consumption data. This separate process of calculation of energy end-uses in the buildings may render Smart-E less flexible to be used in varied problem formulations.

Good et al. (2016) used an RC-network as the underlying simulation approach for the building space heating sub-model in a domestic multi-energy model. Other sub-models for building energy end-uses were employed to calculate DHW, cooking, and appliance needs. The model can be used to assess the impact of electro-thermal technologies, such as heat pumps and combined heat and power units, in aggregations of dwellings. The main contribution of the study is the flexibility of the model to realistically simulate diversity and coincidence of various energy demand profiles within and across the collection of buildings. Although very suitable for distribution network impact studies and for demand side flexibility assessments, the model may require significant adaptation to be used with DER options other than electro-thermal technologies.

McKeena and Thomson (2016) presented the integrated version of CREST, designed to model building thermal-electric demand. Created primarily for low-voltage network analyses, the model can also be used for calculating demand of urban energy systems. CREST comprises several sub-models for the simulation of energy use in buildings, including occupancy, appliances, lighting, thermal demand, PV, and solar thermal collector. An RC-network model is used as the underlying physical representation of the building thermal demand sub-model. Similarly to the work of Good et al. (2015), CREST accounts for diversity in the demand of loads within a building and between buildings. The model has a one-minute resolution and was constructed in an open-source Excel VBA environment. The authors highlight that the simplifications of their modeling approach were aimed for statistical accuracy of the collection of modeled buildings rather than absolute accuracy of any one individual building within the group. As a limitation, the

model was not designed to handle demand response applications nor building-to-building interactions.

Fonseca et al. (2016) developed the computational model City Energy Analyst (CEA) for the analysis and optimization of energy systems in neighborhoods. Very comprehensive in scope and conveniently integrated in a single interface, CEA comprises sub-models for energy generation/conversion, storage, and distribution on the supply side. For the demand side, CEA uses a RC-network model based on the standard ISO 13790, as defined in Fonseca and Schlueter (2015). The City Energy Analyst model was programmed in Python, in hourly time-steps, and has additional algorithms for analysis and visualization of data. Despite the good balance between model complexity and simulation accuracy, Fonseca et al. (2016) reported relatively high computational run times for optimization studies in CEA. Furthermore, the model library only carries building archetypes for the Swiss-European context (City Energy Analyst, 2017a). Demand response analysis is not included in the current simulation modules. Nevertheless, CEA is under ongoing progress, which makes it a promising tool for various applications in urban energy flow analysis (City Energy Analyst, 2017b).

Table 2 summarizes the most relevant features of the studies and respective tools discussed in this section.

Table 2 – Capabilities and limitations of various simulation efforts for neighborhood energy models.

Author(s)	Model Specification / (Building simulation engine)	Model Features								
		Low requirement of building input data	Low effort to input data	Low computational need	Easily scalable to neighborhood applications	Allows peer-to-peer integration	Allows demand-response analysis	Allows co-simulation with other DER	High flexibility for changing build. inputs	High flexibility for changing scenarios
Reinhart et al. (2013)	Umi (EnergyPlus)				✓					
He et al. (2013)	125 houses with diff. behavior (EnergyPlus)				✓				✓	✓
Orehounig et al. (2014)	~300 buildings repres. in 6 models (EnergyPlus)					✓				
Robinson et al. (2009)	CitySim (RC in Java/C++)	✓			✓					
Lee (2012)	Multi-model platform (RC in Excel VBA)	✓	✓		✓					
Zhao (2012)	Multi-model platform (RC in Excel VBA)	✓	✓		✓		✓			
Quan et al. (2015)	Multi-model platform (RC in Excel VBA)	✓	✓		✓					
Chassin et al. (2014)	GridLAB-D (RC, using the ETP approach)	✓			✓	✓	✓	✓		
Patteeuw et al. (2015)	25 buildings with diff. user behavior (RC in Matlab)	✓		✓			✓	✓		
Berthou et al. (2015)	Smart-E (RC)	✓	✓		✓	✓	✓			
Good et al. (2016)	Multi-dwellings (RC)	✓			✓	✓	✓			
McKeena and Thomson (2016)	CREST (RC in Excel VBA)	✓	✓	✓	✓				✓	✓
Fonseca et al. (2016)	City Energy Analyst – CEA (RC in Python)	✓	✓		✓	✓				✓
This study	Multi-model platform (RC in Excel VBA)	✓	✓	✓	✓	✓	✓	✓	✓	✓

RC means “Resistance-Capacitance” network models. ETP refers to the term “Equivalent Thermal Parameter” approach, which employs a simplified version of an RC-network model.

2.5.2 Proposed Modeling Methodology

The modeling approach proposed in this thesis incorporates the positive aspects gathered from several other relevant studies, as presented in the previous sub-section, concerning model flexibility, accuracy, speed, and practicality.

It is implemented in a multi-model calculation platform, where several simulation models run simultaneously. Each model (either a building energy model or a DER model) is programmed in a dynamic sequential format in which the calculation outputs of every time-step are used as inputs in the following time-step. The novelty of the proposed approach lies on the possibility to intervene at any time-step in any individual model, even allowing peer-to-peer interactions, as depicted in Figure 13.

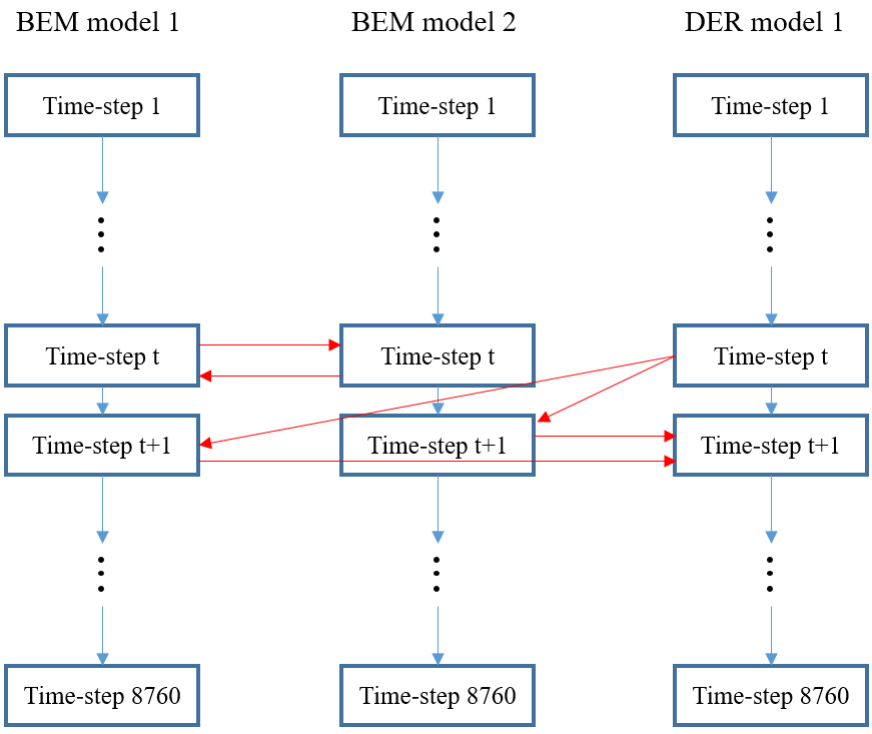

Figure 13 – Multi-model flexibility and integration

Every model in the platform runs under the same hourly scale with 8760 calculation instances for a simulation year. In this manner, additional modules can be used in the neighborhood model for input/output data management, transaction data management, and control strategies. This modeling flexibility allows the co-simulation of BEMs with varied types of complex DER strategies, such as demand response and microgrid interactions, in many possible combinations.

Figure 14 illustrates the overall interconnection scheme between models at every time-step of the simulation platform. The building energy models use the reduced order resolution described previously, and allow the representation of diverse load profiles as each EPC engine runs individually with its own set of input data. This same independence allows the consideration of differences in microclimate conditions between buildings, if needed, as in the work of Quan et al. (2015).

Once in operation, the neighborhood model is updated every time an input or control is changed, resulting in 8760 new sets of interconnected outputs in only a few seconds. Such simulation speed facilitates the application of algorithms for optimization and risk analysis, which require several hundreds or even thousand or runs to come to a result.

The advantages and capabilities of the proposed modeling approach in contrast with other efforts are presented in Table 2 in the previous sub-section. However, it is important to highlight that those performance comparisons do not address the whole range of possible questions or problem formulations that may render some of those models more appropriate.

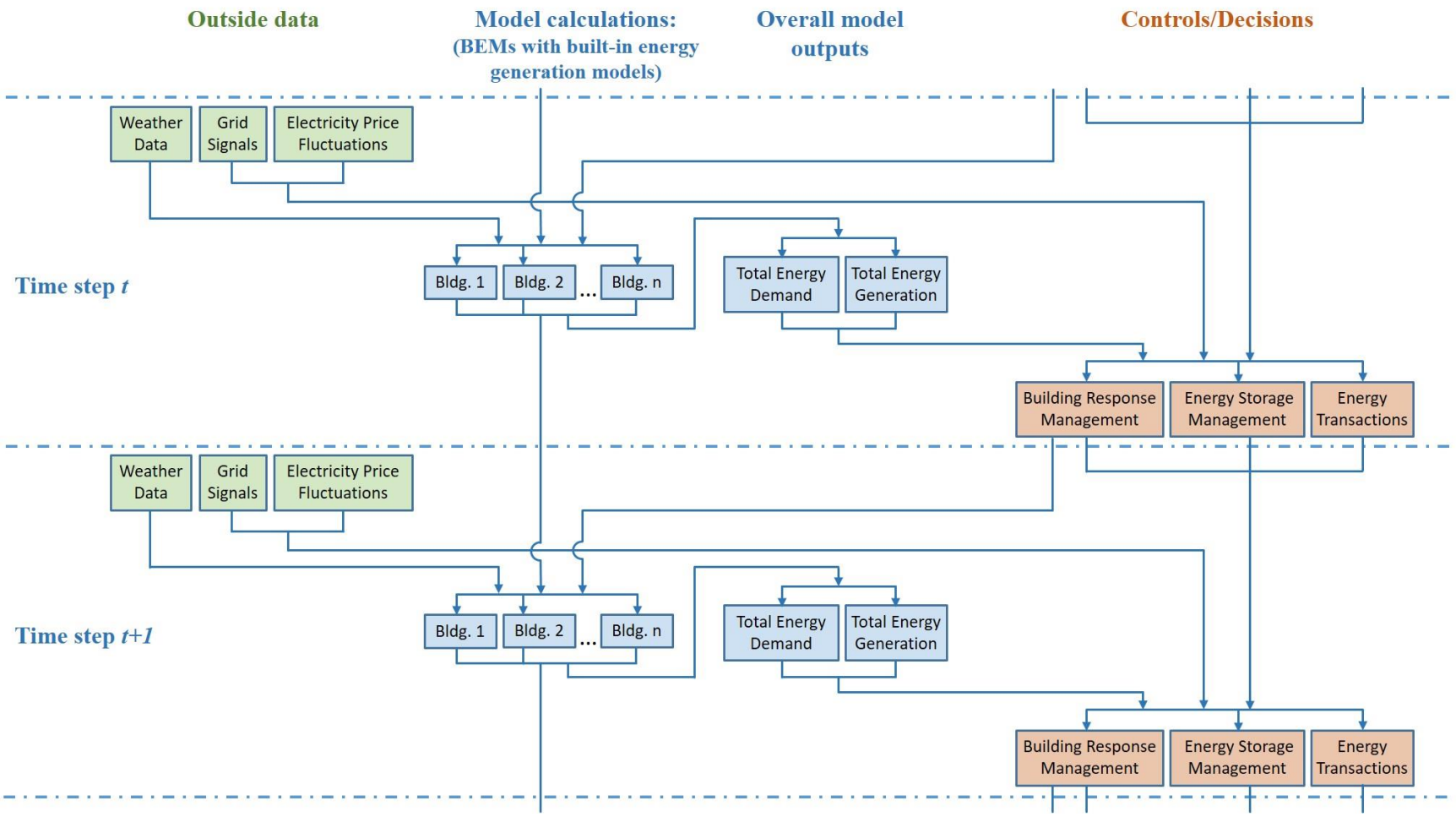

Figure 14 – Neighborhood energy modeling platform. Integrated calculation and decision making at the hourly resolution.

CHAPTER 3. COMPARISON AND VALIDATION OF THE REDUCED ORDER MODEL AGAINST A HIGH-FIDELITY MODEL

3.1 Introduction

This chapter addresses the second research question stated in section 1.3: *How do reduced order models compare with higher order models for supporting decision-making towards the selection of design and engineering parameters related to energy performance and flexibility at the neighborhood scale?*

Such comparison exercise is only meaningful when we explicitly define the application purpose for which the models are being used. In this research, we are specifically interested in understanding how the models compare with regards to supporting decision-making towards the selection of building design and building engineering parameters for improving energy performance and energy flexibility at the neighborhood scale. The output resolution, in this case, necessarily involves a great amount of aggregation, for which we believe simplified models should be sufficient and computationally more appropriate, as investigated in this chapter.

To set the stage to answer this question, we develop a neighborhood energy modeling platform based on the EPC tool, which we are calling EPC_Nhood. On the other hand, we create the counterpart high-fidelity representation of the neighborhood with the aggregation of outputs of multiple EnergyPlus building models.

The idea is to have a fair number of buildings, from different typologies, that can be used as a virtual community test bed. With this experiment framework, we can assess the applicability and reliability of our reductionist modeling approach for simulating performance indicators[6] related to energy flexibility at the community scale.

The stock of buildings under experimentation comprises eight low-rise multi-family residential buildings, one medium office building and one retail strip mall building located in the city of Miami, Florida, US. This variety intends to represent some distribution of building types within a neighborhood, where different occupancy patterns and demands can be observed. The selection of Miami as a reference location is based on a few criteria: (i) we want to test a major city in the east coast, since next chapter uses a location in the west coast; (ii) we look for a location that is preferably cooling dominated, as to represent higher demands of electricity for cooling throughout the year, and especially during summer months; (iii) the city needs to have readily available building model prototypes for both commercial and residential buildings in the DOE – Building Energy Codes Program's database (DOE, 2017b).

It is important to highlight that, as the experimentation phase of this research was coming to an end, the city of Miami and the surrounding region were already suffering dire consequences of Hurricane Irma, one of the hardest to hit the US. Such reality puts even more relevance to the location selected for this case study and the type of studies conducted in the later parts of this thesis.

[6] Performance Indicators (PIs) are quantifiable indicators that adequately represent a particular performance requirement (Augenbroe, 2011).

The building models in the DOE database were developed by the Pacific Northwest National Laboratory (PNNL), which were designed to be simulated in the EnergyPlus engine. This database provides a suite of prototype buildings that covers commercial buildings, mid- to high-rise residential buildings, single-family detached houses, and multi-family low-rise apartment buildings across all U.S. climate zones (DOE, 2017b).

The selected prototypes were created as to be code compliant with the International Energy Conservation Code – IECC (ICC, 2017), versions 2012 (residential) and 2015 (medium office and strip mall). For this test, the files are updated to the latest available version of EnergyPlus: V. 8.7.0 (DOE, 2017c).

For each selected PNNL prototype, an equivalent EPC (hourly version) model is created following the definition of inputs of the original PNNL's (.idf) files as close as possible, thus preserving the geometry of the building, the thermal properties of the whole envelope, and the simplified representation of the systems and their efficiencies.

The occupancy schedules and related energy end-use patterns are the ones already defined in the original PNNL prototypes, established with an hourly resolution.

Regarding distributed energy resources, the neighborhood model considers the option of having rooftop solar PV in several buildings and batteries for energy storage, both solutions that can be shared by the entire community and can be set up in different arrangements. These DER implementations are intended to represent modes of energy generation, energy storage, and the combination of both for providing energy interactions between buildings and their resources in a connected neighborhood.

The construction of the detailed community energy model, in face of all the hurdles and limitations discussed in the previous chapter, imposes a challenge on how to simulate multiples buildings with multiple DER interactions using EnergyPlus. To overcome these difficulties, we simulate each detailed building energy model separately in the EnergyPlus engine, and combine the hourly outputs as to represent the total electricity demand for the entire community throughout a typical year using the TMY3 climate dataset for Miami international airport. The outputs of these simulations are later used to draw the curves of observed discrepancies (later in this chapter identified as "model form uncertainty") between these detailed building models and their counterparts in the reduced order community model.

For the simulation of the reduced order community model, the preprocessing phase is not necessary, since all prototype-based building energy models can be simulated concurrently (co-simulated). In addition, the energy storage intelligence and the energy transaction modules can run seamlessly in the same computational platform. These characteristics provide enormous advantages in terms of modeling flexibility. Such benefits are fundamental for the neighborhood performance analyses and measures that are later investigated in this thesis.

It must be highlighted that, as a designed case, this virtual test bed eliminates all modeling issues related to input information. In this sense, all input ignorance is not relevant to this validation. The focus is on the energy outcomes for the designed virtual community, and how they are influenced by the deliberate model form reduction approach.

3.2 Model Comparison: EnergyPlus and EPC Calculator

Physics-based building energy models are used to simulate energy consumption from different building systems. As explained in 2.2.1, consumption due to lighting, equipment, appliances, plug-loads, and other miscellaneous uses do not usually require complex simulation methods since they are based on usage schedules. The main purpose of a building energy model is therefore to simulate the physical phenomena related to the heat balance of the considered thermal zone(s). Once the thermal needs of a building throughout the simulation period are known, it is possible to calculate the energy required by the (also modeled) HVAC system to cope with such cooling and heating needs. An important feature of the model is the way the HVAC system is modeled, i.e. whether the HVAC system's dynamic interaction with the building is modeled explicitly and concurrently, or as stand-alone system that merely delivers the thermal needs generated by the building. The latter case can take the simplest form in that we merely multiply aggregated thermal needs with a macro efficiency coefficient.

In section 2.2.3, we present EnergyPlus as the reference detailed building energy model and EPC calculator as the reduced order alternative for neighborhood-scale modeling. In this section, we compare the two simulation engines and describe the main reduction aspects that should be observed when going from the high-fidelity EnergyPlus to the simplified EPC calculator.

When comparing the two modeling approaches, we are interested in the methods used to represent the building as a physical entity, where we can mathematically translate

the physical phenomena that govern the heat transfer balance within the building, and hence solve the resulting mathematical equations.

3.2.1 Building Physical Representation and Heat Balance Calculation

To calculate the heat balance within a building zone it is necessary to understand and to quantify the heat dynamics occurring in that environment. This involves complex and overlapping phenomena such as thermal transmission by conduction, convection, and radiation, heat flow by ventilation, thermal energy storage, and internal and solar heat gains.

By discretizing the building components into a set of nodes, one can establish a more trackable physical representation through which these dynamics occur. Each node necessarily lumps the physical properties of the building component it represents. Therefore, the number of nodes and their spatial distribution dictate the resolution of the model.

By defining elements as the physical connection between nodes, it is possible to mathematically describe the heat dynamics happening within the building zone. This can be used as the core structure of a physics-based building thermal model, where the state variables can be tracked at the node level.

To illustrate this physical representation, we consider a building component (such as a wall, roof, or slab) discretized into *n* nodes as shown in Figure 15. θ_i are the nodes for which we want to track state variables, in this case temperatures. R_{i_i+1} is the thermal

resistance between nodes θ_i and θ_{i+1}. C_i are the capacitances associated with nodes θ_i and with their related mass and heat capacity.

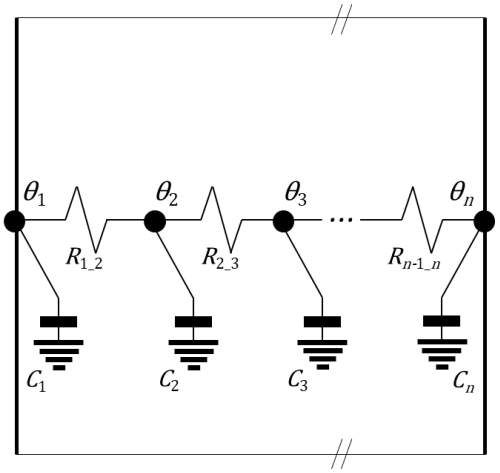

Figure 15 – Nodal representation of a building component with thermal resistance and thermal mass

If nodes θ_1 and θ_n are system boundaries where the state variables, in this case the temperatures, are known at each time-step, the equations that describe the heat transfer occurring between the connected nodes can be written in a matrix format, as follows:

$$\begin{bmatrix} 1 & 0 & 0 & \vdots & 0 \\ -\frac{1}{R_{1\_2}} & \frac{1}{R_{1\_2}}+\frac{1}{R_{2\_3}} & -\frac{1}{R_{2\_3}} & \vdots & 0 \\ 0 & -\frac{1}{R_{2\_3}} & \frac{1}{R_{2\_3}}+\frac{1}{R_{3\_4}} & \vdots & 0 \\ \cdots & \cdots & \cdots & \ddots & \cdots \\ 0 & 0 & 0 & \vdots & 1 \end{bmatrix} \begin{bmatrix} \theta_1 \\ \theta_2 \\ \theta_3 \\ \vdots \\ \theta_n \end{bmatrix} + \begin{bmatrix} C_1 & 0 & 0 & \vdots & 0 \\ 0 & C_2 & 0 & \vdots & 0 \\ 0 & 0 & C_3 & \vdots & 0 \\ \cdots & \cdots & \cdots & \ddots & \cdots \\ 0 & 0 & 0 & \vdots & C_n \end{bmatrix} \begin{bmatrix} \frac{\partial \theta_1}{\partial t} \\ \frac{\partial \theta_2}{\partial t} \\ \frac{\partial \theta_3}{\partial t} \\ \vdots \\ \frac{\partial \theta_n}{\partial t} \end{bmatrix} = \begin{bmatrix} f_1 \\ f_2 \\ f_3 \\ \vdots \\ f_n \end{bmatrix} \quad (1)$$

This formulation is defined, for short, as:

$$S\underline{\theta} + M\underline{\dot{\theta}} = \underline{f} \quad (2)$$

Where:

S = the stiffness matrix;

$\underline{\theta}$ = the vector of the state variables;

M = the mass matrix;

$\underline{\dot{\theta}}$ = derivative of $\underline{\theta}$, as a function of time;

$\underline{f}$ = the vector of inputs.

For the boundary nodes θ_1 and θ_n , where the temperatures are known for each time-step, the corresponding heat balance equation is overwritten by an assignment statement where f_1 and f_n assume the values of boundary temperatures. In the other nodes where temperature is unknown and there is heat load Φ_i (either from internal or solar heat gains), f_i assumes the values of Φ_i. For the other cases, f_i equals zero.

The above approach can easily be extended to all components and their interactions at the boundary, which occur mostly through convective and longwave radiative exchanges. The resulting set of ordinary differential equations (ODEs) can be solved analytically. However, the ODE dimensionality for a whole building can easily exceed 500. For a high-resolution model of a large building it can lead to multiples of that.

As the set of equations increase and the analytical solution becomes too hard to handle, a numerical integrator is required. Several numerical methods with different orders

of approximation can be used to solve this set of ODEs. The choice of the method determines the allowable simulation time-step size, and is based on the required accuracy, and the available computational power.

3.2.1.1 EnergyPlus approach

EnergyPlus is an integrated simulation engine, in which building, system, and plant models are solved simultaneously as depicted in Figure 16 (DOE, 2017d),

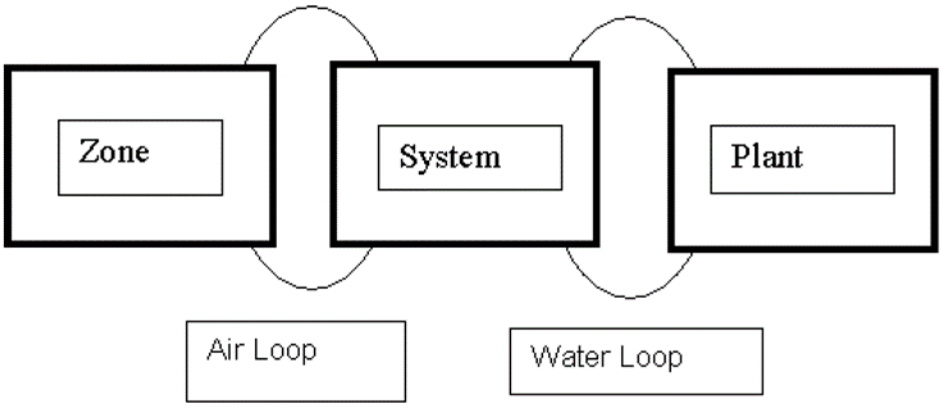

Figure 16 – Simultaneous simulation scheme of EnergyPlus (DOE, 2017d)

In the air loop, the "building zone" and the "air system" models are integrated for the calculation of energy and moisture balances for the zone air. EnergyPlus uses a predictor-corrector[7] approach to solve the resulting ordinary differential equations. This reflects the interactive and concurrent simulation of the building-HVAC pair.

[7] The heat load is assumed as a starting point to give a demand to the air system. Then a simulation of the air system provides the actual supply capability and the zone temperature is adjusted, if necessary (DOE, 2017d).

For a multiple-zone model, the zone air temperature needs to be calculated for each zone. The solution scheme for the heat balance at each zone air node follows Equation 3.

$$C_{air}\frac{d\theta_{air}}{dt} = \sum_{i=1}^{N_{sl}} \Phi_i + \sum_{i=1}^{N_{surfaces}} h_i A_i(\theta_{s,i} - \theta_{air}) + \sum_{i=1}^{N_{zones}} \dot{m}_i C_p\left(\theta_{air,i} - \theta_{air}\right) + \dot{m}_{inf} C_p(\theta_e - \theta_{air}) + \dot{m}_{sys} C_p(\theta_{sup} - \theta_{air}) \quad (3)$$

Where:

$C_{air}\frac{d\theta_{air}}{dt}$ = energy stored in zone air;

$\sum_{i=1}^{N_{sl}} \Phi_i$ = sum of the convective internal loads;

$\sum_{i=1}^{N_{surfaces}} h_i A_i\ (\theta_{s,i} - \theta_{air})$ = convective heat transfer from the zone surfaces;

$\sum_{i=1}^{N_{zones}} \dot{m}_i C_p\ (\theta_{air,i} - \theta_{air})$ = heat transfer due to interzone air mixing;

$\dot{m}_{inf} C_p(\theta_e - \theta_{air})$ = heat transfer due to infiltration of outside air;

$\dot{m}_{sys} C_p(\theta_{sup} - \theta_{air}) = \Phi_{sys}$ = air systems output;

$C_{air} = \rho_{air} C_p C_T$;

ρ_{air} = zone air density;

C_p = zone air specific heat;

C_T = sensible heat capacity multiplier[8].

In order to calculate the derivative term with respect to time, an approximation may be used. EnergyPlus uses a third order finite difference approach, shown in Equation 4.

[8] This value can be greater than 1.0 to increase the simulation stability by decreasing the zone air temperature deviations, or to try and account for the additional capacitance in the air loop (DOE, 2017d).

$$\left.\frac{d\theta_{air}}{dt}\right|_t \approx (\delta t)^{-1}\left(\frac{11}{6}\theta_{air}^{t} - 3\theta_{air}^{t-\delta t} + \frac{3}{2}\theta_{air}^{t-2\delta t} - \frac{1}{3}\theta_{air}^{t-3\delta t}\right) + O(\delta t^3) \qquad (4)$$

And the resulting zone temperature equation is calculated according to Equation 5.

$$\theta_{air}^{t} = \left[\sum_{i=1}^{N_{sl}} \Phi_i + \sum_{i=1}^{N_{surfaces}} h_i A_i \theta_{s,i} + \sum_{i=1}^{N_{zones}} \dot{m}_i C_p \theta_{air,i} + \dot{m}_{inf} C_p \theta_e + \dot{m}_{sys} C_p \theta_{sup} - \left(\frac{C_{air}}{\delta t}\right)\left(-3\theta_{air}^{t-\delta t} + \frac{3}{2}\theta_{air}^{t-2\delta t} - \frac{1}{3}\theta_{air}^{t-3\delta t}\right)\right] \qquad (5)$$
$$/ \left[\left(\frac{11}{6}\right)\left(\frac{C_{air}}{\delta t}\right) + \sum_{i=1}^{N_{surfaces}} h_i A_i + \sum_{i=1}^{N_{zones}} \dot{m}_i C_p + \dot{m}_{inf} C_p + \dot{m}_{sys} C_p\right]$$

This default approximation used in EnergyPlus is referred to as the "3rdOrder-Backward-Difference" method for the "Zone-Air-Heat-Balance-Algorithm" object.

The heat transfer through the building envelope, as depicted in Figure 17, involves conduction and convection. Convective heat transfer occurs between the external environment node and the nodes at external surfaces, as well as between the zone air nodes and the nodes at internal surfaces. The conduction through the walls is calculated in EnergyPlus by a "Conduction Transfer Function" solution, which employs a state-space solution method.

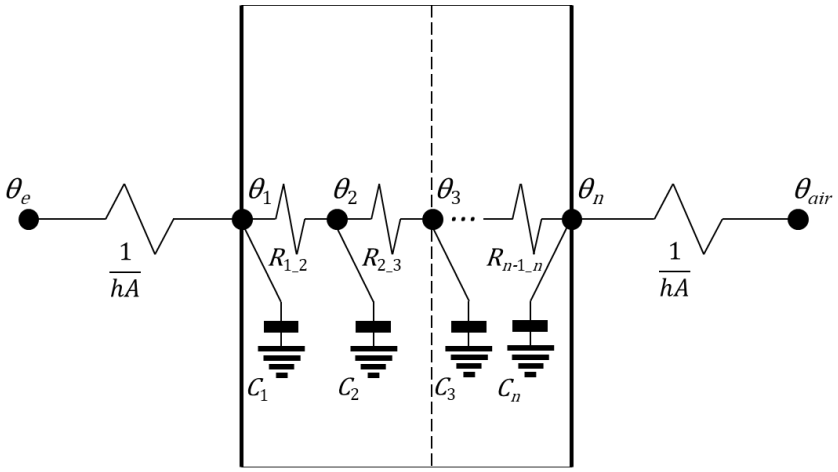

Figure 17 – Conduction through a wall with *n* nodes and convection at both sides

The parameters of thickness, conductivity, density, and specific heat are specified for each material layer of the building envelope. EnergyPlus divides every layer into between 6 and 18 nodes, plus nodes at the interface between two layers (DOE, 2017d).

The heat transfer through windows is calculated according to Equation 6, where window U-values include interior and exterior surface heat transfer coefficients (film resistances), as well as the resistance of the bare window itself, without thermal mass.

$$\frac{1}{U} = R_{e,w} + R_{l,w} + R_{air,w} \tag{6}$$

Where:

U = window conductance (U-value) with convective films;

$R_{e,w}$ = the resistance of the exterior film, occurring between the external environment node and the node at the external surface of the window;

$R_{l,w}$ = the conductive resistance of the bare window (without the film coefficients), occurring within the length of the window;

$R_{air,w}$ = the resistance of the interior film, occurring between the zone air node and the node at the internal surface of the window.

With regards to solar heat gains, EnergyPlus calculates the absorption of direct and diffuse solar in the external nodes of the opaque surfaces, as well as the gains due to transmission through the windows. In the latter case, the model calculates the distribution of short-wave radiation (beam solar and diffuse solar) inside each thermal zone, and the amount that is absorbed on the internal surfaces and the amount that is transmitted back to the external environment.

3.2.1.2 EPC Calculator approach

The simple hourly calculation method used in the EPC calculator is based on the methodology described in ISO 13790:2008, in which the building is represented by a resistance-capacitance lumped model with five resistances and one capacitance (ISO, 2008). In this approach, as illustrated in Figure 18, the whole building is reduced into only three nodes. The zone air node (θ_{air}) lumps all internal zones of the building. The lumped envelope is divided into the mass node (θ_m), the only one with thermal mass, and the internal surface node (θ_s).

The interaction of the building with the external environment occurs by coupling these nodes with the external environment node (θ_e), and the air supply node (θ_{sup}).

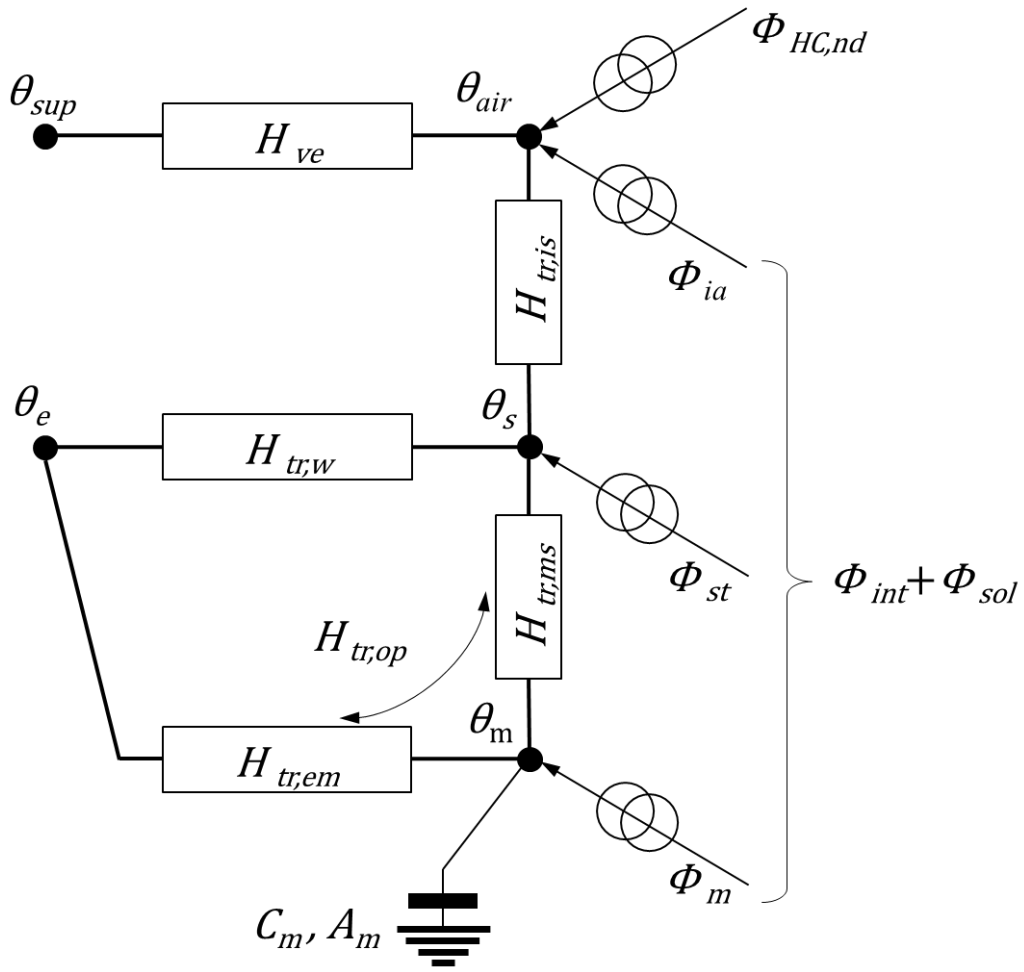

Figure 18 – 5R1C thermal network used in EPC

In this simplified nodal network, the heat transfer between nodes (H) is defined as follows.

H_{ve} is the heat transfer by ventilation, which directly connects the zone air node (θ_{air}) to the supply air node (θ_{sup}).

Heat transfer by transmission through the envelope occurs between the external environment node (θ_e) and the internal surface node (θ_s). It is separated into the window

portion ($H_{tr,w}$), with zero thermal mass, and the opaque portion ($H_{tr,op}$), with thermal mass. $H_{tr,op}$ is split into $H_{tr,em}$ and $H_{tr,ms}$, where $H_{tr,em}$ connects the external environment node (θ_e) with the mass node (θ_m), and $H_{tr,ms}$ connects the mass node (θ_m) with the internal surface node (θ_s). The thermal mass is represented by a single thermal capacity, C_m, located between $H_{tr,ms}$ and $H_{tr,em}$.

Finally, $H_{tr,is}$ is the coupling conductance between the internal surface node (θ_s) and the zone air node (θ_{air}).

Figure 19 illustrates the thermal transmittance scheme that takes place through the entire opaque envelope with convection at both sides. This is a very simplified discretization when compared to the approach of the detailed building model, as previously depicted in Figure 17.

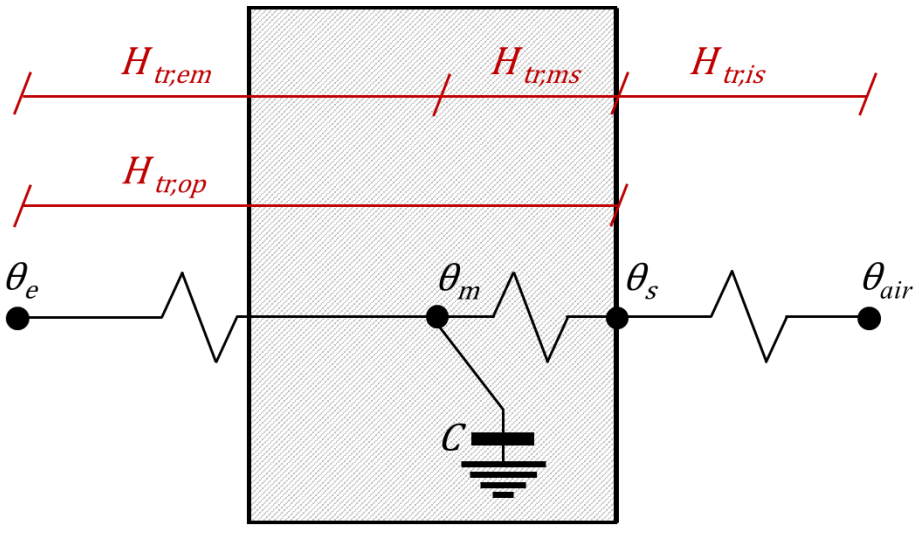

Figure 19 – Thermal transmittance scheme through the entire opaque envelope with convection at both sides (adapted from Gorrino, 2011)

$H_{tr,op}$ is calculated through Equation 7.

$$H_{tr,op} = \sum_{i} U_{op,i}\, A_{op,i} \tag{7}$$

Where:

$U_{op,i}$ = the thermal transmittance of the opaque surface type *i* of the building envelope, expressed in W/(m^2·K);

$A_{op,i}$ = the total area of opaque surface type *i* of the building envelope, expressed in square meters.

Since $H_{tr,op}$ is split into $H_{tr,em}$ and $H_{tr,ms}$, it is necessary to calculate these two components. $H_{tr,ms}$ is calculated first, through Equation 8.

$$H_{tr,ms} = h_{ms}\, A_m \tag{8}$$

Where:

h_{ms} = the heat transfer coefficient between the building mass (θ_m) and the surface node (θ_s). h_{ms} is fixed at 9.1 W/(m^2·K);

A_m = the effective mass area, expressed in square meters; A_m is calculated as a function of the overall heat capacity of the building, in the form $A_m = \varsigma\, Af$, where ς varies from 2.5 to 3.5 according to the building heat capacity class.

Then, $H_{tr,em}$ is calculated from the difference between $H_{tr,op}$ and $H_{tr,ms}$, as defined in Equation 9.

$$H_{tr,em} = 1/\left(\frac{1}{H_{tr,op}} - \frac{1}{H_{tr,ms}}\right) \quad (9)$$

The coupling conductance $H_{tr,is}$, between the air node (θ_{air}) and the surface node (θ_s) is calculated through Equation 10,

$$H_{tr,is} = h_{is}\, A_t \quad (10)$$

Where:

h_{is} = the heat transfer coefficient between the air node (θ_{air}) and the surface node (θ_s). h_{is} is fixed at 3.45 W/(m^2·K).

A_t = the area of all surfaces facing the building zone, equal to $\Lambda_{at}\, A_f$, expressed in square meters.

A_f = the conditioned floor area, expressed in square meters.

Λ_{at}= the dimensionless ratio between A_t and A_f; Λ_{at} is assumed to be equal to 4.5.

The coupling conductance through the windows ($H_{tr,w}$) is calculated through Equation 11.

$$H_{tr,w} = \sum_i U_{w,i}\, A_{w,i} \quad (11)$$

Where:

$U_{w,i}$ = the thermal transmittance of the glazing surface type i of the building envelope, expressed in W/(m^2·K);

$A_{w,i}$ = the total area of glazing surface type *i* of the building envelope, expressed in square meters.

Solar (Φ_{sol}) and internal heat gains (Φ_{int}) are distributed in the form of Φ_{ia} over the zone air node (θ_{air}), in the form of Φ_{st} over the internal surface node (θ_s), and in the form of Φ_m over the mass node (θ_m), as depicted in Figure 18. These are calculated through Equations 12 to 14.

$$\Phi_{ia} = 0.5\Phi_{int} \tag{12}$$

$$\Phi_m = \frac{A_m}{A_t}(0.5\Phi_{int} + \Phi_{sol}) \tag{13}$$

$$\Phi_{st} = \left(1 - \frac{A_m}{A_t} - \frac{H_{tr,w}}{9.1A_t}\right)(0.5\Phi_{int} + \Phi_{sol}) \tag{14}$$

With this mathematical formulation, all parameter and load values are defined at any given hour, except the heating or cooling need ($\Phi_{HC,nd}$), which must be calculated.

The numerical solution used in this approach is based on a Crank-Nicolson scheme considering a time-step of one hour. With such numerical approximation, the temperature θ_m^t is calculated at the end of the time-step from the previous value $\theta_m^{t-\delta t}$, through Equation 15.

$$\theta_m^t = \frac{\left\{\theta_m^{t-\delta t}\left[(C_m/3600) - 0.5 \times (H_{tr,3} + H_{tr,em})\right] + \Phi_{mtot}\right\}}{\left[(C_m/3600) + 0.5 \times (H_{tr,3} + H_{tr,em})\right]} \quad (15)$$

Where:

$$\Phi_{mtot} = \Phi_m + H_{tr,em}\,\theta_e + \frac{H_{tr,3}\langle\Phi_{st} + H_{tr,w}\,\theta_e + H_{tr,1}\left\{\left[(\Phi_{ia} + \Phi_{HC,nd})/H_{ve}\right] + \theta_{sup}\right\}\rangle}{H_{tr,2}} \quad (16)$$

$$H_{tr,1} = \frac{1}{1/H_{ve} + 1/H_{tr,is}} \quad (17)$$

$$H_{tr,2} = H_{tr,1} + H_{tr,w} \quad (18)$$

$$H_{tr,3} = \frac{1}{1/H_{tr,2} + 1/H_{tr,ms}} \quad (19)$$

For any time-step, the average temperatures at the building nodes are given by Equations 20 to 22.

$$\theta_m = (\theta_m^t + \theta_m^{t-\delta t})/2 \quad (20)$$

$$\theta_s = \frac{\left\{H_{tr,ms}\,\theta_m + \Phi_{st} + H_{tr,w}\,\theta_e + H_{tr,1}\left[\theta_{sup} + (\Phi_{ia} + \Phi_{HC,nd})/H_{ve}\right]\right\}}{(H_{tr,ms} + H_{tr,w} + H_{tr,1})} \quad (21)$$

$$\theta_{air} = \frac{(H_{tr,is}\,\theta_s + H_{ve}\,\theta_{sup} + \Phi_{ia} + \Phi_{HC,nd})}{(H_{tr,is} + H_{ve})} \quad (22)$$

Since this is a single zone building model, the different zones of a building with different characteristics must be summarized into a single set of inputs. For this, weighted average values based on conditioned floor area are used.

Equation 23, for example, is used to find the heating set point of the single-zone representation, based on different set-points of a multiple-zone configuration. The averaging is done on an hourly basis.

$$\theta_{int,H,set} = \frac{\sum_s A_{f,s}\theta_{int,s,H,set}}{\sum_s A_{f,s}} \quad (23)$$

Where:

$\theta_{int,s,H,set}$ = the set-point temperature for heating of space s;

$A_{f,s}$ = the conditioned floor area of space s.

The same is done for cooling set-points, and for the other building usage inputs, such as occupancy, appliances, and lighting schedules. In this manner, all heat gains are lumped into the single-zone air node.

3.2.2 HVAC System Representation

Once the building thermal model is mathematically resolved, there remains the necessity to model the HVAC system that will cope with the required heating and cooling

needs. The reduced order and the detailed models also diverge in the way this is done, as briefly explained below.

3.2.2.1 EnergyPlus approach

As mentioned before, energy plus simulates the air zone heat balance and the HVAC system operation simultaneously, in a loop-based interactive formulation. Nevertheless, air recirculation and system controls make the algebraic solution impossible to be solved directly. Therefore, EnergyPlus uses numerical strategies such as iterative methods, and partial decoupling for solving the HVAC system model.

The systems are represented at a fairly high level of detail, based on a mix of thermodynamic and empirically based relationships, sometimes reflecting the actual sequencing of certain equipment as defined in factory manuals. This fact renders the HVAC system modules rather opaque and in some cases more detailed than necessary for a predictive simulation which by necessity is based on idealizations of the actual building and its HVAC systems.

3.2.2.2 EPC Calculator approach

In the EPC calculator, the HVAC system simulation is completely uncoupled from the building thermal simulation. The calculator considers that all the heating or cooling needs are fully supplied by the HVAC system at every hour.

The system heat losses are indicated via an overall system efficiency. In this case, the conversion can be found through Equations 24 and 25.

$$Q_{H,sys} = \frac{Q_{H,nd}}{\eta_{H,sys}} \tag{24}$$

$$Q_{C,sys} = \frac{Q_{C,nd}}{\eta_{C,sys}} \tag{25}$$

Where:

$Q_{H/C,sys}$ = the energy use for the heating or cooling system including system losses;

$Q_{H/C,nd}$ = the energy need for heating or cooling, serviced by the considered heating system;

$\eta_{H/C,sys}$ = the overall system efficiency for the heating or cooling system, including generation, electronics, transport, storage, distribution and emission losses.

This simplification not only reduces the simulation overload, but also reduces significantly the amount of input data required to run the building models.

For every HVAC system type, EPC also calculates the electricity consumption from auxiliary systems, i.e. pumps and fans. This is done by associating every system type with a factor that is used to calculate the auxiliary consumption. This HVAC type specific factor was pre-calibrated on an average over many buildings, climates and situations. It is well recognized that it is a crude approximation that can severely over or underestimate the auxiliary system consumption. It is not uncommon to perform a case specific calibration step to determine the auxiliary system consumption factor before using EPC calculator. For some HVAC types, the same should be done for the COP factor in order to increase the

overall accuracy of the HVAC consumption which can be considered the Achilles heel of the EPC calculator.

3.3 Case Study: Miami Community Energy Model

As explained earlier, this case study comprises a community with ten buildings. Among them, eight residential buildings are considered identical for the sake of the simulation. They are, therefore, represented by a single building energy model, whose outcomes are multiplied by eight. One medium office and one retail strip mall have one separate representative building energy model each. With this configuration, the whole community is constructed with only three building model prototypes.

The building models are simulated both in EnergyPlus and in the EPC Calculator, and the deviations on the outputs due to model form simplification are observed.

Different DER options with similar costs are tested in the reduced order community model to find the order of preference in terms of their ability to reduce the occurrence of high electricity demand peaks during critical days.

Hence, the ranking of the DER alternatives under well-defined performance indicators are used as a rational test to verify whether and how disturbances to the reduced order model, including model form simplification, can affect the reliability of the simulations.

3.3.1 PNNL prototypes

The first EnergyPlus-ready building prototype selected from the PNNL suite is a low-rise multi-family residential building. It is a 2,000 m^2 three-story building founded on a concrete slab, with an air source heat pump for heating and cooling. As depicted in Figure 20, the building has 18 apartments, each one represented by a different zone in the original PNNL prototype.

For this study, all day types in the original idf files are reduced to regular week days and weekends, thus eliminating special days as well as daylight saving time. This is done to decrease the noise in the simulation outcomes and to control for the variables of interest in the virtual experiment.

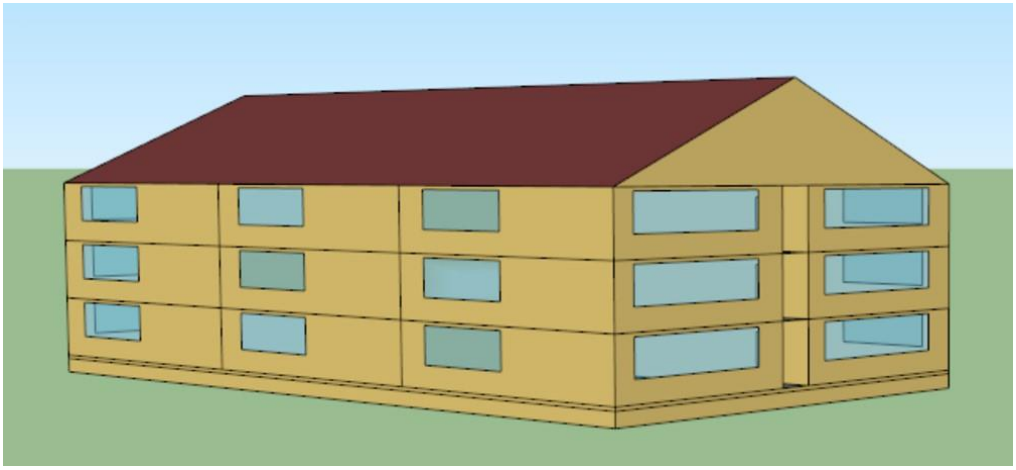

Figure 20 – Multi-family Residential Building Prototype

The other building prototype is a three-story medium office building with 4,980 m^2 of gross floor area, as showed in Figure 21. This PNNL prototype has 18 building zones that are divided according to building internal location. As before, all days are adjusted to week days and weekends only, without special days and daylight saving time.

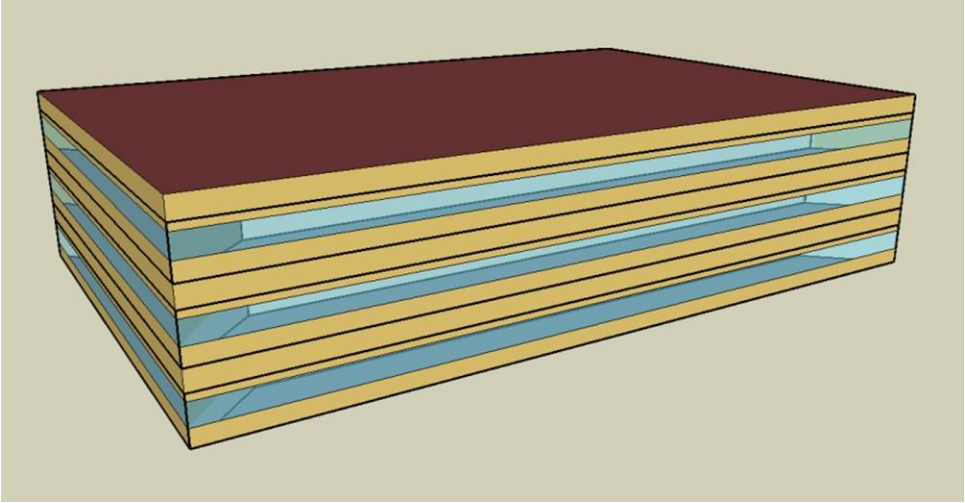

Figure 21 – Medium Office Building Prototype

The third building, a retail strip mall, is represented by a one-story building prototype with 10 zones, each one related to a different retail store (Figure 22). The stores range between three types, each one having its own pattern of electricity consumption. In the same fashion, days and time are adjusted to regular week days and weekends.

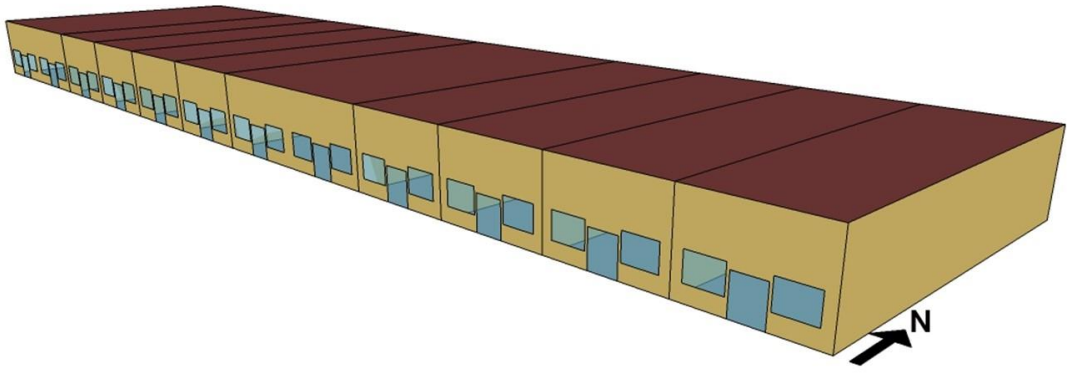

Figure 22 – Retail Strip Mall Building Prototype

3.3.2 Reduced Order Building Models

For each PNNL prototype prepared for EnergyPlus, an equivalent EPC building model is created. The inputs used in the EPC models are retrieved from the idf files, as to maintain the envelope fidelity with regards to orientation, dimensions, window-to-wall ratios, and U-values. In each created reduced order building model, the multiple zones of the counterpart detailed model are translated into a single zone that holds the weighted average pattern of usage drawn from all zones. This enables the definition of representative general week-days and weekends schedules for occupancy, lighting usage, and appliances usage for each reduced order building model.

As per the original PNNL prototypes, the sources of energy for thermal end-uses for cooling, heating, and domestic hot water – DHW vary according to Table 3. Therefore, cooling demands impact electricity consumption in all buildings belonging to the community. The outcomes of energy demand from end-uses supplied by natural gas are not considered in the community energy simulations, since we are targeting overall electricity consumption.

Table 3 – Sources of Energy for End-Uses

Building Type	**Sources of Energy**		
	Cooling	**Heating**	**DHW**
Residential	Electricity	Electricity	Electricity
Medium Office	Electricity	Natural Gas	Natural Gas
Retail Strip Mall	Electricity	Natural Gas	Electricity

It is important to clarify that the pattern of DHW usage defined in the original PNNL residential prototype follows a one-case scenario of summation of individual uses

of different domestic appliances at specific hours, which results in a unique curve of DHW electricity demand with very high spikes at isolated hours and low consumption at other hours. When we consider a collection of eight residential buildings totaling 128 apartments, it becomes reasonable to assume that such spikes will be somewhat levelized. To address this issue and avoid unrealistic peak demands for DHW in specific hours, the DHW consumption for the residential buildings is pre-processed. For that, we average the original DHW calculated by EnergyPlus for one year, at every three hours, so that the spikes are smoothed in those intervals.

The resulting DHW outcomes are then added to the other end-use calculations in both EPC and EnergyPlus models, so that they do not affect the overall discrepancies between the two model representations of the residential building.

It is important to note that this adjustment could be pursued by the estimation of realistic DHW consumption patterns based on stochastic occupant models. Nevertheless, our simple approach achieves the same end goal and is therefore adequate for the validation exercise.

Regarding cooling loads and respective energy consumption, all EPC building models have their inputs for cooling COP – for full and partial loads (COP100, COP75, COP50, COP25) – calibrated using the cooling outcomes of the correspondent EnergyPlus. This is done to pursue the maximum approximation of outcomes of the limited system's representation of EPC to the detailed calculations held in the EnergyPlus models.

Figure 23 to Figure 28 show the electricity consumption by end-use for each building type in typical winter and summer days.

Residential building end-use electricity consumption: **Lighting**

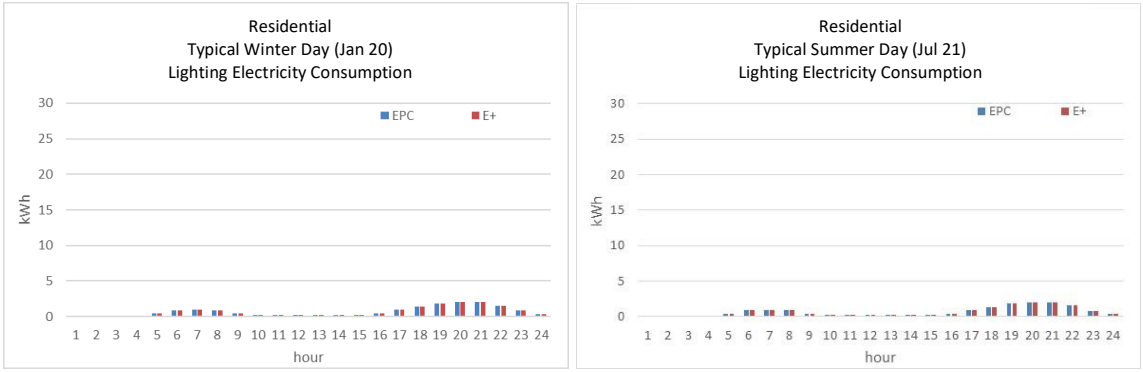

Residential building end-use electricity consumption: **Appliances**

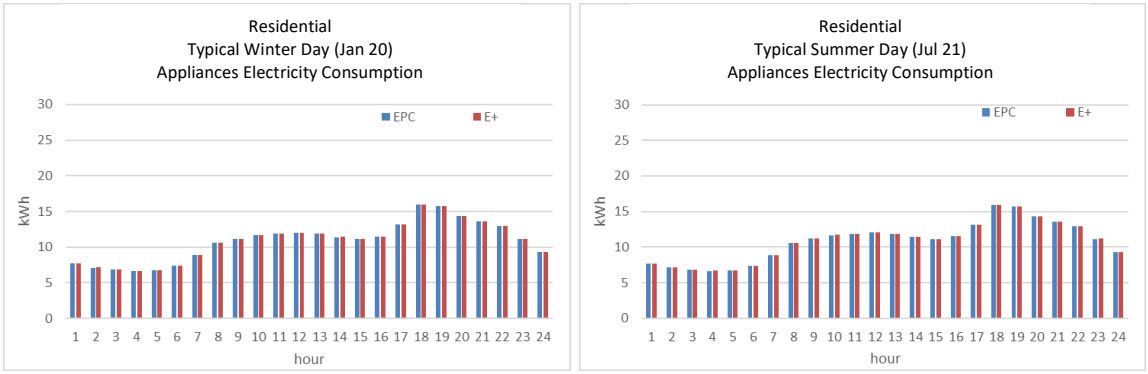

Residential building end-use electricity consumption: **Cooling**

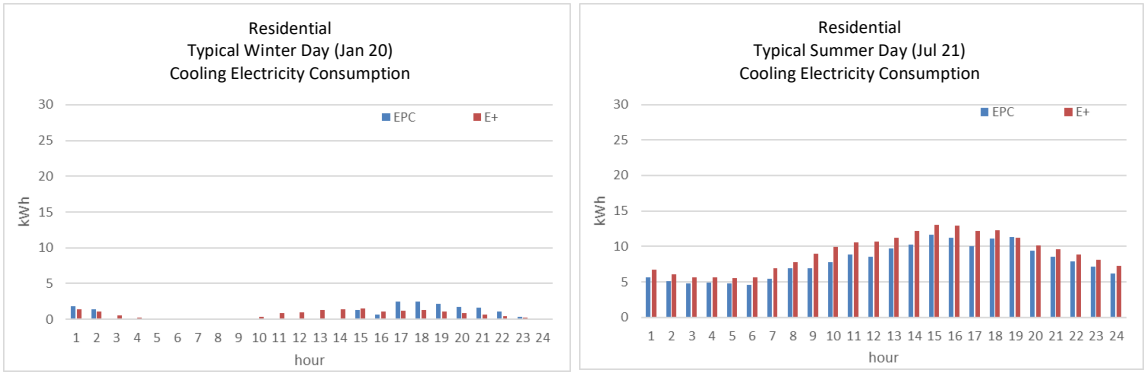

Figure 23 – Residential Building Electricity Consumption by End-Use in Typical Days: lighting, appliances, cooling

(left: typical winter day; right: typical summer day)

Residential building end-use electricity consumption: **Fans**

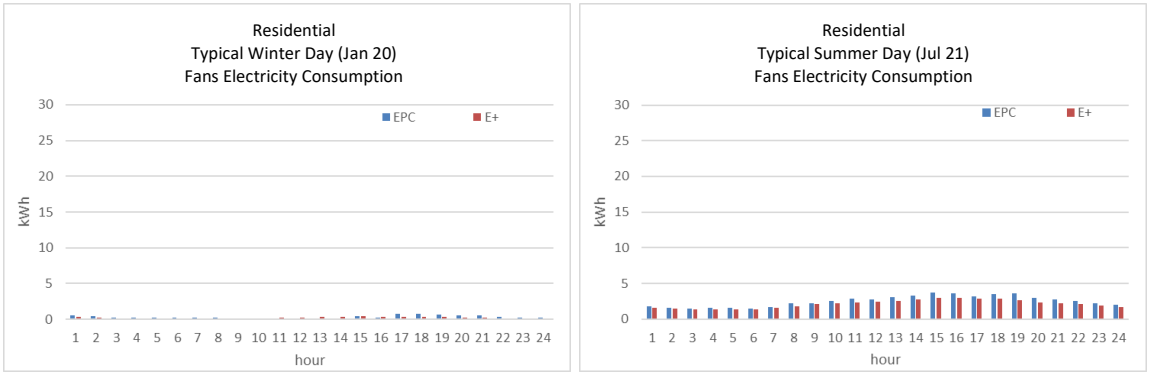

Residential building **TOTAL** electricity consumption

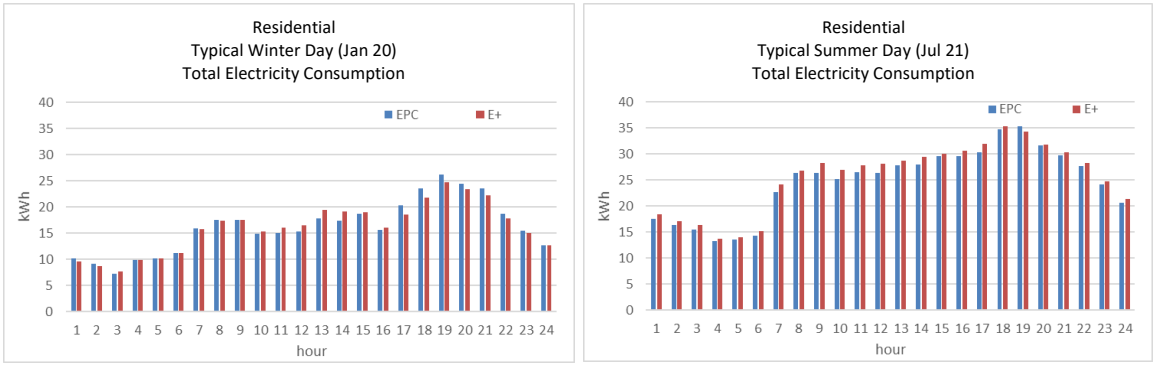

Figure 24 – Residential Building Electricity Consumption by End-Use in Typical Days: fans, total

(left: typical winter day; right: typical summer day)

Medium office end-use electricity consumption: **Lighting**

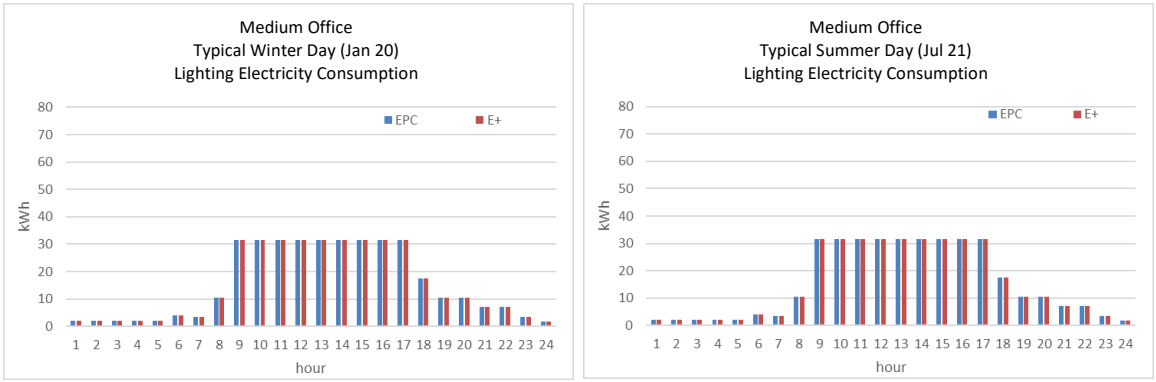

Medium office end-use electricity consumption: **Appliances**

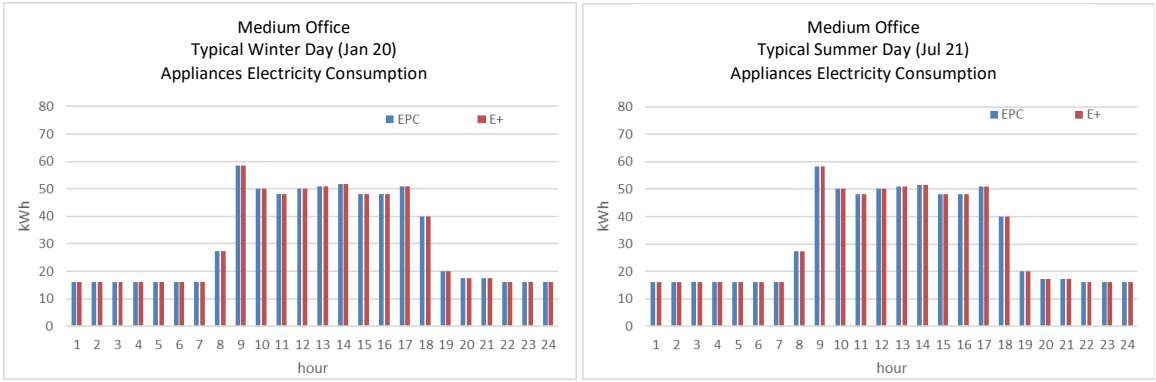

Medium office end-use electricity consumption: **Cooling**

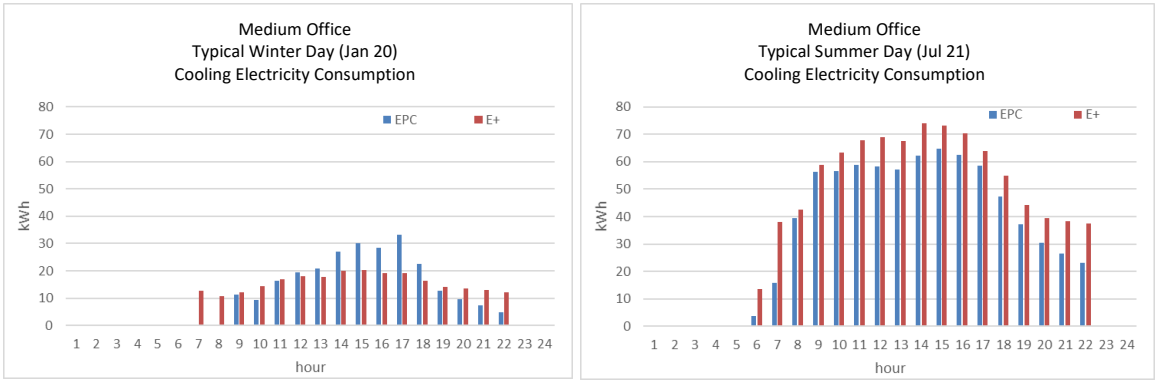

Figure 25 – Medium Office Building Electricity Consumption by End-Use in Typical Days: lighting, appliances, cooling

(left: typical winter day; right: typical summer day)

Medium office end-use electricity consumption: **Fans**

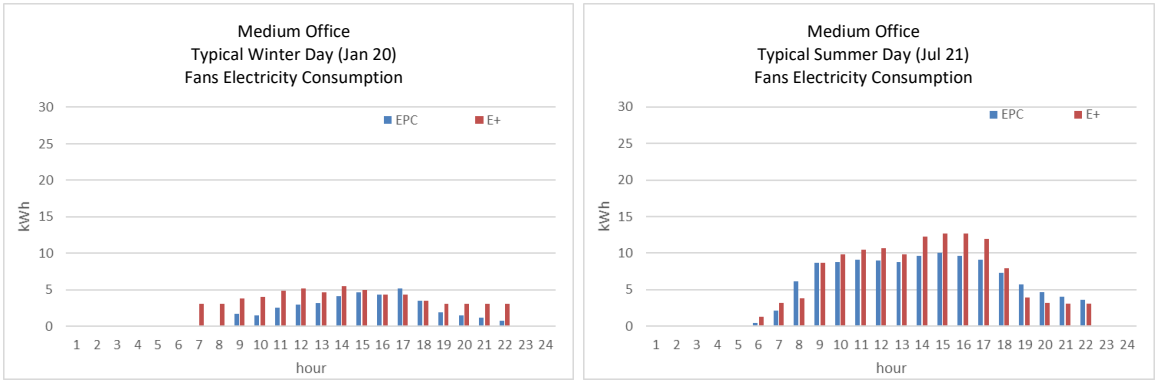

Medium office **TOTAL** electricity consumption

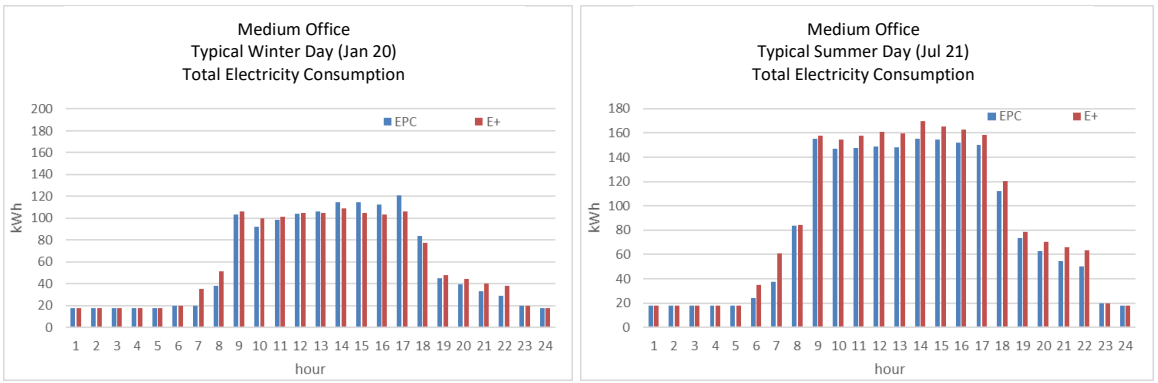

Figure 26 – Medium Office Building Electricity Consumption by End-Use in Typical Days: fans, total

(left: typical winter day; right: typical summer day)

Retail strip mall end-use electricity consumption: **Lighting**

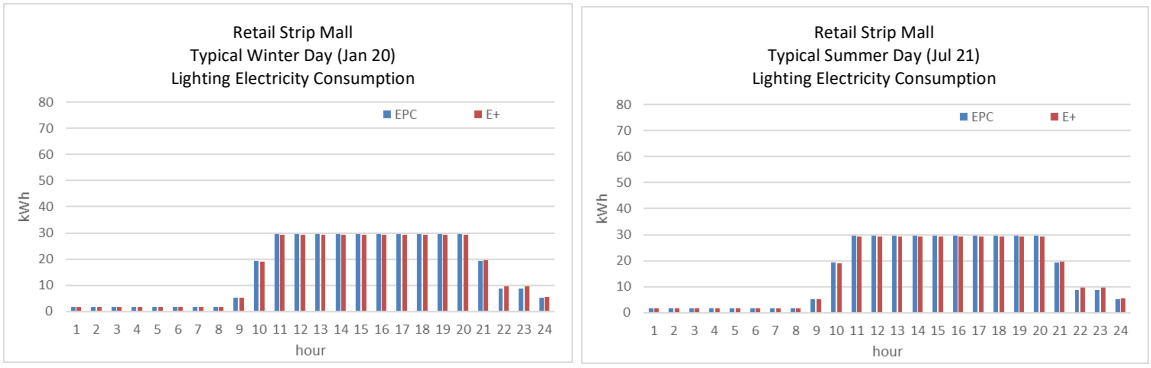

Retail strip mall end-use electricity consumption: **Appliances**

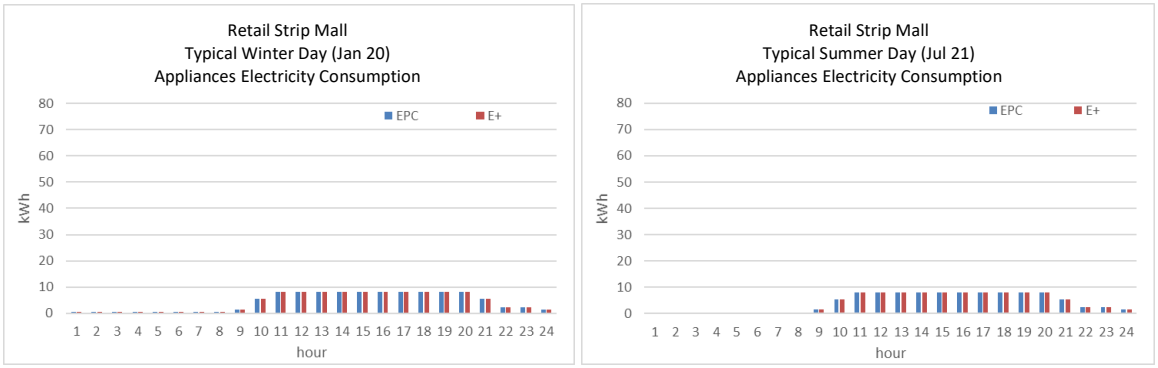

Retail strip mall office end-use electricity consumption: **Cooling**

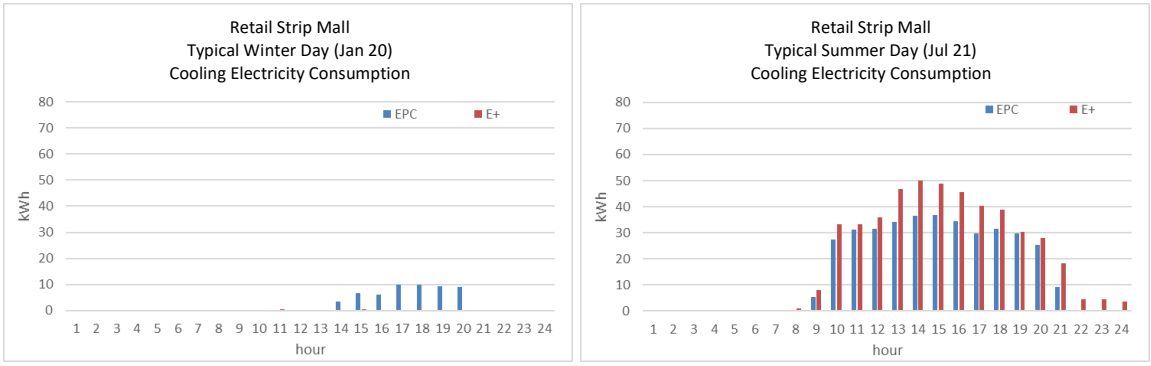

Figure 27 – Retail Strip Mall Building Electricity Consumption by End-Use in Typical Days: lighting, appliances, cooling

(left: typical winter day; right: typical summer day)

Retail strip mall end-use electricity consumption: **DHW**

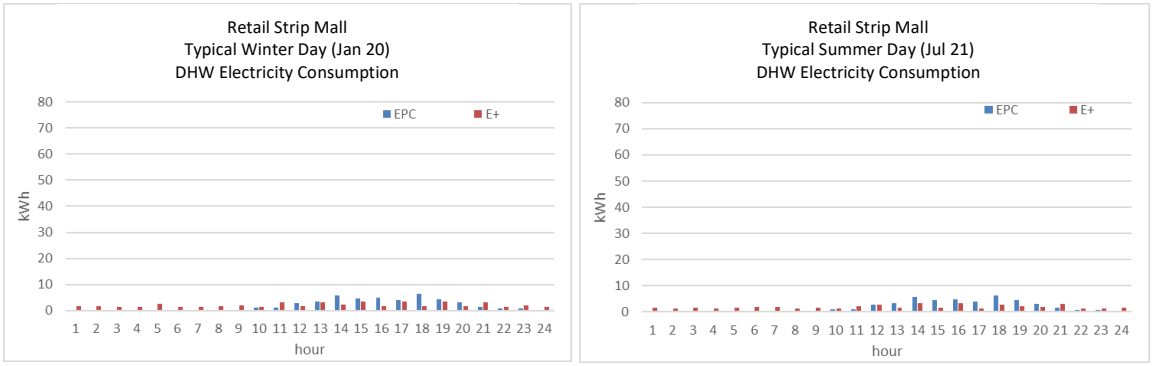

Retail strip mall end-use electricity consumption: **Fans**

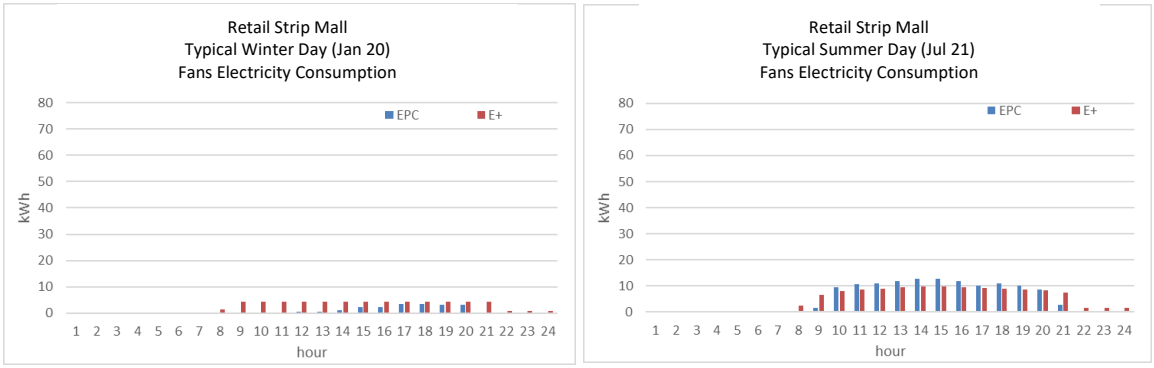

Retail strip mall **TOTAL** electricity consumption

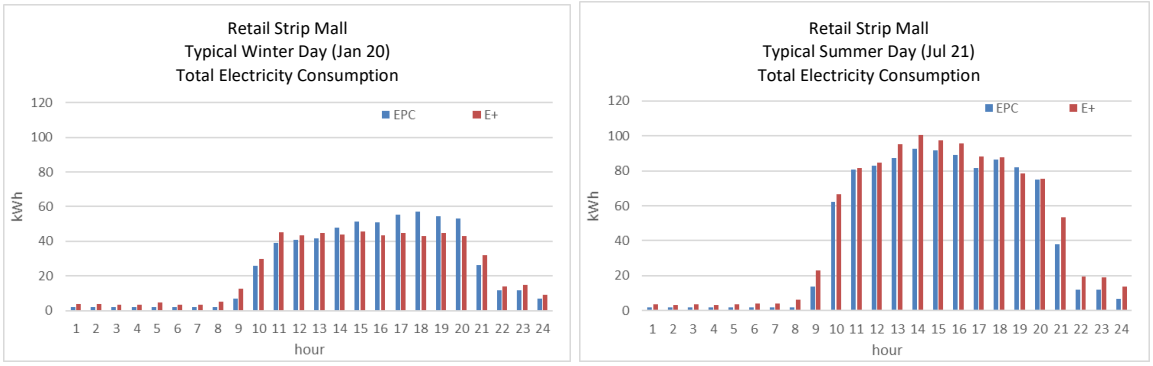

Figure 28 – Retail Strip Mall Building Electricity Consumption by End-Use in Typical Days: DHW, fans, total

(left: typical winter day; right: typical summer day)

From Figure 23 to Figure 28, we observe that our reduced order EPC building models generate electricity demands by end-use that are very close to the ones generated by the correspondent EnergyPlus models, being virtually identical for lighting and appliances. As expected, there are some discrepancies in the electricity demand for cooling, due to limitations in the reduced order models for representing both the internal thermal needs and the cooling systems themselves. However, we must highlight that those figures illustrate extreme situations (winter and summer heights) for which the electricity demand for cooling in the EPC models are only slightly higher or lower, respectively, than the ones in the higher order models. Therefore, we can expect that for non-extreme days those discrepancies would be even less significant.

In any case, the total electricity consumption per building type on those extreme days are very similar in terms of both pattern and magnitude.

By putting together the total electricity consumption in an entire year for each building type, calculated from both modeling tools, we can compare the discrepancies on the output figures at the hourly resolution. The curves depicted in Figure 29 are derived from this comparison. These are the basis for the model form uncertainties investigated in section 3.4.2.3.

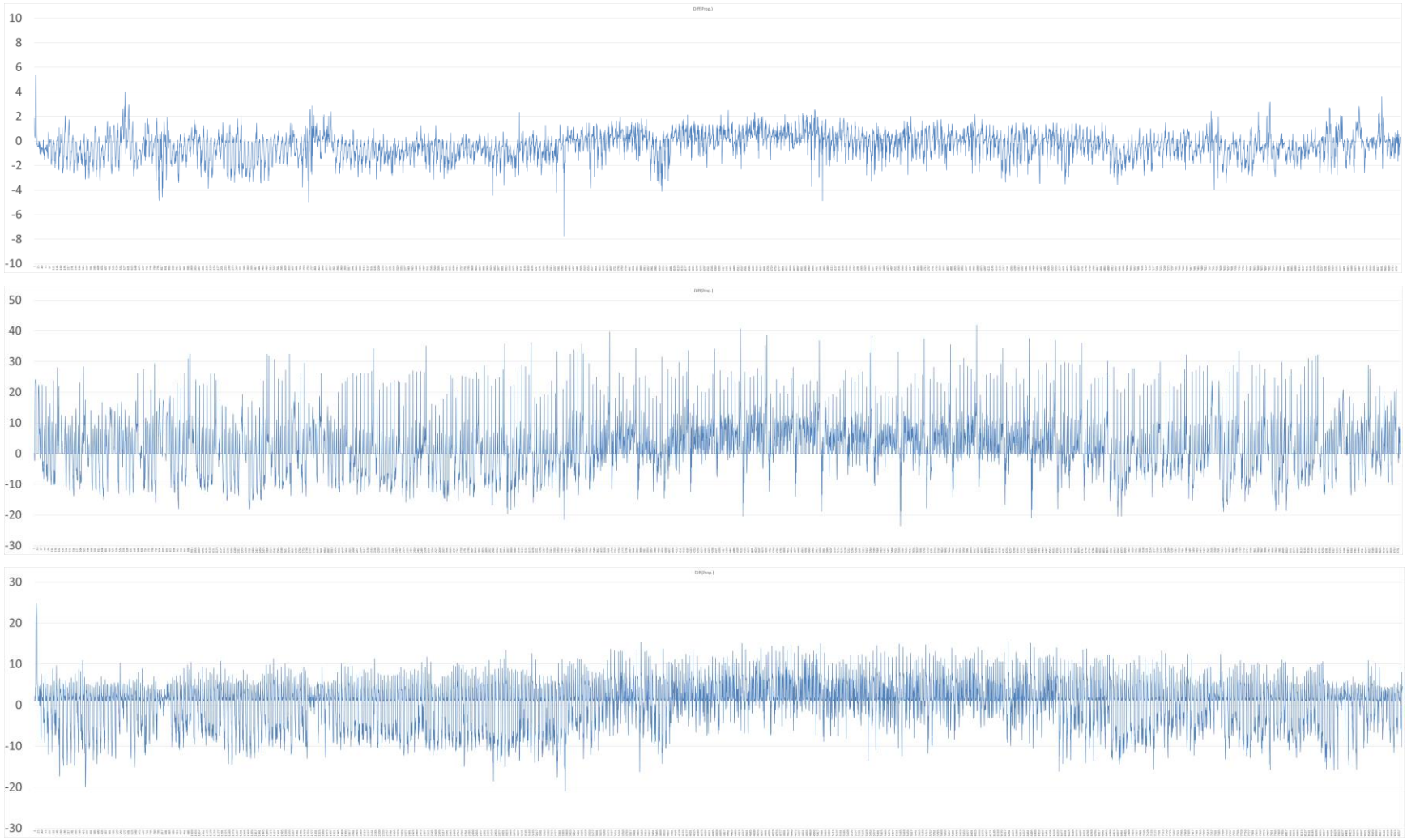

Figure 29 – Observed discrepancies for total hourly electricity consumption (kWh) for each building type in one year (top: residential building; middle: medium office; bottom: retail strip mall)

3.3.3 Comparison between Community Energy Models

Using the same extreme days for winter and summer, we can compare more closely the total hourly electricity consumption for the entire collection of buildings according to the outcomes of the reduced order and the higher order models. As depicted in Figure 30, the comparison of hourly values for extreme days show great similarity in both pattern and magnitude.

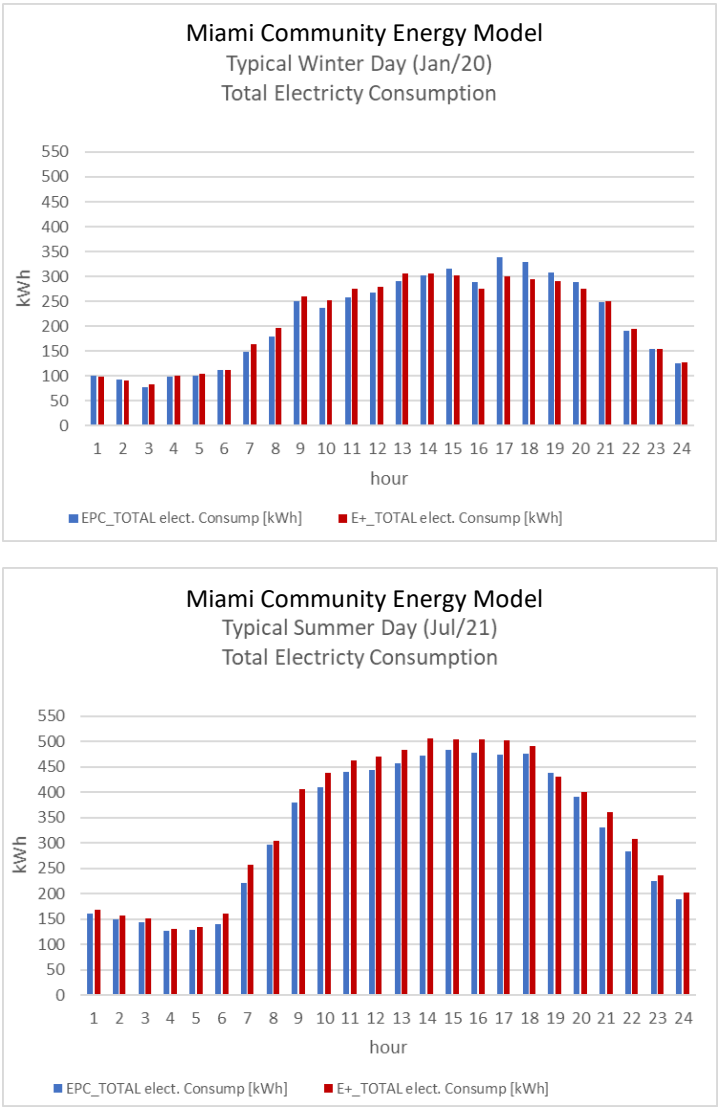

Figure 30 – Total hourly electricity consumption for the collection of buildings (top: typical winter day; bottom: typical summer day)

To have a more comprehensive comparison between the two modeling approaches, we use the annual load duration curve – LDC as a means for constructing a performance indicator. Figure 31 presents the LDC constructed from the outcomes of both modeling approaches. The horizontal axis indicates the total number of hours in a year for which the electricity load (kWh) is exceeded.

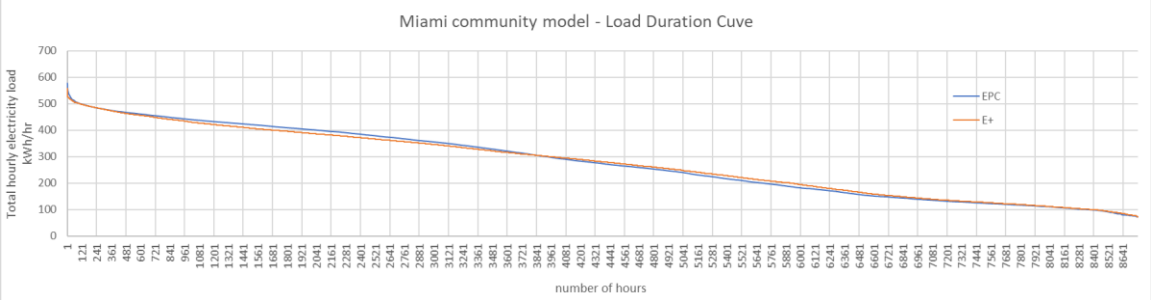

Figure 31 – Load Duration Curves for the Miami community model: total hourly loads (red: values from EnergyPlus models; blue: values from EPC models)

It is relevant to note that the two LDCs are nearly identical, hinting that the two sets of outputs apparently have great similarity. However, we must acknowledge that the LDC collapses all dynamic effects into a surrogate measure. For instance, if we have a large random error the LDC will still show nearly identical except at the very top, which is the most sensible part of the curve.

With these considerations, a performance indicator (*PI*_1) is defined according to Equation 26, which can be used to investigate the impacts of the discrepancies between the models. For reference, *PI*_1 before any DER implementation gives 481 for the EnergyPlus outcomes and 483 for the EPC_NHood outcomes.

*PI*_1 is also used to verify the effects of implementation of the DER alternatives proposed in the next section.

$$PI\_1 = 0.6 \times P98^{th}[\text{LCD}] + 0.4 \times P95^{th}[\text{LCD}] \quad (26)$$

Where:

$P98^{th}$[LCD] = 98th percentile of LCD, or the value below which 98% of loads fall;

$P95^{th}$[LCD] = 95th percentile of LCD, or the value below which 95% of loads fall.

3.3.4 DER Alternatives

Three options of distributed energy resources are considered for reducing peak loads, as measured by *PI*_1, in the Miami community energy model. They are listed in Table 4, and include solutions for solar generation (PV), energy storage (battery), and the combination of those.

For simplicity, we are assuming that all alternatives have the same cost and similar implementation conditions. Therefore, the resulting energy performance of the community under each alternative is the sole object of investigation.

Table 4 – DER alternatives considered in the validation exercise.

DER alternatives	
Option 1	PV
Option 2	Battery
Option 3	PV+battery

To render these assumptions reasonable, a market value of Rooftop PV is calculated for the suitable roof areas of the entire collection of residential buildings. This value is taken as the reference investment cost, and represents DER option 1 (PV). The excess generated energy in any given time, if any, is sold back to the grid at the avoided cost tariff. For the cost of the PV systems, a life cycle of 20 years is considered.

Table 5 – DER option 1 – solar generation

Photovoltaic panels (PV)	
Total PV area (m^2)	2,080
Peak power coefficient (kW/m^2)	0.15
Net Present Cost - NPC (US$)	**$858,000**

We assume that the batteries involved in options 2 and 3 have a life cycle of 5 years. To size these options, we consider that their total cost should not deviate from +/- 1% of total cost of option 1, so they could be considered all cost-equivalent.

Option 2 consists of a pack of stationary batteries serving the neighborhood. The batteries are used to store energy during off-peak periods and release energy back to the buildings during on-peak hours.

An optimization algorithm is applied on EPC_Nhood to find the best discharge scheme for the pack of batteries, by varying the discharge hours and discharge rate to minimize *PI*_1, but constraining the cost to +/- 1% of the total cost of option 1. The resulting specification of DER option 2 is presented in Table 6.

Table 6 – DER option 2 – energy storage

Energy Storage (Battery)	
Total Capacity (kWh)	589.60
Net Capacity (kWh)	530.64
Round-trip efficiency	80%
Maximum hourly discharge (kWh)	76.08
Discharge hours	12, 13, 14, 15, 16, 17, 18, 19, 20, 22, 23
Net Present Cost - NPC (US$)	**$861,910**

DER option 3 is composed of a combination of PV and battery technologies. The optimization algorithm is also used in EPC_NHood to find a best solution for minimizing *PI*_1, with the same cost constraint mentioned before. In this case, the algorithm searches for the best combination of PV array size, battery capacity, discharge hours, and discharge rate. The derived solution is presented in Table 7.

Table 7 – DER option 3 – solar and storage

Solar+Storage (PV with Battery)	
Battery	
Total Capacity (kWh)	176
Net Capacity (kWh)	158.40
Round-trip efficiency	80%
Maximum hourly discharge (kWh)	37.88
Discharge hours	13, 17, 18, 19, 22, 23
Battery - NPC (US$)	**$257,290**
PV	
Total PV area (m^2)	1,440
Peak power coefficient (kW/m^2)	0.15
PV - NPC (US$)	**$594,000**
Total NPC (US$)	**$851,290**

3.4 Validation of the reduced order modeling approach

In this section, we investigate the adequacy of our reduced order modeling approach for testing the performance of different DER alternatives for reducing peak loads within the Miami community model.

It must be clear that a validation of this nature must be case specific to be meaningful. In other words, when comparing two models, one can only draw relevant conclusions on the adequacy of the models if he knows what the models are being used for.

In our study, we first make clear what performance indicators we are using to evaluate technological decision at the community level. Then we use the discrepancies in the outputs between the reduced order and the detailed models as a proxy for the model form uncertainty quantification. Finally, we investigate the robustness of decisions based on the outcomes of the reduced order EPC_NHood platform.

The key criterion for this analysis is the ranking of DER alternatives in terms of how they can promote the improvement of *PI*_1, as defined by Equation 26. The lower the value of *PI*_1, the better the alternative. Since they all have the same overall cost, it becomes a straightforward comparison.

3.4.1 Deterministic Simulation

In the first part of the validation exercise, we simply run a single simulation of EPC_NHood under the implementation of each one of the DER alternatives. Due to the

deterministic nature of this analysis, all simulations have fixed (assumed as "known") inputs, therefore resulting in a unique set of outputs from which *PI*_1 can be calculated.

The intention is to create a baseline ranking of preferred alternatives for the upcoming uncertainty analyses.

According to Figure 32, "PV+battery" DER option ranks 1st with the lowest *PI*_1 (414), followed by "PV" (424), and "Battery" (438).

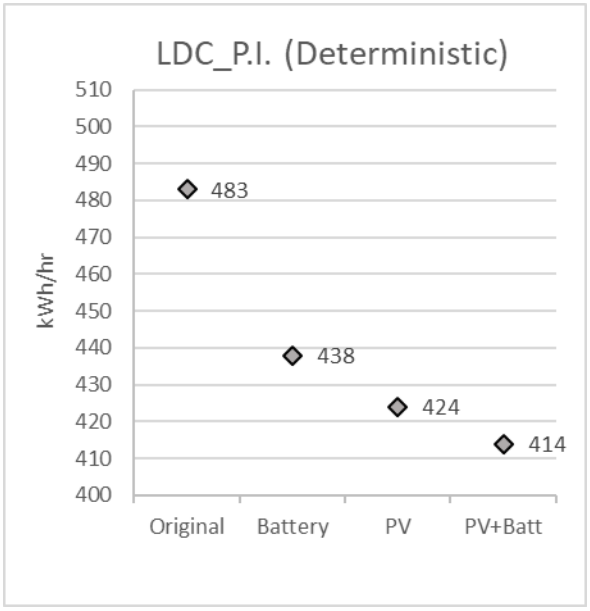

Figure 32 – Performance of DER options via deterministic simulation

3.4.2 Uncertainty Analysis

For this part of the validation exercise, we investigate how different sorts of uncertainties affect the objectivity of our reduced order model in evaluating and ultimately ranking the performance of the available DER alternatives for reducing peak loads. We

look at the impacts of scenario, parameter, and model form uncertainties, with special interest in the latter.

3.4.2.1 Scenario Uncertainty

In this research, we are calling scenario uncertainty the set of simulation inputs that are related to the usage of the buildings, more specifically represented by patterns of occupancy and schedules of average appliance and lighting usage. These patterns are typically inserted in building simulation models by means of usage intensity values, and schedules that modulate how these values vary throughout the day.

Table 8 shows the default intensity values for occupancy, appliances, and lighting for the building types belonging to EPC_NHood.

Table 8 – Building usage intensity

Building Models	Default values		
	Occupancy (person/m^2)	Appliance (W/m^2)	Lighting (W/m^2)
Medium Office	0.0538	14.5400	7.9438
Residential	0.0179	9.7570	1.0230
Retail Strip Mall	0.0861	4.3000	14.9500

According to the original PNNL prototypes, the variations of these intensity values follow the curves represented as “regular variation” in Figure 34 to Figure 36.

To provide some degree of uncertainty in the definition of these inputs, we segment those profiles into nine parts, each one linked to a “scenario uncertainty multiplier”. These multipliers can affect, independently, different groups of hours of each schedule according to Table 9. Therefore, a total of 18 multipliers can promote additional modulations on

different parts of those three profiles. They enable up to +/- 10% variation in each segment of the “regular variation” curves. All multipliers follow a random probability that follows the normal distribution depicted in Figure 33.

Table 9 – Relation between scenario uncertainty multipliers and affected hours

Scenario Uncertainty Multiplier	Affected hours
Sched_Occ/App/Light_(BuildingType)1	1, 2, 3
Sched_Occ/App/Light_(BuildingType)2	4, 5, 6
Sched_Occ/App/Light_(BuildingType)3	7, 8, 9
Sched_Occ/App/Light_(BuildingType)4	10, 11, 12
Sched_Occ/App/Light_(BuildingType)5	13, 14, 15
Sched_Occ/App/Light_(BuildingType)6	16, 17
Sched_Occ/App/Light_(BuildingType)7	18, 19
Sched_Occ/App/Light_(BuildingType)8	20, 21
Sched_Occ/App/Light_(BuildingType)9	22, 23, 24

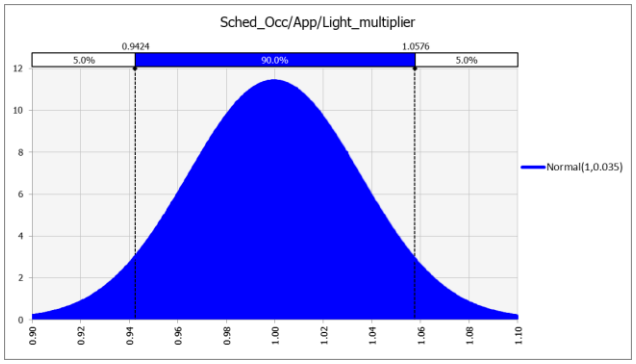

Figure 33 – Probability density function for scenario uncertainty multipliers

It must be noted that the same would be achieved by more realistic patterns of occupancy and building usage based on stochastic occupant models. However, our simple approach achieves the same end goal and is therefore adequate for the verification/validation purpose. Figure 34 to Figure 36 present the possible range of variation of schedules, with the lower and upper bounds for each segment of the curves. The colored background indicates the segments of hours affected by each multiplier.

Figure 34 – Medium office building schedules – range of variation and respective regions of influence of multipliers

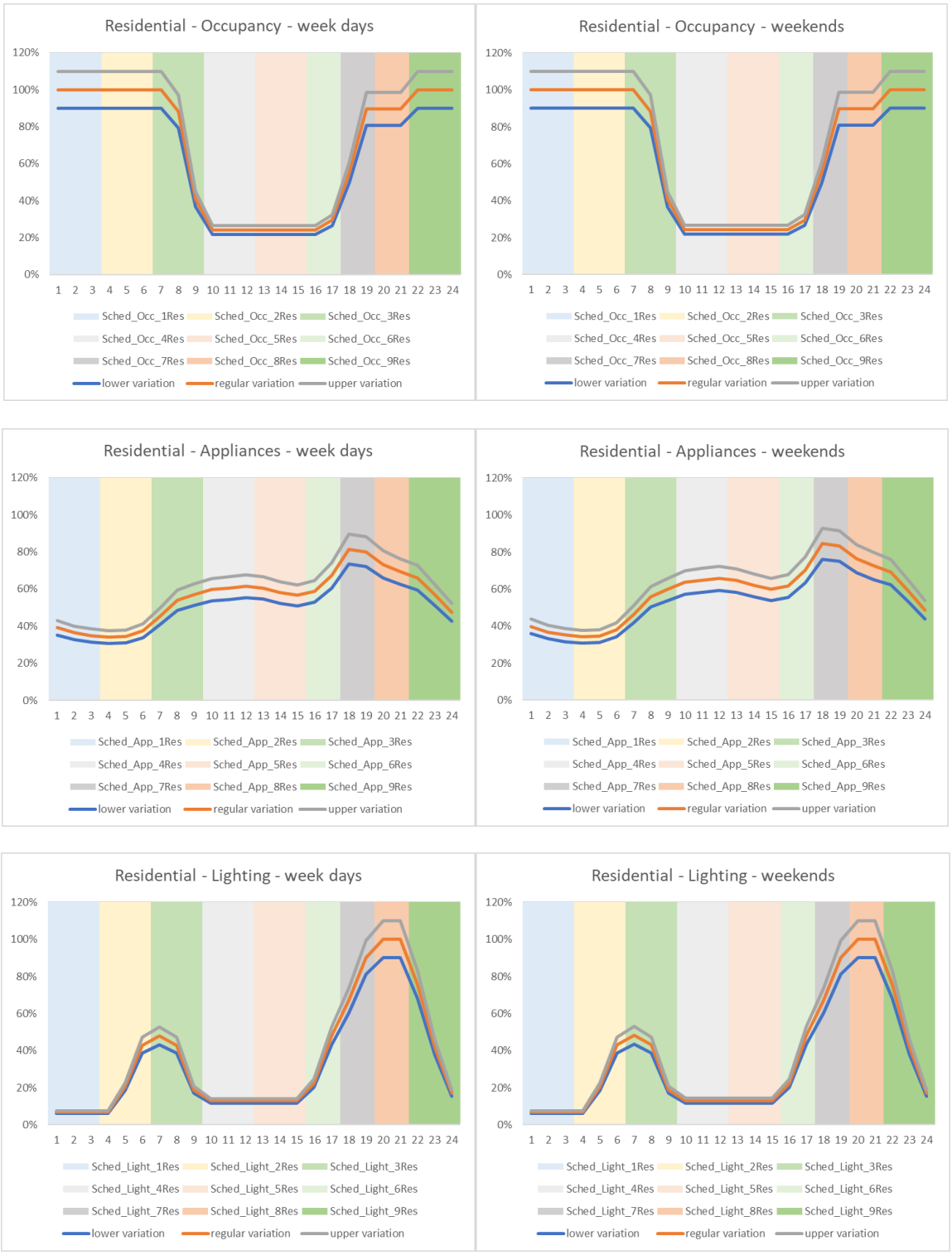

Figure 35 – Residential building schedules – range of variation and respective regions of influence of multipliers

Figure 36 – Retail strip mall building schedules – range of variation and respective regions of influence of multipliers

3.4.2.2 Parameter Uncertainty

For parameter uncertainty, we are looking for relevant building input parameters that might significantly impact the overall energy demand. We select cooling coefficient of performance (cooling COP) and envelope U-values as key inputs related to building thermal performance.

To create the intended variability in the determination of cooling COP in the building models, we use probability density functions for the COPs of each building type according to Figure 37 to Figure 39. Those distributions are skewed to the right, in such a manner that the 5% highest values are closer to the expected COP value than the 5% lowest values. This means that higher values of COP are unlikely to happen, but when they happen they are not significantly higher than the originally assumed values. On the other hand, lower values of COP are limited by a further lower boundary, thus possibly achieving significantly lower values in a few simulation trials. In other words, we are assuming that in face of several uncertain factors that may affect such systems their overall COPs could be higher than the estimated values, but are more likely to be lower.

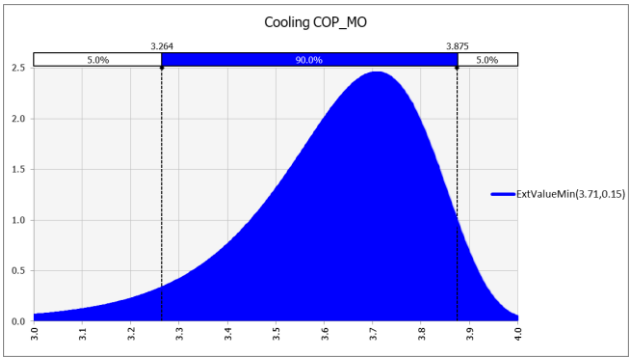

Figure 37 – Probability density function for cooling COP uncertainty: Medium office building

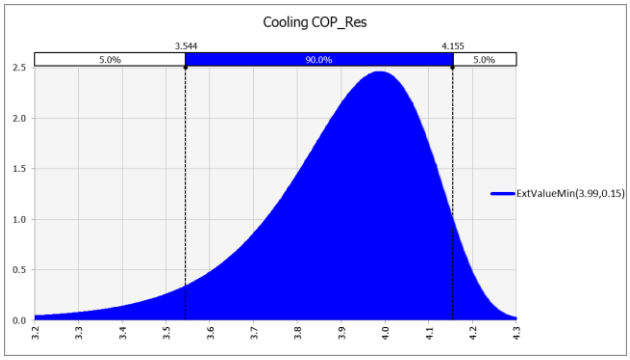

Figure 38 – Probability density function for cooling COP uncertainty: Residential building

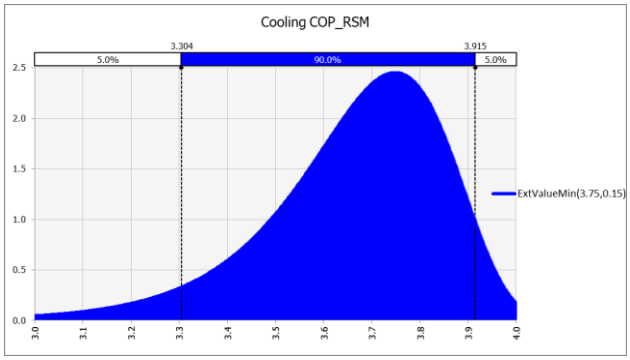

Figure 39 – Probability density function for cooling COP uncertainty: Retail strip mall building

With regards to U-value uncertainties, we take a more conservative approach, in which we assume that those values can only be equal or higher (meaning less thermal resistance) to the expected values. The reasoning behind these assumptions is that even if the layers and respective U-values of the envelope components are well known, there could always be failures in the construction process and flaws in maintenance that would end up increasing the U-values.

To promote this intended U-value variability, we apply independent multipliers to the U-values of walls, windows, and roofs of each building model. These multipliers follow the distribution presented in Figure 40, and are related to each envelope according to Table 10.

Table 10 – Relation between parameter uncertainty multipliers and U-values

Parameter Uncertainty Multiplier	U-value default input [W/(m^{2}K)]
U-value Roof_MO	0.273
U-value Wall_MO	0.437
U-value Window_MO	2.848
U-value Roof_Res	0.189
U-value Wall_Res	0.494
U-value Window_Res	1.692
U-value Roof_RSM	0.273
U-value Wall_RSM	0.437
U-value Window_RSM	2.848

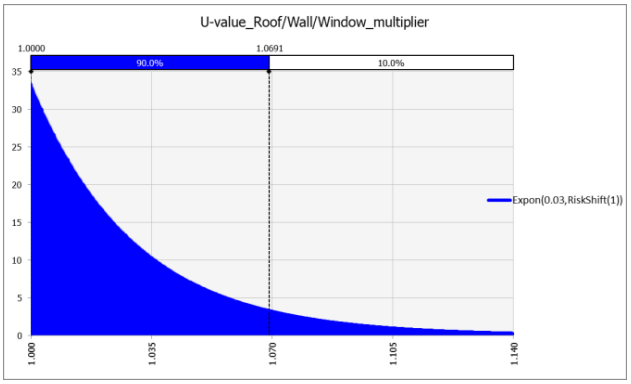

Figure 40 – Probability density function for envelope U-value multiplier

3.4.2.3 Model Form Uncertainty

Another source of uncertainty comes from the model form simplification intrinsic to our modeling approach. In this context, we want to know whether and how this model form reduction affects the outcomes of the simulations with possible impacts in its adequacy for supporting decision making.

As a proxy for model form uncertainty, we are using the observed hourly discrepancies between the overall electricity consumption calculated from the reduced order building models and from their higher order counterparts, as depicted in Figure 29. Even though these values are related to a one-case comparison, we expect that by investigating their influence within the uncertainty analysis we can have a good grasp of their relative significance in the decision-making process.

Those series of discrepancies are added as "noise" to the outputs of the reduced order building models. The incidence of such noise in the model form uncertainty analysis is governed by three factors:

(i) Proportionality factor: in each simulation trial, each hourly discrepancy is reduced or increased proportionally to the ratio between the current EPC model electricity demand output and the original EPC output;

(ii) Weekly randomness factor: a weekly randomness is applied to the series of "noise" of each building model by allowing +/- 10% of variation at every week, separately, in each simulation trial;

(iii) Incidence factor: the whole series of discrepancy values is multiplied to the incidence factor, which is depicted in Figure 41. This means that there is a different incidence of model form "noise" for each building model in each simulation trial.

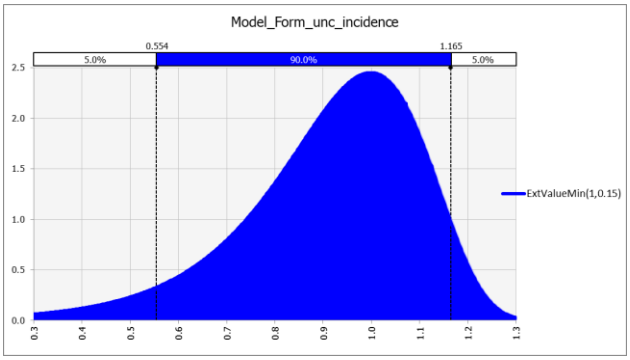

Figure 41 –Probability density function for model form uncertainty incidence

Another probability density function for model form incidence, with 50% higher values as depicted in Figure 42, is created for testing the effects of an exaggerated model form uncertainty.

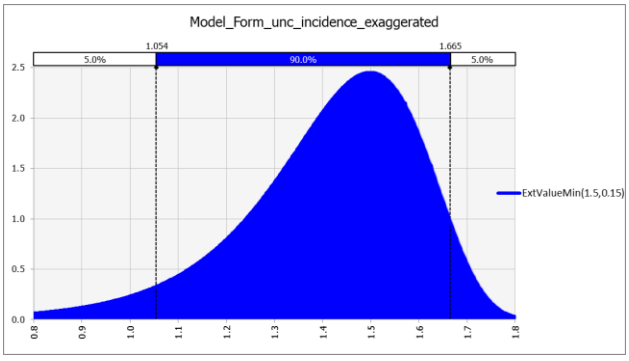

Figure 42 – Probability density function for exaggerated model form uncertainty incidence

3.5 Results and Analysis

Each uncertainty analysis is carried out with 500 random simulations. The following sections show how different combinations of uncertainties in our EPC_NHood model affect its role for evaluating and ranking the DER options.

3.5.1 Influence of Combined Scenario and Parameter Uncertainties

In the first round of analyses, we are investigating the impacts of combined scenario and parameter uncertainties. Figure 43 shows how the simulated performance of the DER options are altered under these uncertainties. When comparing with Figure 32, we see that there is little impact in the relative performance between the DER options. *PI*_1 values are slightly higher than the correspondent values from the deterministic simulation, but not enough to impact the performance ranking.

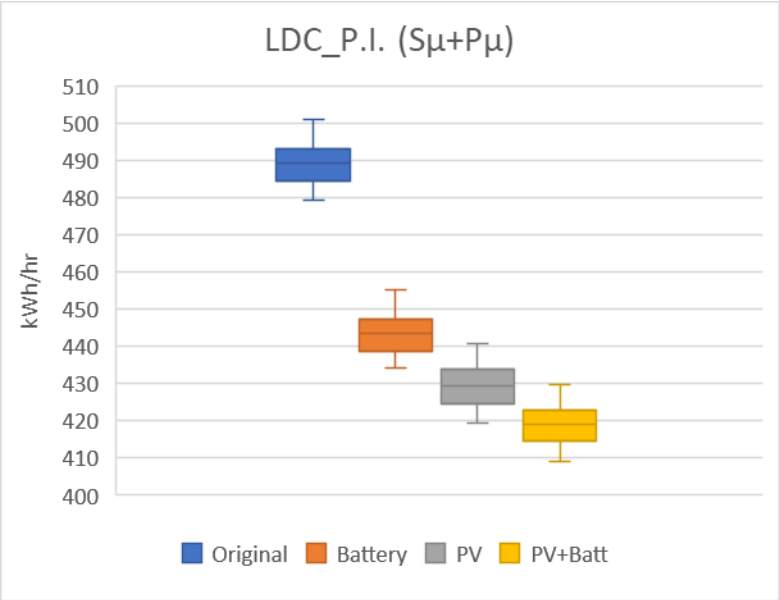

Figure 43 – Performance of DER options under combined scenario and parameter uncertainty

3.5.2 Influence of Model Form Uncertainties

In the second case, we are investigating the impacts of model form uncertainties alone, and with the other sources of uncertainty.

Figure 44 and Figure 45 present the results related to the simulations under combined scenario, parameter, and model form uncertainties. Comparing Figure 44 with Figure 43, we note that there are rather insignificant variations in the relative preference of alternatives when model form uncertainty is added to the analysis. This is corroborated by the tornado plots of Figure 45, where model form uncertainty is almost absent.

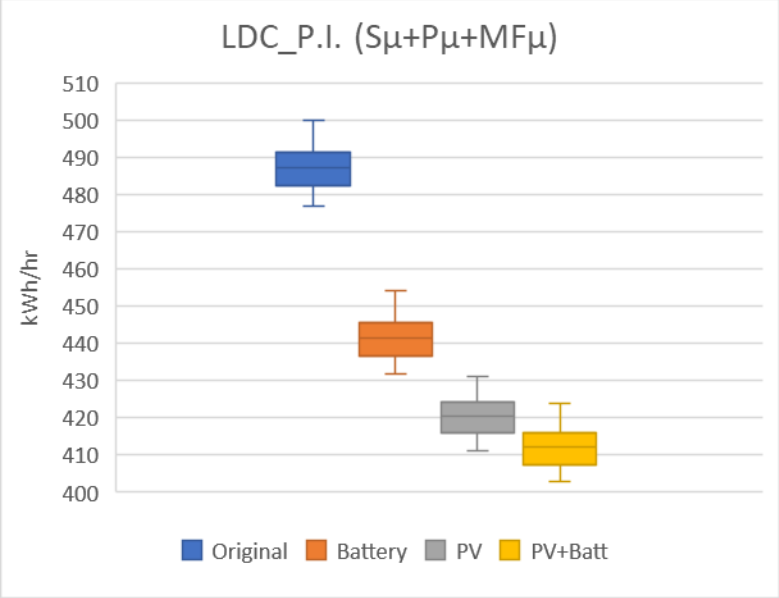

Figure 44 – Performance of DER options under combined scenario, parameter and model form uncertainty

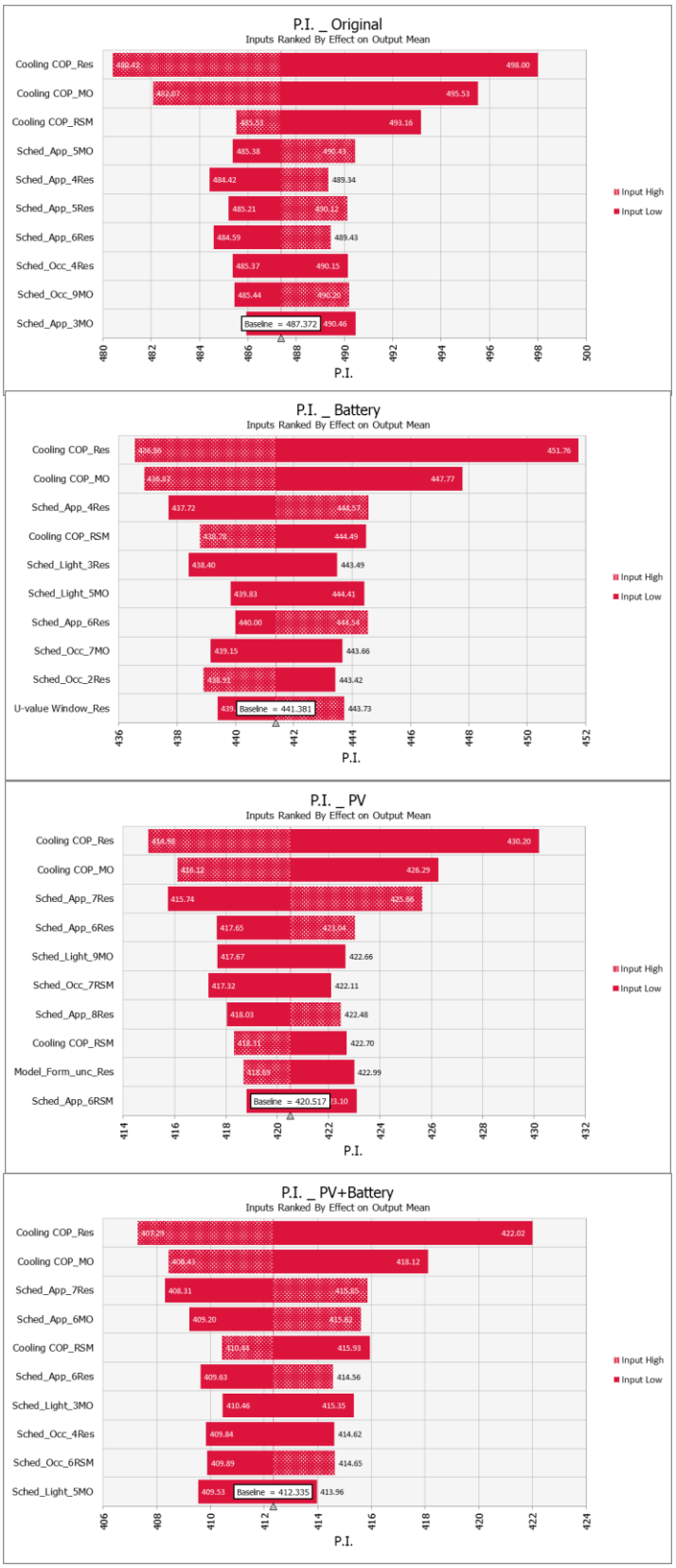

Figure 45 – Influence of uncertainties over DER options performance

For the case of exaggerated incidence of model uncertainty, the relative order of preference among DER alternatives still remains the same. There is an approximation between alternatives “PV” and “PV+Battery” (see Figure 46), but not sufficient to alter the original ranking of DER alternatives (Figure 32).

From Figure 47, we observe that the exaggerated model form uncertainty for medium office now comes to evidence in all four sets of simulations. However, this source of uncertainty, despite being exaggerated, is still of lower relevance when compared to the uncertainties related to Cooling COP in all buildings, as well as to those related to appliances usage in the residential buildings.

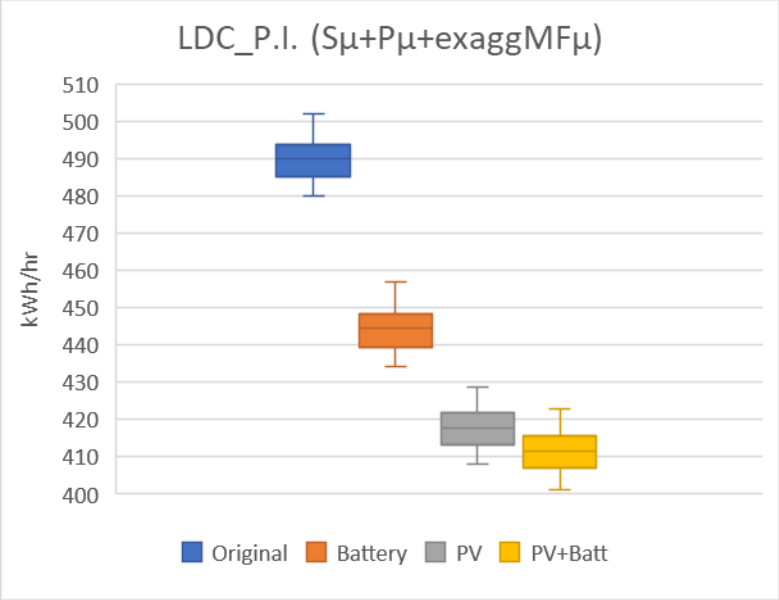

Figure 46 – Performance of DER options under combined scenario, parameter and exaggerated model form uncertainty

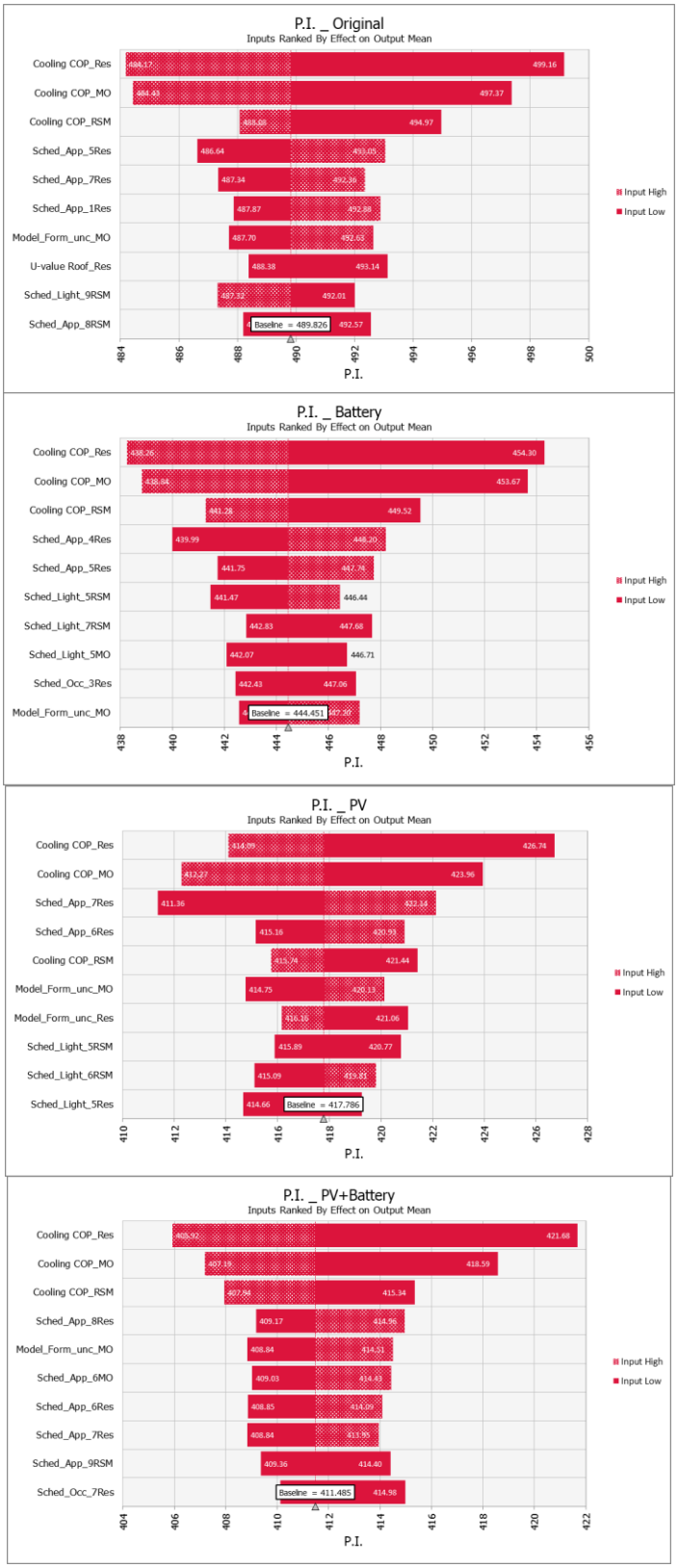

Figure 47 – Influence of uncertainties over DER options performance, including exaggerated model form uncertainty

Finally, when simulating the community under model form uncertainty alone, we see rather small effects in the calculated performance of the DER options. The addition of such simulation "noise" results in a slight reduction of *PI*_1 for all options (Figure 48), when compared to the outputs of the deterministic simulation (Figure 32). Nevertheless, the relative performance among alternatives sees no meaningful difference.

The sensitivity analysis presented in Figure 49 shows the range of variation in the outputs due to the influence of model form uncertainty. The horizontal bars are significantly narrower when compared to the more impacting inputs from the previous cases. It is interesting to note that the model form uncertainty for the medium office buildings is more impactful in the simulation of the "original" and "battery" DER options. Model form uncertainty related to the residential buildings has more effect on the "PV" and "PV+Battery" solutions.

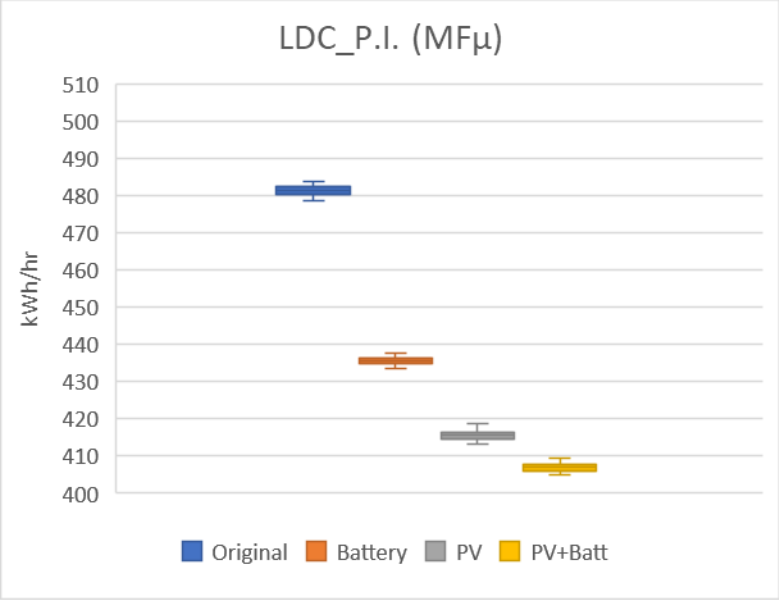

Figure 48 – Performance of DER options under model form uncertainty alone

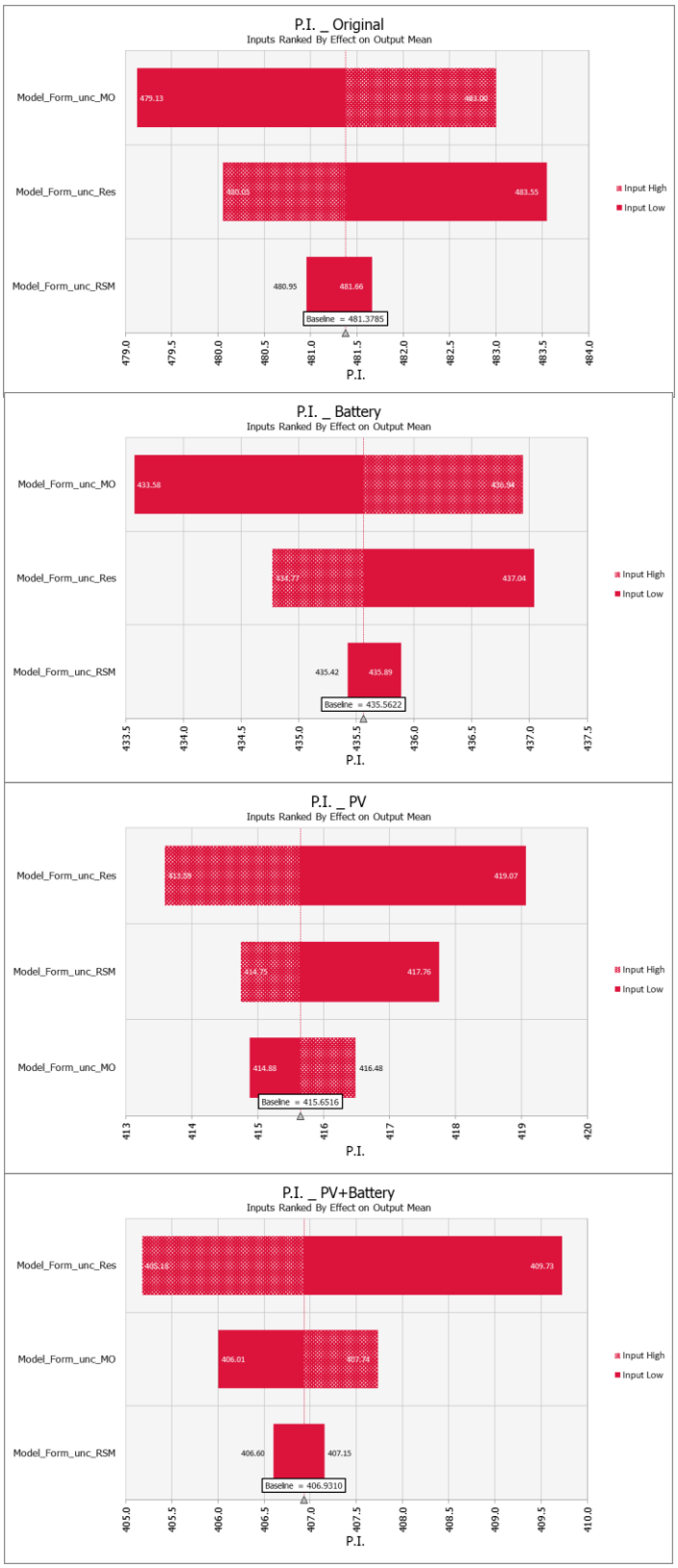

Figure 49 –Influence of model form uncertainty alone over DER options performance

3.6 Conclusions

The results obtained through the various uncertainty analyses conducted in this chapter serve as a robust means for validating our reduced order modeling approach. According to the findings, uncertainties due to model form reduction play a far less relevant role when optimizing or designing DER alternatives for communities than other sources related to parameter and scenario uncertainty.

The combination of different forms of uncertainty and the addition of exaggerated model form uncertainty in the form of "noise" to the outputs are not sufficient to disturb the adequacy of the model for supporting decision making.

We must emphasize that, while EPC_NHood proves to be adequate to model the particular case under study, further investigation might be needed to test whether there are limitations to specific situations involving other building types and other performance indicators that might be more sensitive to model form uncertainties.

Nevertheless, the scope of buildings involved in our analysis and the scale of investigation render this approach readily adequate for a broad range of similar applications.

Furthermore, the impact of model form uncertainty on the outcomes revealed to be so insignificant for this test case, when compared to input uncertainties, that it is fair to expect that it would remain a factor of minor relevance in most problems dealing with similar performance measures and within a similar scale.

CHAPTER 4. APPLICATION OF THE REDUCED ORDER MODEL TO AN EXISTING SOLAR NEIGHBORHOOD

4.1 Introduction

Physics-based experiments designed to predict the behavior of real world physical entities or to understand physical phenomena are a common practice in many scientific disciplines. As illustrated in Figure 50, such experiments can be carried out in the real facilities, in scale models, in computational models or through hybrid (both physical and computational) models (Augenbroe, 2004).

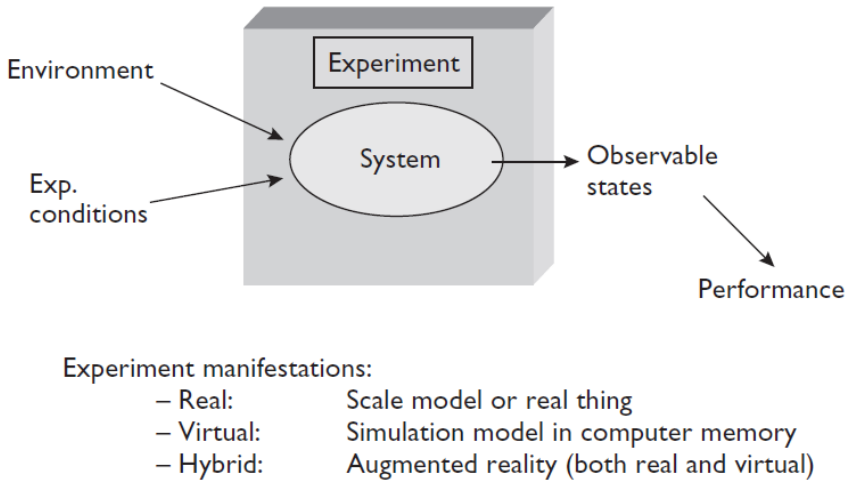

Figure 50 – Experiment manifestations: simulation viewed as a (virtual) experiment (Augenbroe, 2004)

Due to practical and economic reasons, virtual experiments carried out in computational models are usually the preferred mode when it comes to testing the

performance of large entities. In building simulation, the main purpose of developing a computational model is to simulate the behavior of as-designed, as-built, and as-operated facilities (Malkawi and Augenbroe, 2004). A reliable computational model should answer the questions of designers, engineers, developers, policy-makers and other stakeholders in relation to how a building or a collection of buildings would perform under given conditions.

Nevertheless, it is not rare to find long-term and expensive experiments that are carried out in existing neighborhoods or urban spaces to assist with the understanding or the evaluation of the behavior of a collection of buildings under novel scenarios. Especially from the side of the electric utility companies, a few pilot projects undertaken in real facilities have been designed to evaluate the performance of the integration of buildings and distributed energy resources, and their capabilities for acting in aggregation for shaping the local energy demand (SMUD, 2015, PECO, 2106).

Although very useful, such full-scale physical models – or real experiments – are not flexible in terms of modeling scenarios. By having a computational model – or virtual experiment – that can answer the same questions investigated in a real setting, the modeler can potentially draw faster outputs and hold a much greater experimental flexibility to further test the performance of the specific built environment under various conditions and scenarios.

In this context, this chapter evaluates the applicability of the modeling approach proposed in this thesis for substituting a full-scale physical experiment. A test case is conducted using an existing residential community in Rancho Cordova, CA with solar

energy generation and battery storage. This neighborhood was the subject of a pilot demonstration project previously conducted by the local utility company. The following section describes the selected community and the test case performed.

With this case study in a real community, this chapter also answers the other part of the research question 1, as stated in section 1.3, with relation to comparison with real data.

4.2 Case Study: 15 homes in Anatolia Smart Grid Pilot Project

The Anatolia III Solar Smart Homes Community is located in the southeast portion of the service territory of the Sacramento Municipal Utility District – SMUD, in the city of Rancho Cordova, CA (SMUD, 2015). Developed as a low density residential, open space project, Anatolia III is composed of 879 residential units, and is surrounded by other residential and commercial developments in the city (City of Rancho Cordova, 2005).

The Anatolia PV and Storage Demonstration Pilot Project was funded by the U.S. Department of Energy, and was conducted by SMUD along with the project partners Navigant consulting, SunPower, GridPoint, and the National Renewable Energy Laboratory – NREL (Rawson, 2013). The project monitored fifteen Residential Energy Storage (RES) units and three Community Energy Storage (CES) units to investigate their ability to solve intermittency and reliability issues associated with high solar PV penetration, as well as the benefits of distributed energy storage for helping utilities with growing peak demand (SMUD, 2015).

Among other objectives, the demonstration project specifically wanted to (Rawson, 2013):

- *Understand how the integration of energy storage could enhance the value of distributed PV resources within the community*;
- *Determine if the addition of energy storage could alleviate the demand during "super-peak" hours, particularly when PV output drops after 5pm*.

To test the applicability of our proposed modeling approach to the solar community of Anatolia, we develop an EPC_NHood model that represents the fifteen households evaluated in the real-scale experiment. General and scarce data for the entire neighborhood retrieved from the pilot project documentation is used to calibrate the community energy model.

Once calibrated, EPC_NHood is used to test different energy storage arrangements for load-shaving that could not be applied in the real-scale project due to practical constraints. Advanced optimization techniques and uncertainty analysis are explored in this context.

4.2.1 Anatolia Community

Among the fifteen homes in the Anatolia Community that were used in SMUD's pilot project, nine homes are located in the southwest part of the community, five homes in the central part, and one home in the northeast portion (see Figure 51). These homes were designed as "Solar Smart" residences, meeting or exceeding the code California Title

24, with 14 SEER air conditioners, EnergyStar qualified windows, and efficient lighting. Each home has a PV system installed with a nameplate capacity between 1.9 and 4.0 kW_{DC} (Navigant, 2012).

Figure 51 – Anatolia Community – Rancho Cordova, Sacramento County, CA: Location of homes monitored in SMUD's pilot project

4.2.2 Building Types

Since no detailed data are available with regards to the buildings' dimensions, the fifteen homes used in the pilot project are inspected through satellite and street-level imagery, and are separated according to their size (number of stores and approximate gross floor area) and orientation. In parallel, we investigate the palette of residential design

options offered by the construction company that built those homes (Lennar, 2017). Three building archetypes are then defined as ideal representatives of the different types of homes within the group of fifteen units. Accounting for the different orientations, eleven building models are created, each one with its own set of basic building inputs as required by the EPC calculator.

4.2.3 DER Technologies

SMUD's pilot project investigated both large energy storage equipment and home-battery solutions, respectively labeled as "community energy storage" – CES and "residential energy storage"– RES. The first technological device had a capacity of 34 kWh (30 kW) and the latter 7.7 kWh (5 kW).

In our community energy model application, we are looking at the performance of individual batteries only, which would be equivalent to SMUD's RES units. Due to the flexibility of our modeling approach, the operation of the home-batteries can be embedded in the community energy model, where we can test and optimize energy storage solutions with regards to their capacity and to charge/discharge schemes.

4.3 Reduced Order Community Energy Model

When dealing with larger energy models with multiple buildings, the manipulation of input data can easily become a problematic part of the simulation exercise. As discussed

in previous sections, there are issues related to accessing detailed building behavior and energy usage information at the scale of individual buildings. Even if such data are available, their treatment and insertion in higher order community energy models still require a great deal of human effort and computational power.

If the access to building data is indeed limited, which is the case in many assessments, the last resort is to represent buildings with equivalent simplifications, such as basic prismatic building shapes, single-zone conditioned volumes, overall U-values for the envelopes, overall systems' efficiencies according to building vintage, and overall energy consumption according to generic available data. Yet, there remains the question on whether to use higher order or reduced order simulation techniques to represent the collection of buildings under these circumstances.

From the previous chapter, we observed that model form uncertainty in reduced order energy models at the community scale is rather insignificant when compared to higher order models. Considering that we used detailed building input information for those analyses, it is not unreasonable to assume that the discrepancies between higher and reduced order models' outcomes would be of the same level or lower when dealing with simplified or generic input data.

The Anatolia case study then becomes an ideal candidate for this evaluation since it is a case where the availability of data related to detailed building specification, occupation patterns, and end-use energy consumption is very limited and generalized for the whole neighborhood. This gives us a great opportunity to show that our approach can

be used to recreate, with good representativeness, a collection of fifteen buildings that are energy-wise equivalent to those used in the SMUD's pilot.

The following sections explain the creation and calibration of such community energy model. We then use this model to test different energy storage arrangements for load-shaving, with a breadth of implementation options and scenario variations that obviously could not be tested in the real-scale project due to time, financial, and practical constraints.

4.3.1 EPC Archetypes

A reduced order EPC model is created for each one of the three building designs selected to represent the fifteen homes in Anatolia. From the specifications provided by the construction company portfolio and by the pilot project documentation (Rawson, 2013, Lennar, 2017), it is possible to define in the EPC archetypes all inputs related to envelope dimensions and thermal properties. Adjustments for building actual orientation result in eleven EPC Archetypes, as listed in Table 11. These sources also enable an initial guess of the HVAC systems efficiencies, as well as lighting and appliances total loads.

Table 11 – Building Archetypes in Anatolia Community Energy Model.

#	Address*	Area [m^2]	Community Location	Archetype (Design)	Building Orientation	Oriented Archetype
1	5xx8 Almond Falls Way	185	Southwest	Berkshire	E	ARCH_01
2	5xx0 Almond Falls Way	260	Southwest	Hawthorne	E	ARCH_03
3	5xx2 Almond Falls Way	185	Southwest	Berkshire	E	ARCH_01
4	5xx5 Almond Falls Way	260	Southwest	Hawthorne	W	ARCH_07
5	11xx7 Aspen Heights Ct	200	Southwest	Preston	S	ARCH_10
6	5xx1 Jade Springs Way	260	Southwest	Hawthorne	NW	ARCH_05
7	5xx9 Jade Springs Way	260	Southwest	Hawthorne	NW	ARCH_05
8	11xx7 Country Garden Dr	200	Southwest	Preston	E	ARCH_08
9	5xx0 Copper Sunset Way	260	Southwest	Hawthorne	SW	ARCH_06
10	11xx9 Country Garden Dr	185	Central	Berkshire	SE	ARCH_02
11	5xx7 Dusty Rose Way	260	Central	Hawthorne	NE	ARCH_04
12	5xx1 Dusty Rose Way	200	Central	Preston	NE	ARCH_09
13	5xx6 Dusty Rose Way	260	Central	Hawthorne	NE	ARCH_04
14	5xx5 Dusty Rose Way	260	Central	Hawthorne	NW	ARCH_05
15	12xx3 Apple Bury Ct	200	Northeast	Preston	SW	ARCH_11

(*) the complete address is omitted to preserve the privacy of residents

As one can see in Table 11, there are two households represented by ARCH_01, two represented by ARCH_04, three represented by ARCH_5, while all the others have an exclusive archetype representation each. This means that the outcomes of the EPC archetypes that represent more than one household are multiplied accordingly in the community energy model.

4.3.2 Community Energy Model

For the EPC_NHood model, we develop a master electronic workbook, which links all eleven EPC archetypes and their multipliers. In this platform, we can program modules to simulate energy storage and energy transaction operations at every hourly step. This environment also allows for calibration, optimization, uncertainty analysis, and other more sophisticated studies at the community scale.

All occupant related inputs, such as thermostat setpoints, occupancy patterns, lighting and appliance usage-level schedules, are initially defined according to usual values as proposed in Wilson et al. (2014) and reference values listed in Augenbroe et al. (2017). Energy for heating and domestic hot water is provided by means of natural gas in the neighborhood, therefore they do not affect the community electricity consumption.

As depicted in Figure 52, information related to energy consumption in the neighborhood is very generic, defined in terms of frequency of daily values. These values are related to the entire neighborhood, and they were observed before any energy storage intervention.

To compare these figures with our reduced order model, we have to scale the original values down to the proportion related to 15 households within one year of simulation. In this manner, the frequency data of the top graph of Figure 52 are scaled from the original 463 days of observation to 365 days, using 1-hour intervals. Similarly, the frequency data from the middle and bottom graphs of Figure 52 are scaled down from 642 days of observation to 365 days, and from 300 households in the neighborhood to 15 households in the connected community.

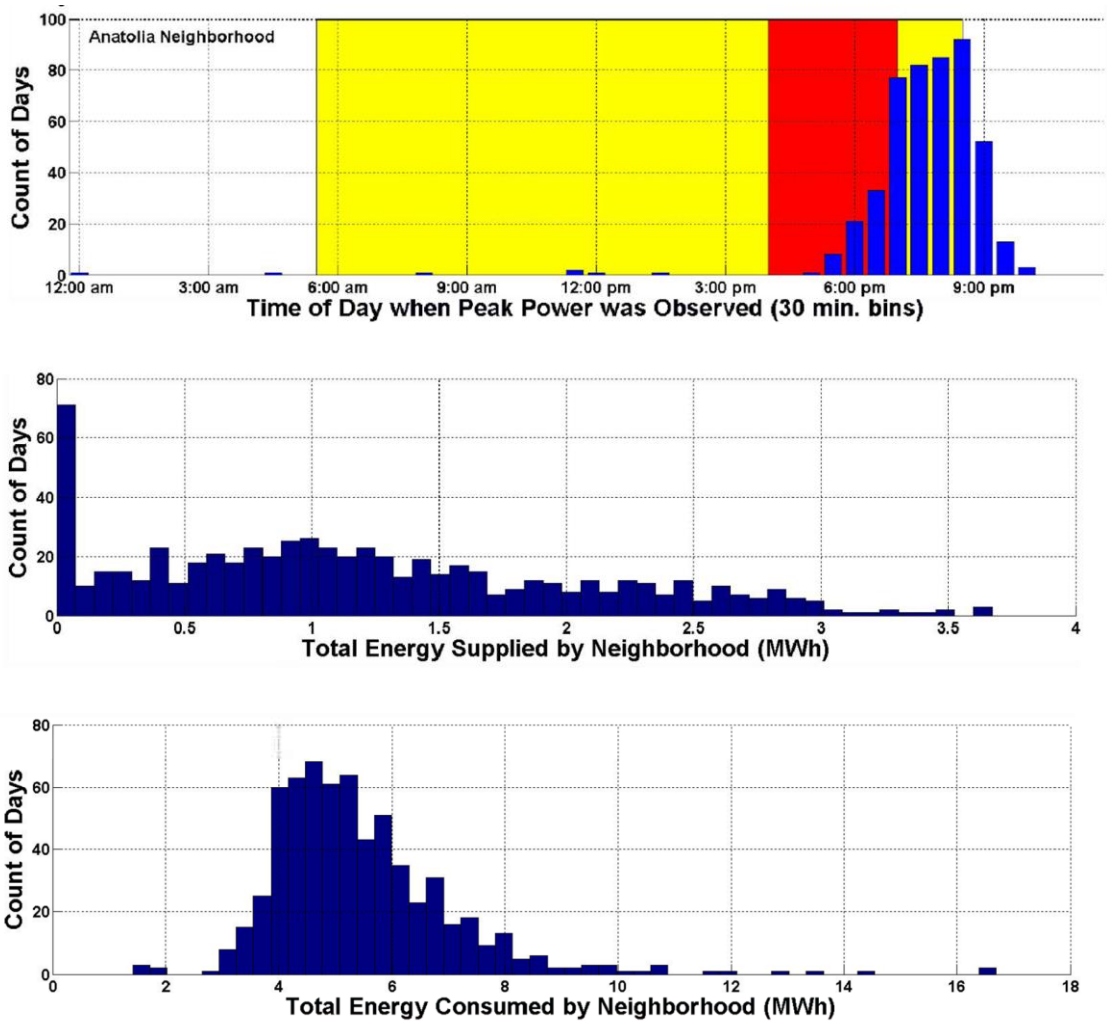

Figure 52 – Anatolia Neighborhood typical energy consumption profile (top: time of day when peak power is observed; middle: total energy supplied by neighborhood; bottom: total energy consumed by neighborhood)

After these adjustments, the generic energy performance data of the neighborhood can be directly compared to the outputs of our reduced order community model. Figure 53 shows the comparison before any calibration of the EPC_NHood model.

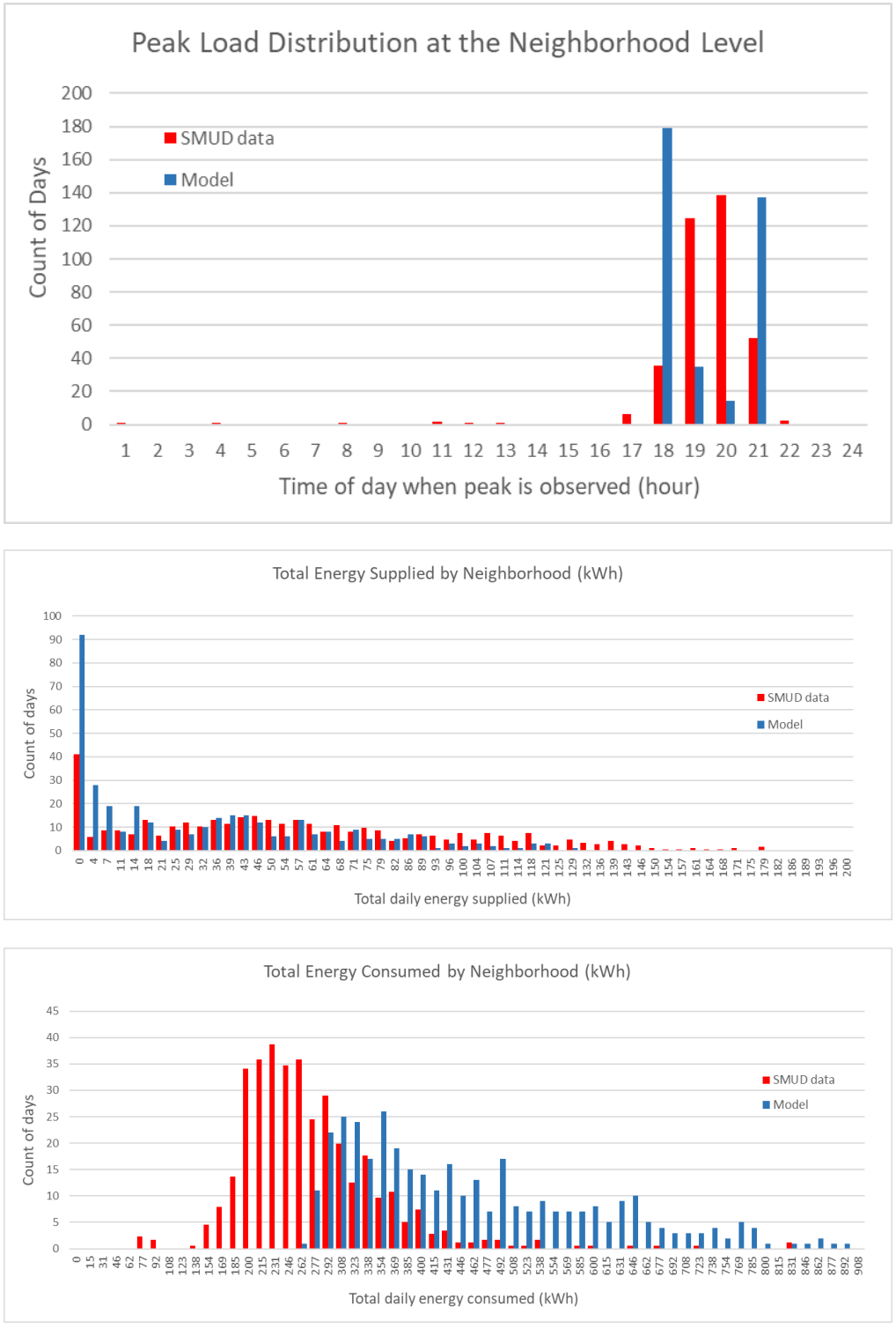

Figure 53 – Energy Performance Comparison (Red: adjusted SMUD data for 15 homes and 365 days; Blue: reduced order community model before calibration)

4.3.3 Calibration

From Figure 53, it is clear that the initial community energy model constructed based on limited knowledge of building specifications and on generic occupancy data is ill-suited to represent the collection of households with the patterns of energy consumption that are typical for that community.

To improve our model, we perform a calibration step to make up for the ignorance assumed in populating the building properties. For this step, we deploy an optimization routine, based on genetic algorithms (GA), to find the set of inputs that minimize the sum of squared errors (SSE) between the outcomes of our model and the real data measured by the SMUD utility company. Equation 27 is used to quantify the total weighted error (δ') considering the three sets of calibration data simultaneously.

$$\delta' = W_1 \times SSE_1 + W_2 \times SSE_2 + W_3 \times SSE_3 \quad (27)$$

Where:

SSE_1 = SSE of the counts of days when peak load is observed at every hour tag;

SSE_2 = SSE of the counts of days of total energy supplied that matches every kWh tag;

SSE_3 = SSE of the counts of days of total energy consumed that matches every kWh tag;

W_i = Weight attributed to each SSE (for i = 1, … , 3).

The EPC_NHood inputs that are subject to calibration are mainly related to building occupancy and usage behavior. Thus, we allow slight variations in the input profiles for

occupancy, lighting usage, and appliances usage by applying variable multipliers linked to different parts of each of those input sets, in a similar way to what was done in section 3.4.2. Along with input schedules, the total loads for lighting and appliances are subject to calibration. In addition, the calibration algorithm looks for a better estimate of the average cooling and heating setpoints.

Regarding the building parameter uncertainties, we consider the coefficient of performance (COP) for cooling as an inevitable calibration variable, since we learned in the previous chapter about its relevance in the sensitivity analysis. In addition, the fan control factor is included as another variable input.

Finally, the average size of rooftop PV per home is also defined as a calibration variable, since we only have an estimate value for the average size of PV arrays, which is in the range between 2.5 to 3.0 kW_{DC} per household.

It must be observed that during the calibration stage, the energy storage module of the EPC_NHood is not being used, since the original SMUD data are related to the solar community energy consumption before the intervention of the batteries.

With an embedded genetic algorithm, the calibration process proceeds to search for the best values for the unknown inputs that minimize δ'.

In the beginning of the calibration, δ' is 73024, with weights: $W_1 = 1$; $W_2 = 1$; $W_3 = 2$. As depicted in Figure 54, after 1800 trials – or generations of potential solutions – the value of δ' shows an impressive reduction, achieving 2389.

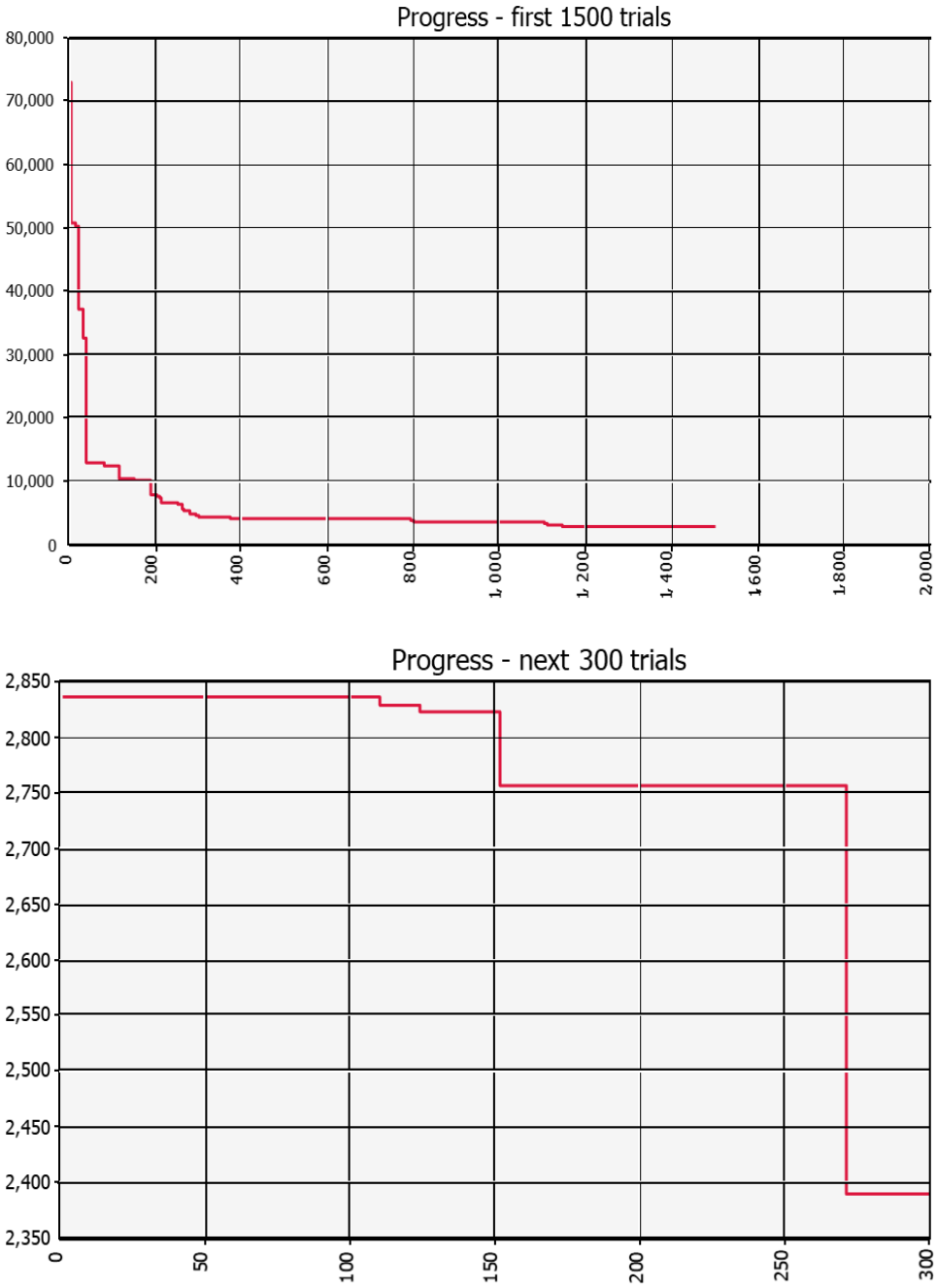

Figure 54 – Minimization of total weighted error (δ') using $W_1 = 1$, $W_2 = 1$, $W_3 = 2$ (top: first 1500 trials; bottom: next 300 trials)

For the final calibration trials, the balance of weights is changed to $W_1 = 1$; $W_2 = 2$; $W_3 = 1$, because SSE_2 is still yielding more discrepancies than the other indicators. Taking

advantage of the relatively quick simulation runtime, another 2500 generations are simulated, beginning with δ' = 3233 (according to the new definition of weights) and reaching a lower value of δ' = 1763 (see Figure 55). For clarification, this value means roughly an average error of only 3 counts of days for each tag of the horizontal axis of the three graphs of Figure 53 (after adjusting for the weights and the squares).

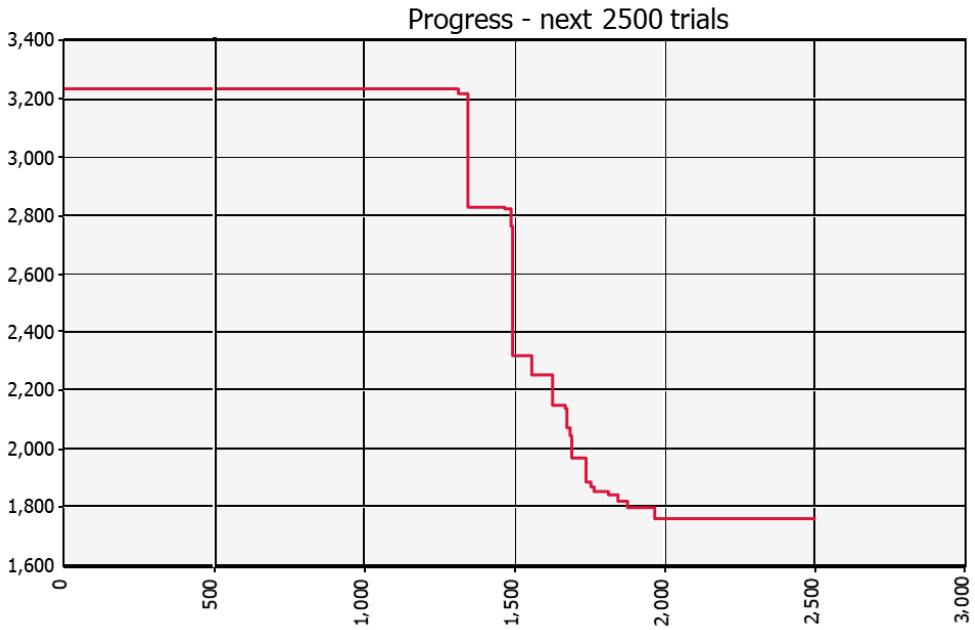

Figure 55 – Minimization of total weighted error (δ') using W_1 = 1, W_2 = 2, W_3 = 1 (final 2500 trials)

Figure 56 to Figure 58 show the comparison of the outputs of our calibrated model with the SMUD's data. The results confirm a very good fit for the community energy model, with p-value for comparison of means higher than 0.05 in all cases.

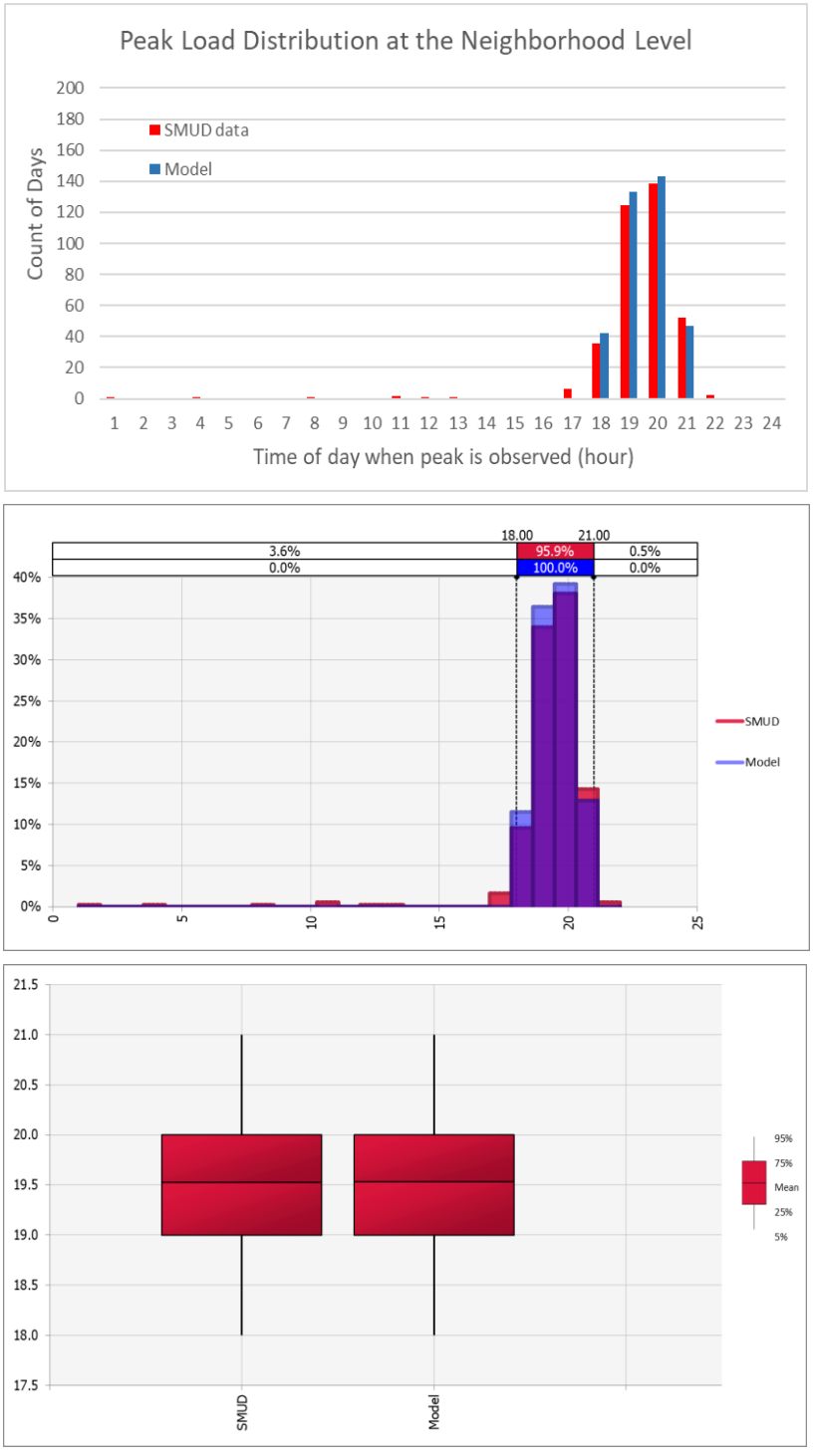

Figure 56 – Calibrated outputs for counts of days when peak load is observed (top: frequency distribution; middle: probability density; bottom: box plot comparison of means – obs.: p-value 0.90)

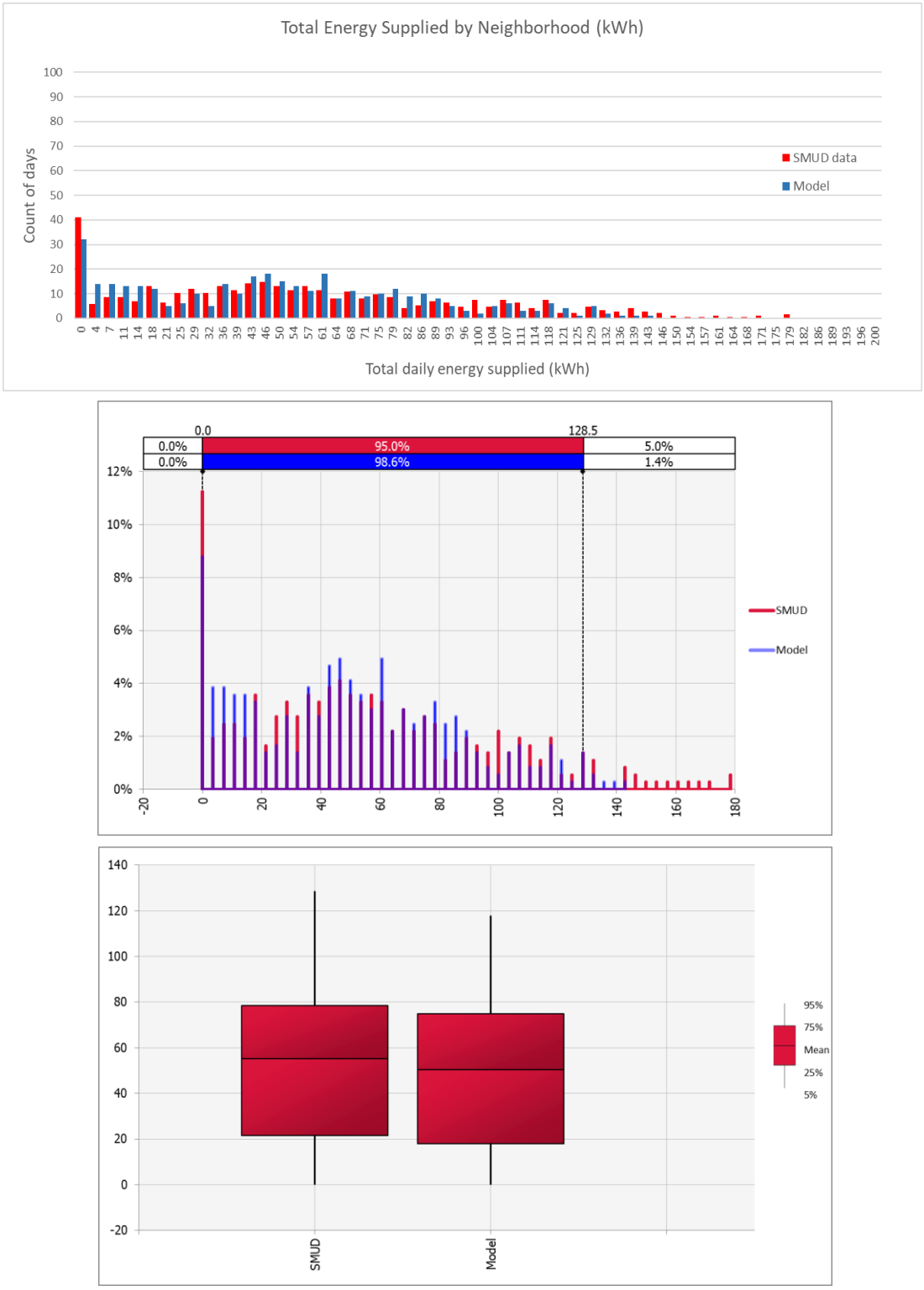

Figure 57 – Calibrated outputs for counts of days of total energy supplied by the neighborhood (top: frequency distribution; middle: probability density; bottom: box plot comparison of means – obs.: p-value 0.09)

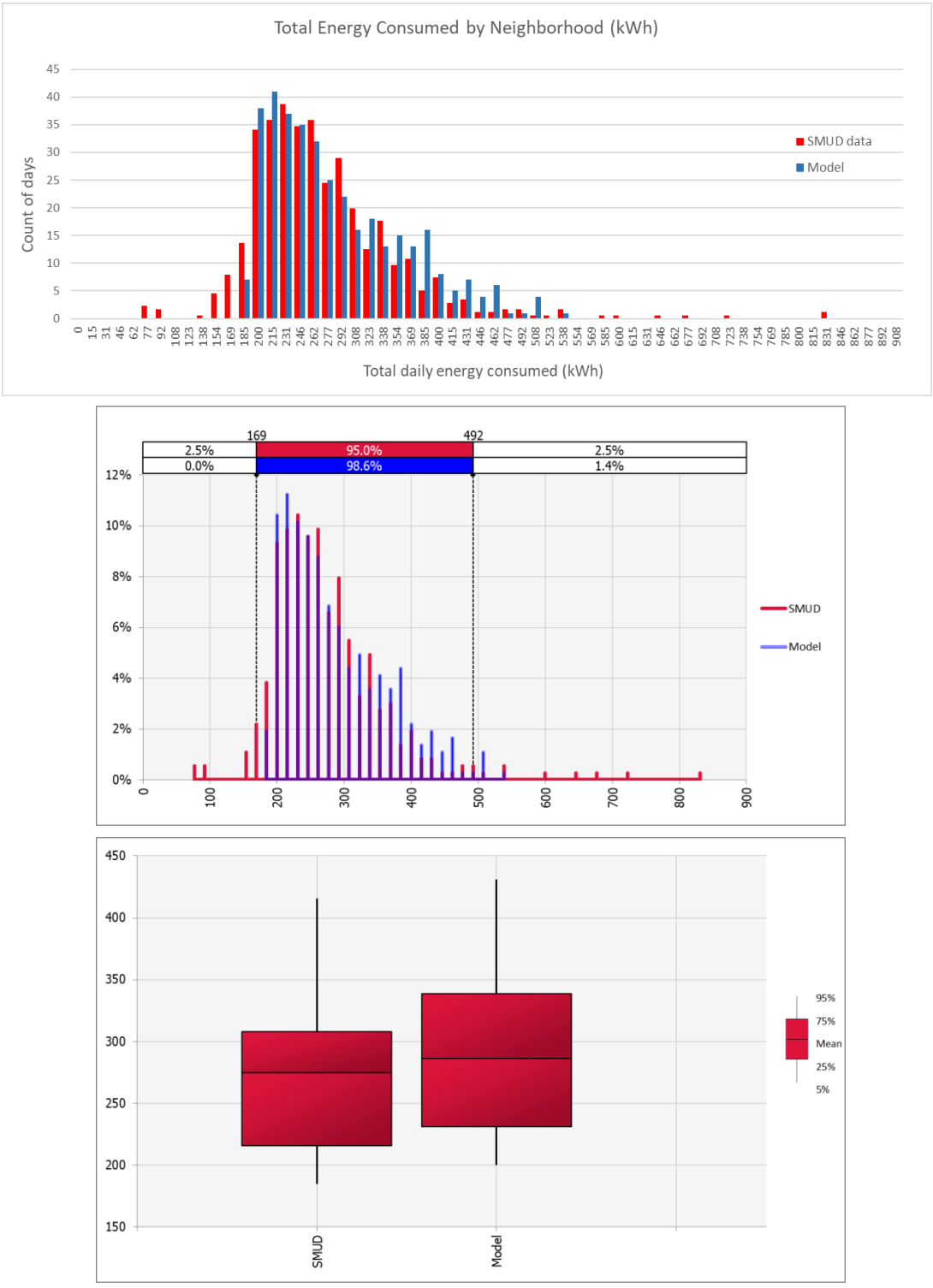

Figure 58 – Calibrated outputs for counts of days of total energy consumed by the neighborhood (top: frequency distribution; middle: probability density; bottom: box plot comparison of means – obs.: p-value 0.06)

We must also emphasize that the total simulation runtime for all those calibration trials is 7hr:30min, in a computer with an intel i7 processor @2.70GHz and 12 GB of RAM. This is quite a small processing time, when we acknowledge that the calibration of the community model consists of eleven individual building energy models running concomitantly for thousands of trials, each trial comprising a generation with a small sample of annual simulations with different input combinations (11BEMs x 4300generations x # of new sets of inputs at each generation). The same process with a more detailed community energy model would certainly require significantly more number of hours, if not days of simulation. For reference, a single building model simulation in EnergyPlus in the same computer takes around three minutes to run. If we assume ten new sets of input data at each generation within the GA process, this entire calibration, if possible at all to be programmed with EnergyPlus, would take roughly a thousand days of computation time in the same computer.

It is worth mentioning, though, that the adequacy of the calibration of a lower order model depends on what the calibrated model is being used for. The EPC_NHood model in this case study is calibrated using overall energy flow figures, and therefore should not be used to assess deep behavior within the collection of buildings. Since the assessments in this case are targeting overall community peak load reduction, we understand that the calibrated EPC_NHood model is adequate. Moreover, we assume that the detailed building information that is not captured in the reduced order modeling approach will not significantly affect the upcoming design and optimization studies that are related to aggregate performance indicators.

4.4 Optimization Assessment

As explained in section 4.2, one of the specific objectives of the SMUD's pilot project in Anatolia was to verify how the addition of energy storage alleviates the demand during "super-peak" hours. The real scale study did find benefits from these measures, and even tested alternatives for optimal dispatch of the batteries for load shifting (SMUD, 2015). However, the demonstration project had limited flexibility to test the performance of the energy storage solutions with relation to scenario and other parameter variability. Outcomes of the pilot project in terms of amount of load shifted per home during the test period helped confirm the positive effects of battery deployment, but could not be used for finding optimized solutions at the community scale.

With our calibrated ECP_NHood model, we have at hand a flexible, manageable and reliable average representation of the homes previously involved in the Anatolia pilot study. We can explore many more situations that were not feasible in the real scale project, with virtually no limits for testing different energy storage arrangements and dispatching solutions.

To set the stage for an adequate simulation-based optimization, we define five different targets for community load-shaving, for which we want to find minimum-cost storage solutions (Table 12).

According to the utility policy in effect at the time of the demonstration project, the "super-peak season" is defined from 4pm to 7pm, during all week-days from June 1st until September 30th, billed at US$ 0.25/kWh. Due to the neighborhood pattern of later peak

loads, the loads from 7pm to 8pm are also included in our analysis at US$ 0.16/kWh. Hence, we consider a total of 348 super-peak hours in our assessments.

Table 12 – Targets to be achieved by optimized energy-storage solutions

Target	Super-peak load threshold [kWh/hr]	Allowable number of unmet hours [count (%)]
I	50	7 (2%)
II	45	7 (2%)
III	40	18 (5%)
IV	35	35 (10%)
V	30	35 (10%)

The reasoning behind the definition of the targets and the respective allowable number of unmet hours is that one could be a bit more tolerant for the occurrences of peak loads beyond the super-peak threshold as it becomes harder to achieve.

4.4.1 Deterministic Optimization

In the first part of the optimization assessment, we want to find optimal energy storage solutions with regards to their capacity and to their discharge schemes. To provide more flexibility in the definition of the potential solutions, the fifteen homes belonging to the community are divided into three groups according to Table 13. Therefore, three distinct individual home-battery solutions can be assigned to the community, one to each group of homes, in terms of both capacity and discharge times. With these variations, we can explore a much larger solution space than what would be possible with a single home-

battery solution. This configuration provides an intermediate freedom of customization when finding the optimized solutions, which lies between a one-fits-all solution and a one-to-one solution. We understand that such intermediate customization assumption is more reasonable for mimicking potential real scale programs driven by a utility company at the neighborhood scale.

Table 13 – Groups of households with distinct battery solutions

Group	Households*
A	1, 3, 4, 8, 9
B	5, 11, 12, 13 ,15
C	2, 6, 7, 10, 14

(*) number tags according to Table 11

For this simulation-based optimization, the objective function (NPC_{tot}) to be minimized is defined according to Equation 28. This cost function calculates the total cost of the battery solutions installed in all three groups of homes, plus the total cost of electricity spent by those households during the critical hours in a period of 20 years. For the batteries, we assume a price tag of US$450/installed kWh[9], with a roundtrip efficiency of 80% and a 5-year lifetime.

$$NPC_{tot} = NPC_{batt} + NPC_{elect} \quad (28)$$

[9] This value is assumed based on Schmidt et al. (2017), whose study projects costs below US$500 kWh^{-1} for mature technologies, which we believe will comprise stationary home-batteries in the near future.

Where:

NPC_{tot} = total net present cost of solution for a 20-year cycle analysis;

NPC_{batt} = net present cost of energy storage solution;

NPC_{elec} = net present cost of billed electricity in super peak seasons.

Considering a deterministic scenario where all simulation inputs of the original calibrated community model are fixed, the optimization variables to be investigated are storage capacity (from 7 to 11 kWh per individual home-battery) and the choice of discharge hours (on/off values at the hour tags 17, 18, 19, 20) for each one of the three groups of households. The optimization is constrained by *PI*_2, which is a performance indicator that measures the total number of hours when the load surpasses the fixed threshold. There is a tolerable value for *PI*_2 for each defined super-peak threshold, as described in Table 12. With these settings, we run a simulation-based optimization for each load reduction target in order to find the best arrangement of battery solutions for the community. In this assessment, we consider that the batteries charge from the grid during off-peak hours and discharge to the households during the critical hours according to the discharge schemes defined for each group of homes.

Figure 59 shows the original values of community electricity demand during super-peak hours. Each cluster of bars represents a sequence of four daily super-peak loads. The horizontal axis units are labeled according to the correspondent hour tag in the sequence of 8760 hours of the simulation year.

Table 14 and Figure 60 to Figure 64 show the optimized solutions for each load reduction target and the resulting electricity consumption during the super-peak season.

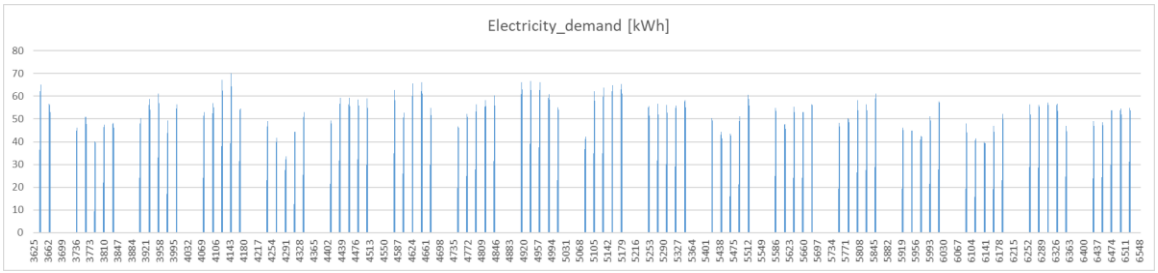

Figure 59 – Electricity demand for the community during the super-peak hours without energy storage solution

Table 14 – Optimized energy-storage solutions for each load reduction Target

Target	Super-peak load threshold [kWh/hr]	Optimized battery solution (capacity ; discharge hour)	NPC_{tot} [US$]	Realized number of unmet hours [count (%)]
I	50	Group A: 7kWh ; 17, 18, 20 Group B: 7kWh ; 17, 20 Group C: 7kWh ; 19, 20	241,680	5 (1.4%)
II	45	Group A: 7kWh ; 18, 19, 20 Group B: 9kWh ; 18, 19, 20 Group C: 7kWh ; 20	245,250	5 (1.4%)
III	40	Group A: 7kWh ; 19, 20 Group B: 8kWh ; 18, 19, 20 Group C: 8kWh ; 18, 20	244,080	16 (4.6%)
IV	35	Group A: 7kWh ; 17, 18, 20 Group B: 8kWh ; 18, 19, 20 Group C: 11kWh ; 19, 20	249,740	33 (9.5%)
V	30	Group A: 11kWh ; 17, 18, 19, 20 Group B: 8kWh ; 18, 20 Group C: 10kWh ; 19, 20	316,270	30 (8.6%)

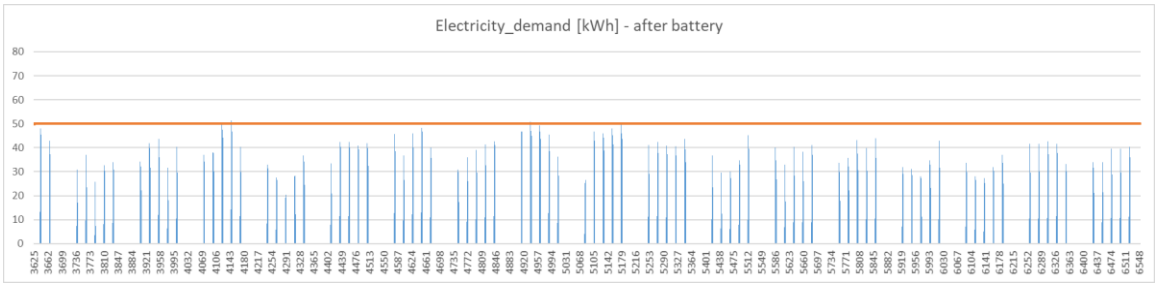

Figure 60 – Electricity demand for the community during the super-peak hours with optimized solution for TARGET I

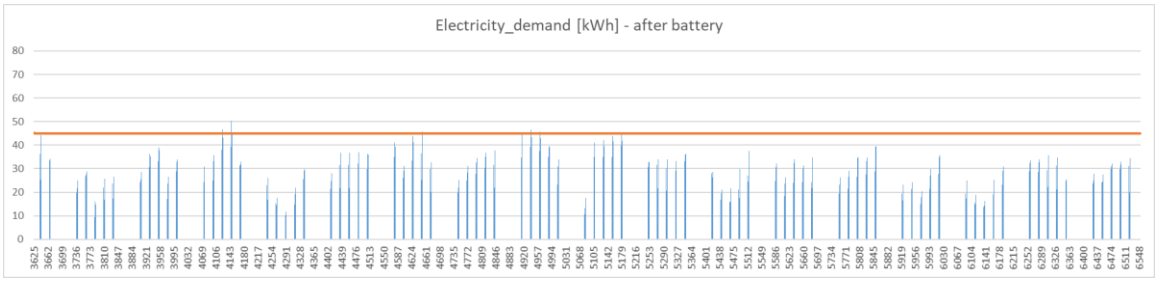

Figure 61 – Electricity demand for the community during the super-peak hours with optimized solution for TARGET II

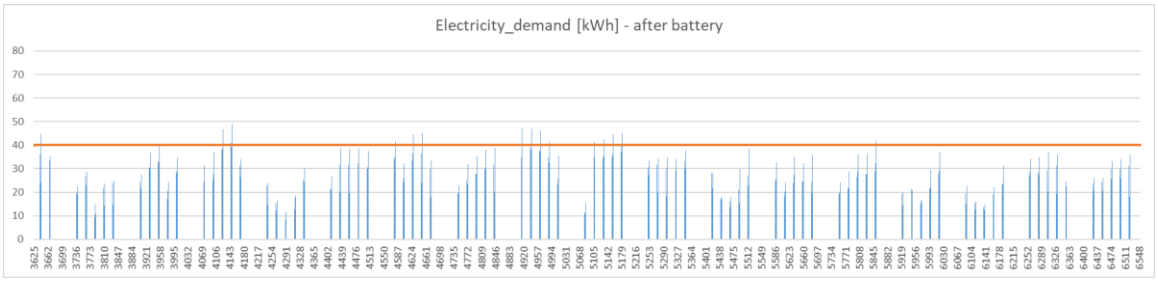

Figure 62 – Electricity demand for the community during the super-peak hours with optimized solution for TARGET III

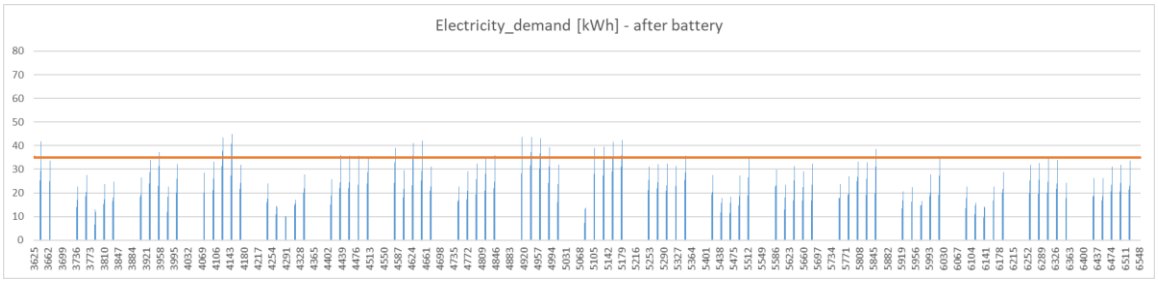

Figure 63 – Electricity demand for the community during the super-peak hours with optimized solution for TARGET IV

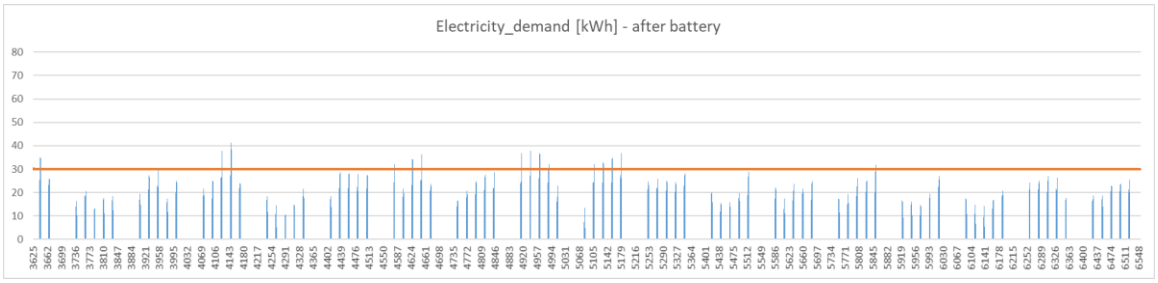

Figure 64 – Electricity demand for the community during the super-peak hours with optimized solution for TARGET V

We observe that it is relatively easy to achieve a solution for Target I with the lowest capacity option (7 kWh) for all three groups of households. The challenge for the optimization algorithm in that case is to find the best scheme for discharging the stored energy during the critical hours so that there is a minimum cost for the remaining electricity to be purchased.

On the other hand, as the target gets more stringent, the optimization solution has to find a good combination of both capacity and discharge scheme for all groups, so that the total NPC remains the lowest as possible. For target V, a solution could only be achieved at a somewhat higher cost.

4.4.2 Uncertainty Analysis

All optimized solutions presented in the previous section are guaranteed to fare well only in the deterministic situations for which they were developed. The question that should be asked now is how these same solutions perform in the presence of uncertainties, which in our case we try to approximate by adding uncertainty to simulation input parameters. This should be an obvious path of inquiry in such optimization assessments. Nevertheless, in complex and heavy models, this implies a cumbersome burden on the modeling exercise, which many modelers might not be willing to face as they are not convinced about its necessity.

In our proposed reduced order approach, uncertainty analysis can be used as a useful additional step of the investigation, where the proposed solutions can be tested to better inform decisions. Since this type of analysis can be carried out within the modeling framework of EPC_NHood, our approach makes it relatively easy and convenient to explore the effects of uncertain inputs in our simulations, more specifically related to scenario and building parameter uncertainties.

4.4.2.1 Scenario Uncertainty

The first set of uncertain inputs are related to the usage of the buildings, which we are calling scenario uncertainty. To create a reasonable range of scenario input variation, we use the same structure developed during the calibration stage (section 4.3.3), and apply the procedure described in section 3.4.2, where the schedules for occupancy, appliances, and lighting are linked to nine multipliers each. By changing the values of such multipliers, the curvatures of the schedules vary at each segment independently, thus providing the

intended variability in occupancy scenarios. For this analysis, we allow each multiplier to result in +/- 10% variation over the original calibrated values for each segment of the schedule curves, following a normal distribution.

Figure 65 to Figure 69 show the density distribution of the performance of the previous solutions based on 500 input samples under scenario uncertainty. In each plot, there is an indication of the percentile that corresponds to the allowable number for unmet hours for each target. We observe that the optimized solutions previously tailored for targets I, III, and V still fare very well under scenario uncertainty, with *PI*_2 surpassing the allowable number of unmet hours only in 1%, 10%, and 5% of the samples respectively.

The solutions developed for targets II and IV have significant fail rates under scenario uncertainty, not meeting the target in 50% and 25% of the samples.

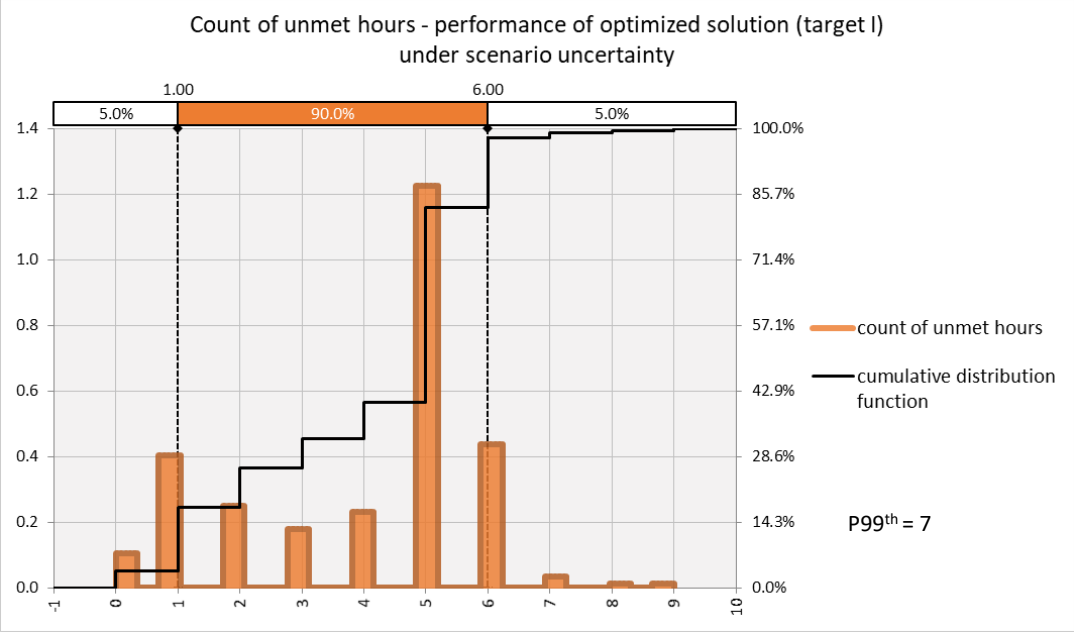

Figure 65 – Performance of optimized solution for TARGET I under scenario uncertainty

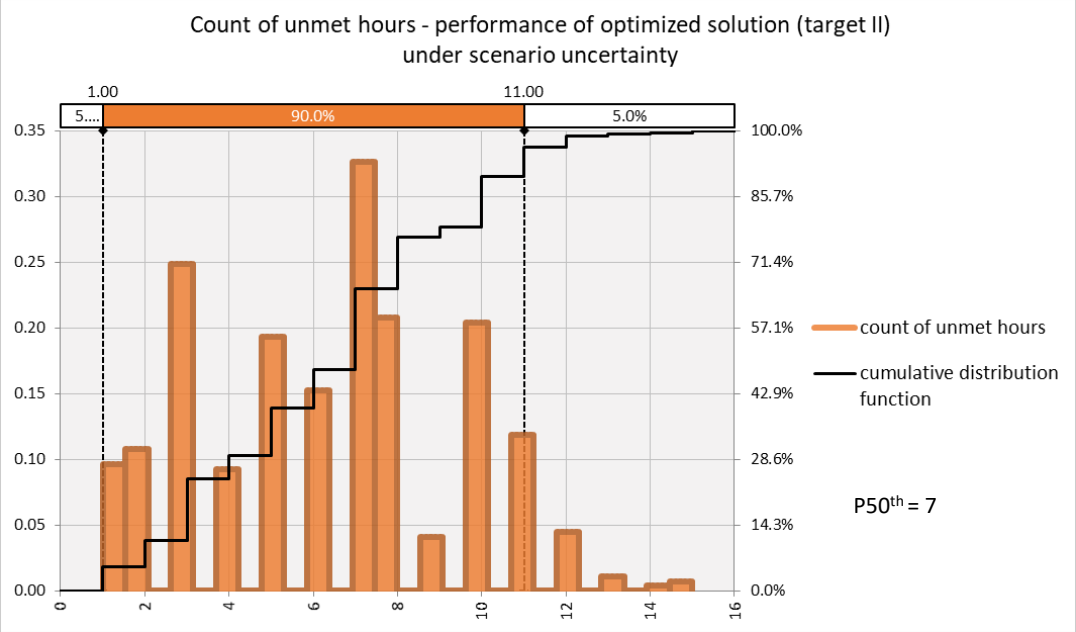

Figure 66 – Performance of optimized solution for TARGET II under scenario uncertainty

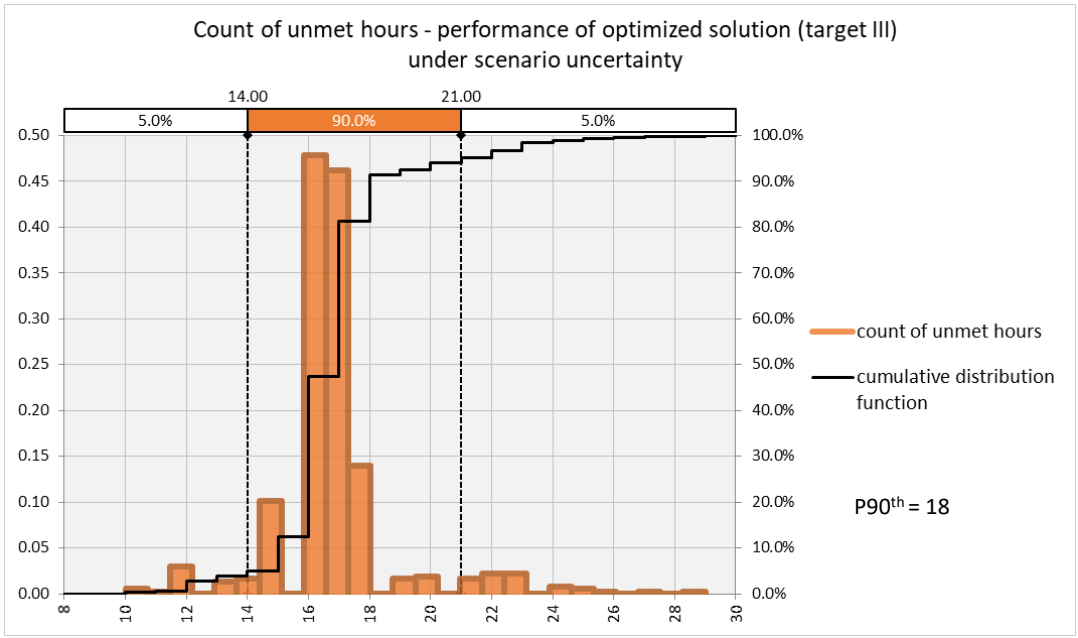

Figure 67 – Performance of optimized solution for TARGET III under scenario uncertainty

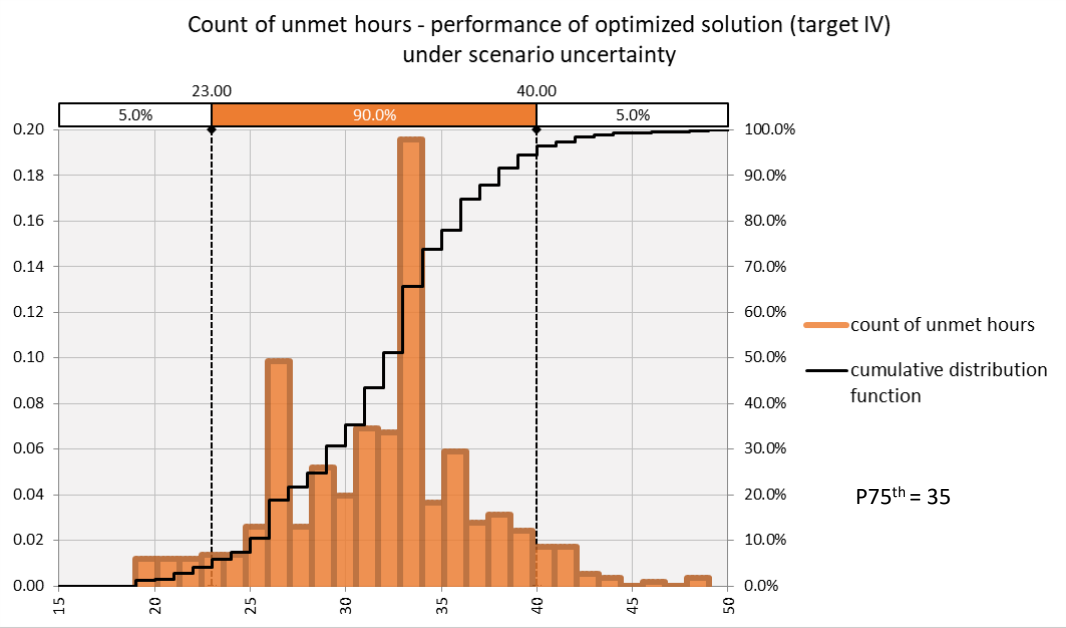

Figure 68 – Performance of optimized solution for TARGET IV under scenario uncertainty

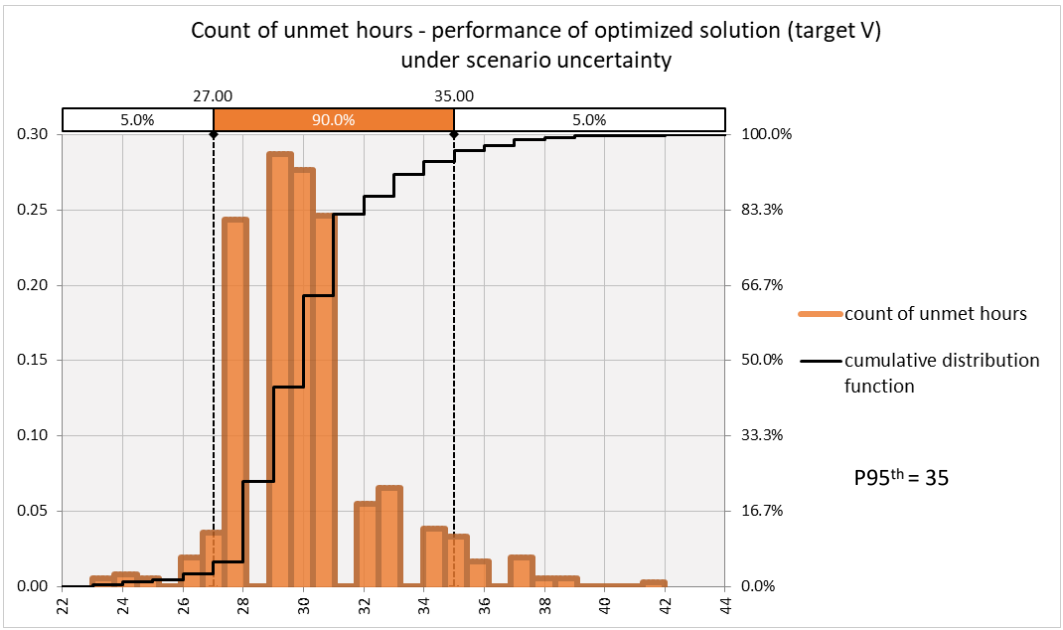

Figure 69 – Performance of optimized solution for TARGET V under scenario uncertainty

4.4.2.2 Parameter Uncertainty

The other set of uncertain inputs are related to the parameters more closely related to the thermal performance of the buildings, namely cooling COP and envelope U-values, which we are calling parameter uncertainty.

The variability of the cooling COP is represented in Figure 70, which follows a distribution skewed to the right, with mode equal to 3.95, and 90% of the values between 3.5 and 4.1. For the envelope U-values, we apply multipliers to the previously calibrated U-values for walls, windows and roofs. These multipliers follow the probability density function represented in Figure 71.

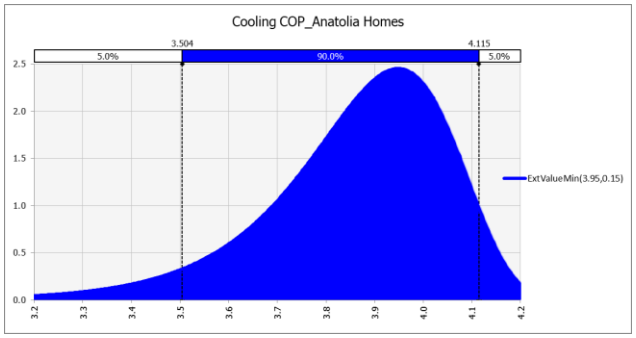

Figure 70 – Probability density function for cooling COP uncertainty

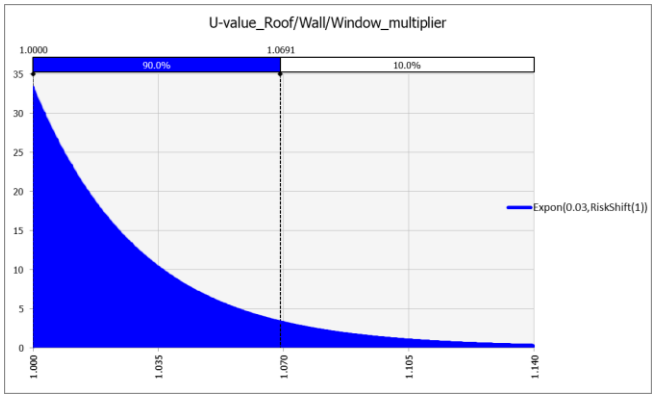

Figure 71 – Probability density function for envelope U-value multiplier

The performance of the optimal solutions under parameter uncertainty is depicted in Figure 72 to Figure 76. Considering the percentiles related to the allowable number for unmet hours for each target, we observe that those previously optimized solutions perform poorly when subject to relatively small variations in relevant building parameters. This is especially true for targets II and III, where only in 25% and 35% of the samples, respectively, the deterministic solution did not fail the tolerated number of unmet hours.

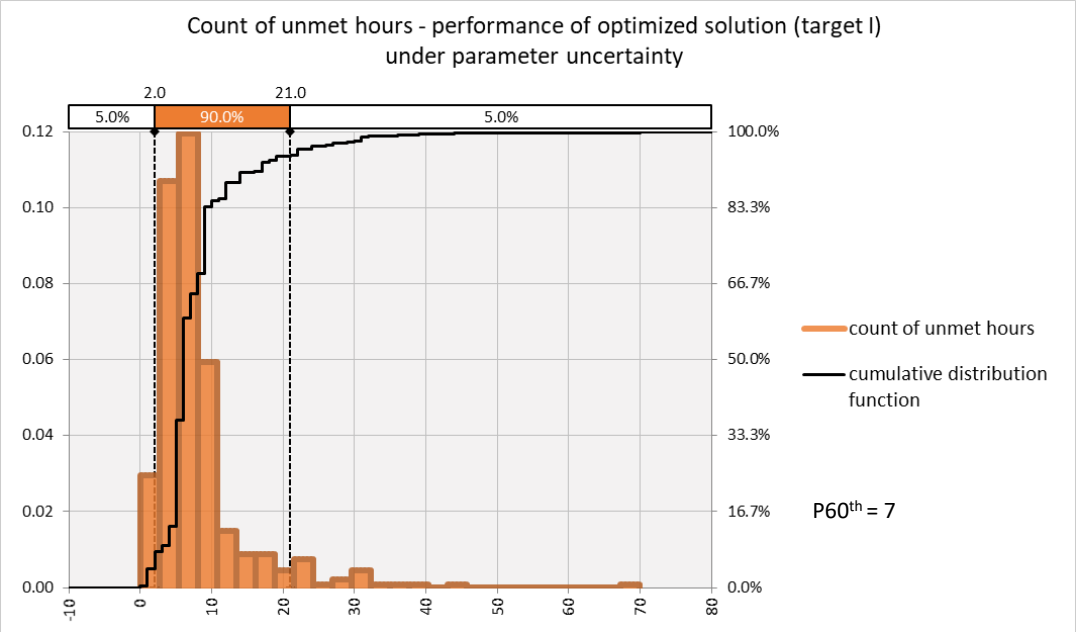

Figure 72 – Performance of optimized solution for TARGET I under parameter uncertainty

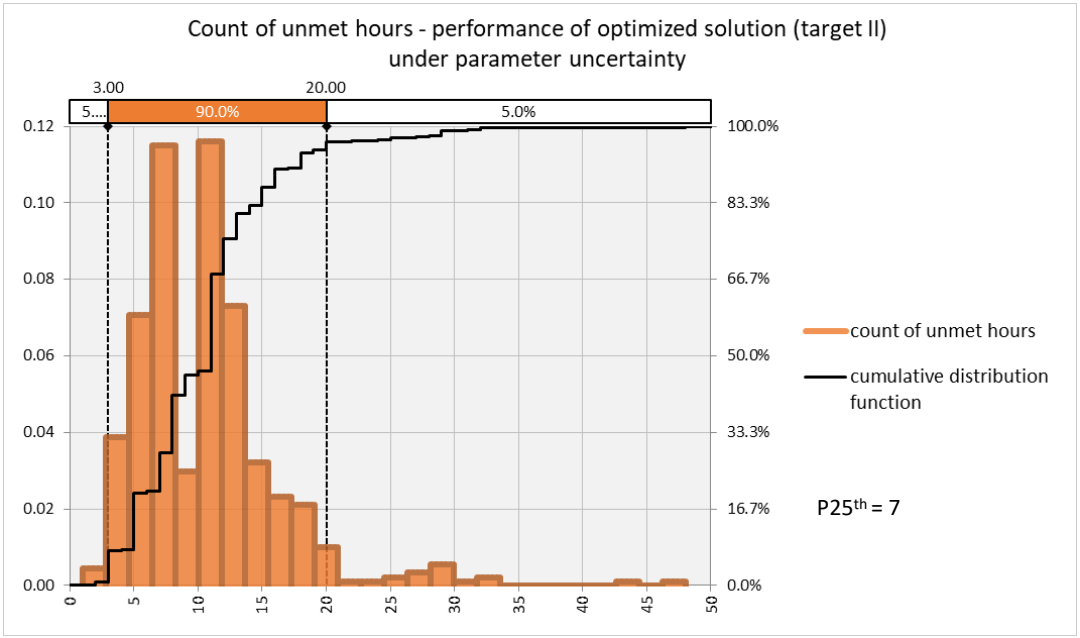

Figure 73 – Performance of optimized solution for TARGET II under parameter uncertainty

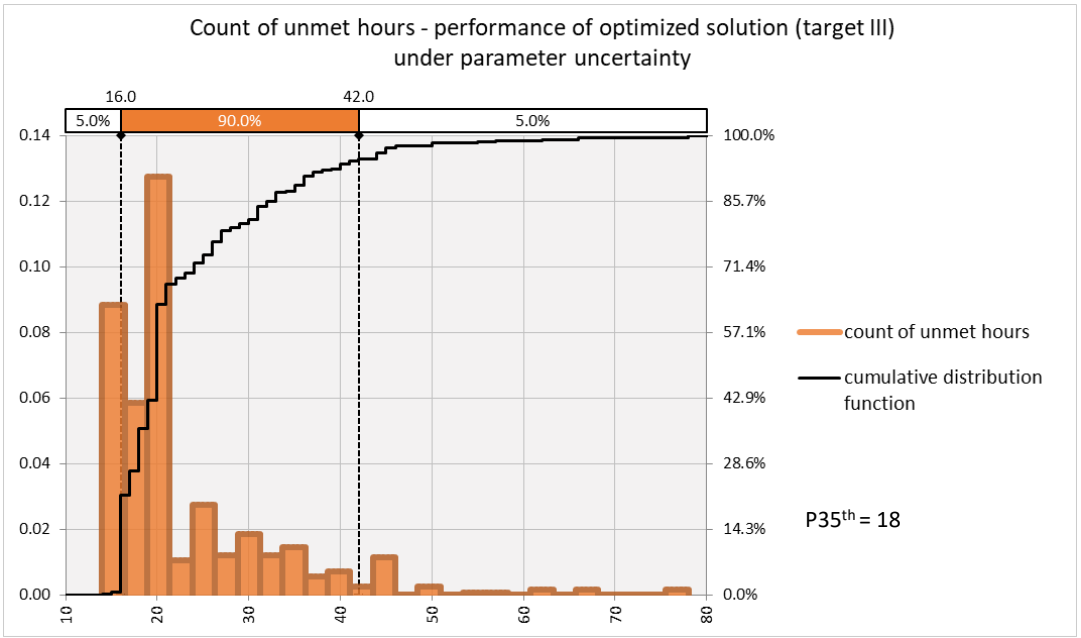

Figure 74 – Performance of optimized solution for TARGET III under parameter uncertainty

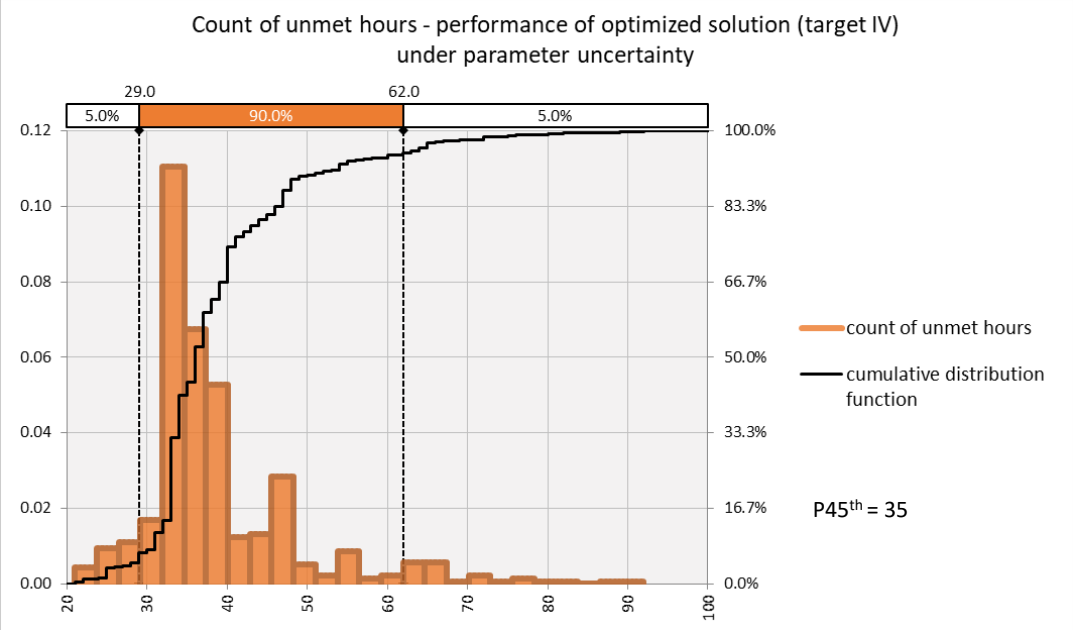

Figure 75 – Performance of optimized solution for TARGET IV under parameter uncertainty

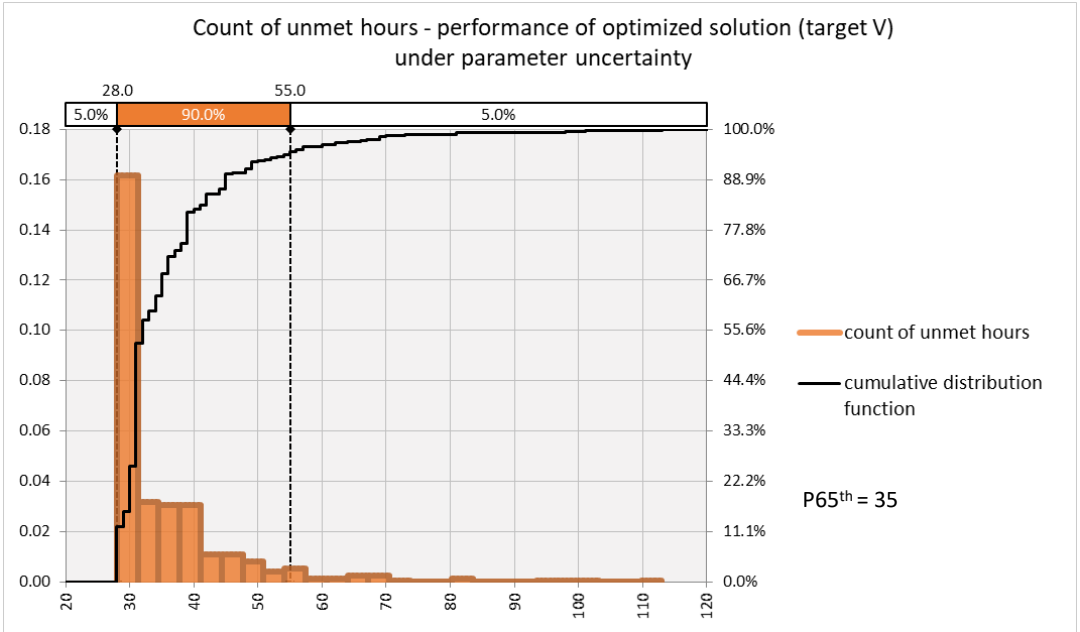

Figure 76 – Performance of optimized solution for TARGET V under parameter uncertainty

4.4.2.3 Combined Scenario and Parameter Uncertainty

To further test the performance of the optimized solutions, we carry out another round of simulations with both scenario and parameter uncertainty.

Figure 77 to Figure 81 show the results with the density distribution of the performance of the optimized solution over 500 samples. In these figures, we add the result of a sensitivity analysis in the form of tornado plots showing the relative importance of the uncertain inputs in each case.

Looking at the percentiles related to the allowable number for unmet hours for each target, we observe that the combination of scenario and parameter uncertainty did not alter in more than 5% the results previously obtained with parameter uncertainty alone. This indicates that the variability in the parameter inputs is most impactful on the outcomes. This is corroborated by the tornado plots, which show that the parameter "cooling COP" prevails in order of importance in all cases. Inputs related to scenario uncertainty, specifically related to the critical hours (see Table 9 for relationship) appear in second place, however with much lower impact on the outcomes.

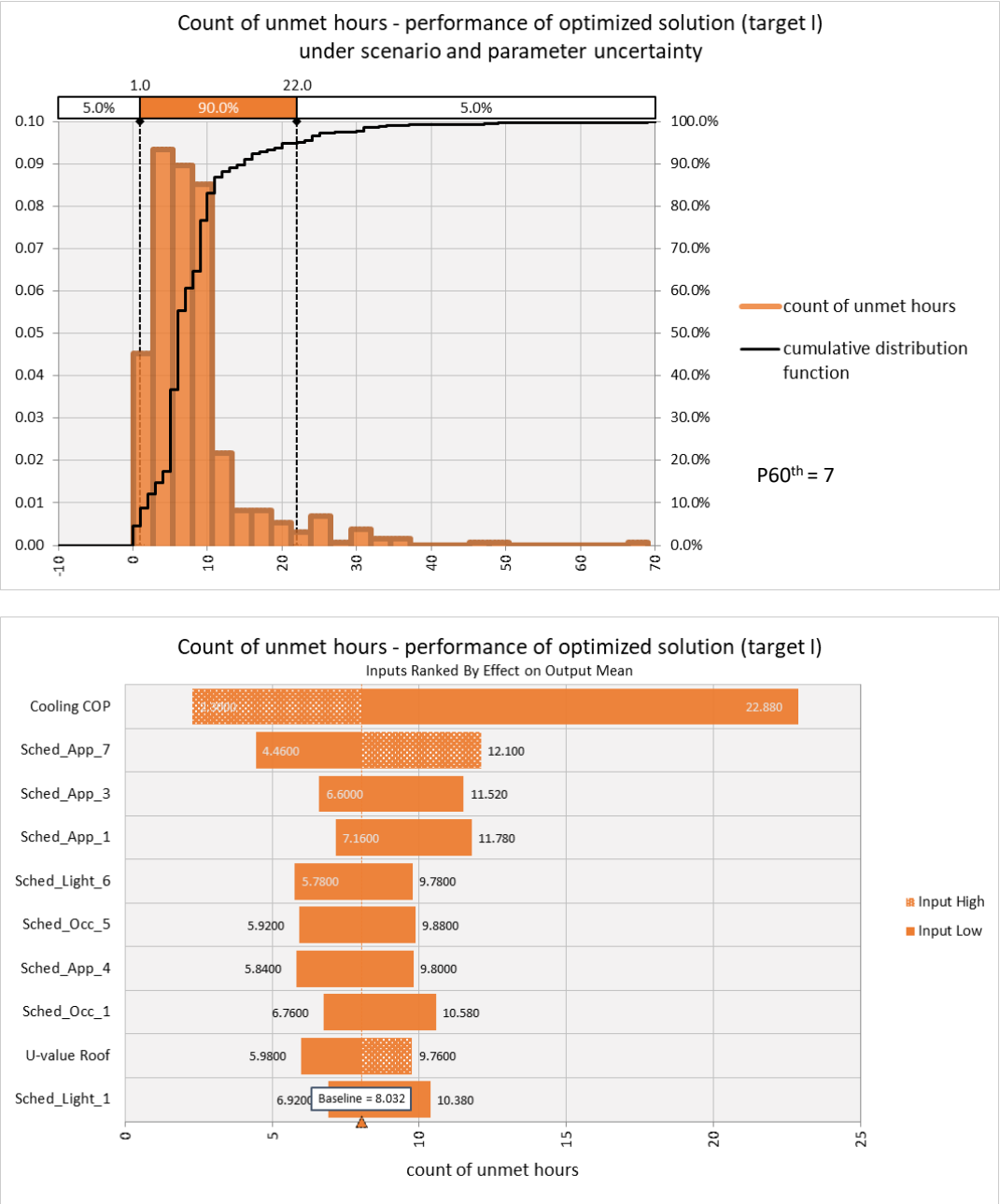

Figure 77 – Performance of optimized solution for TARGET I under scenario and parameter uncertainty (top: density distribution; bottom: sensitivity analysis)

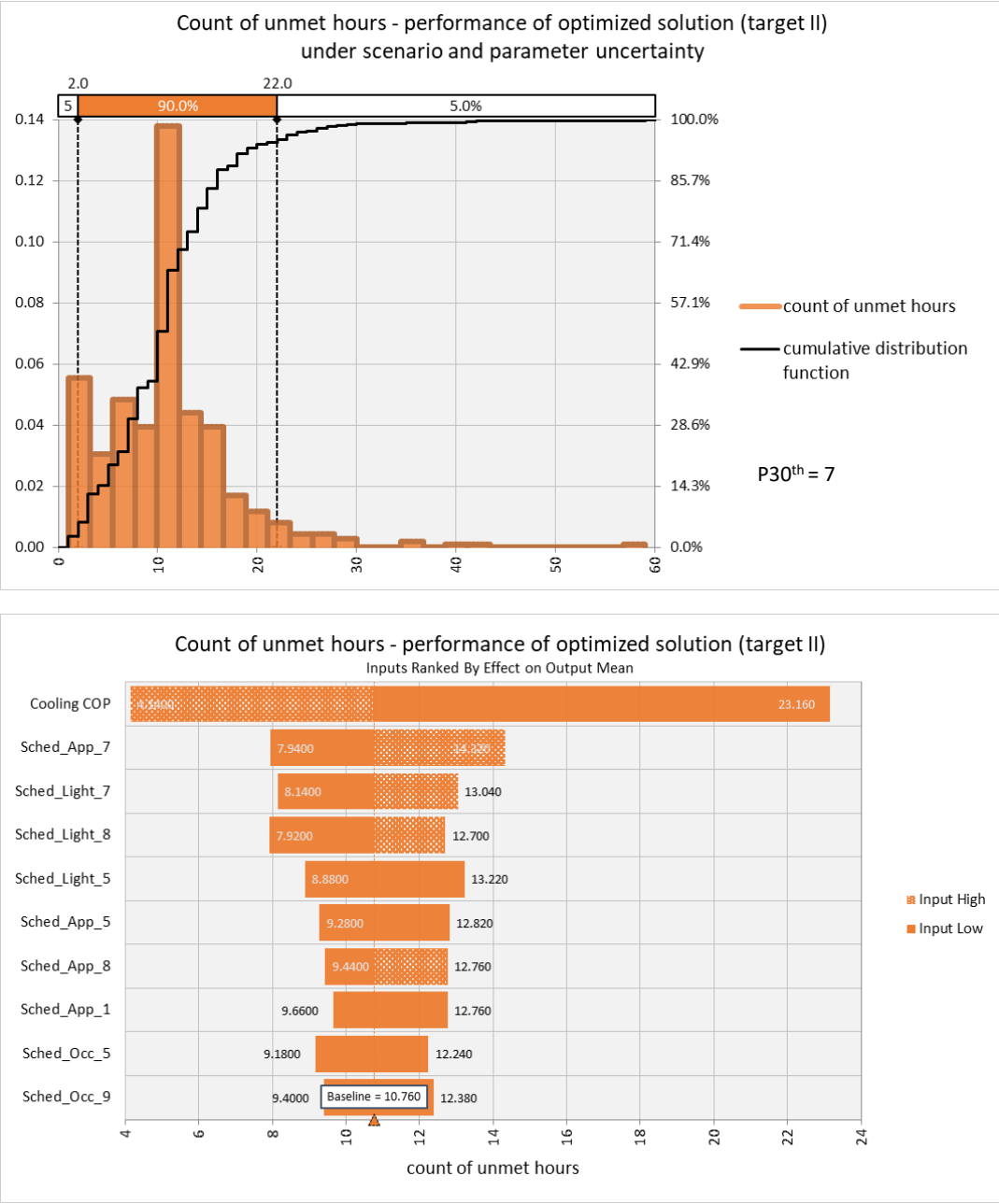

Figure 78 – Performance of optimized solution for TARGET II under scenario and parameter uncertainty (top: density distribution; bottom: sensitivity analysis)

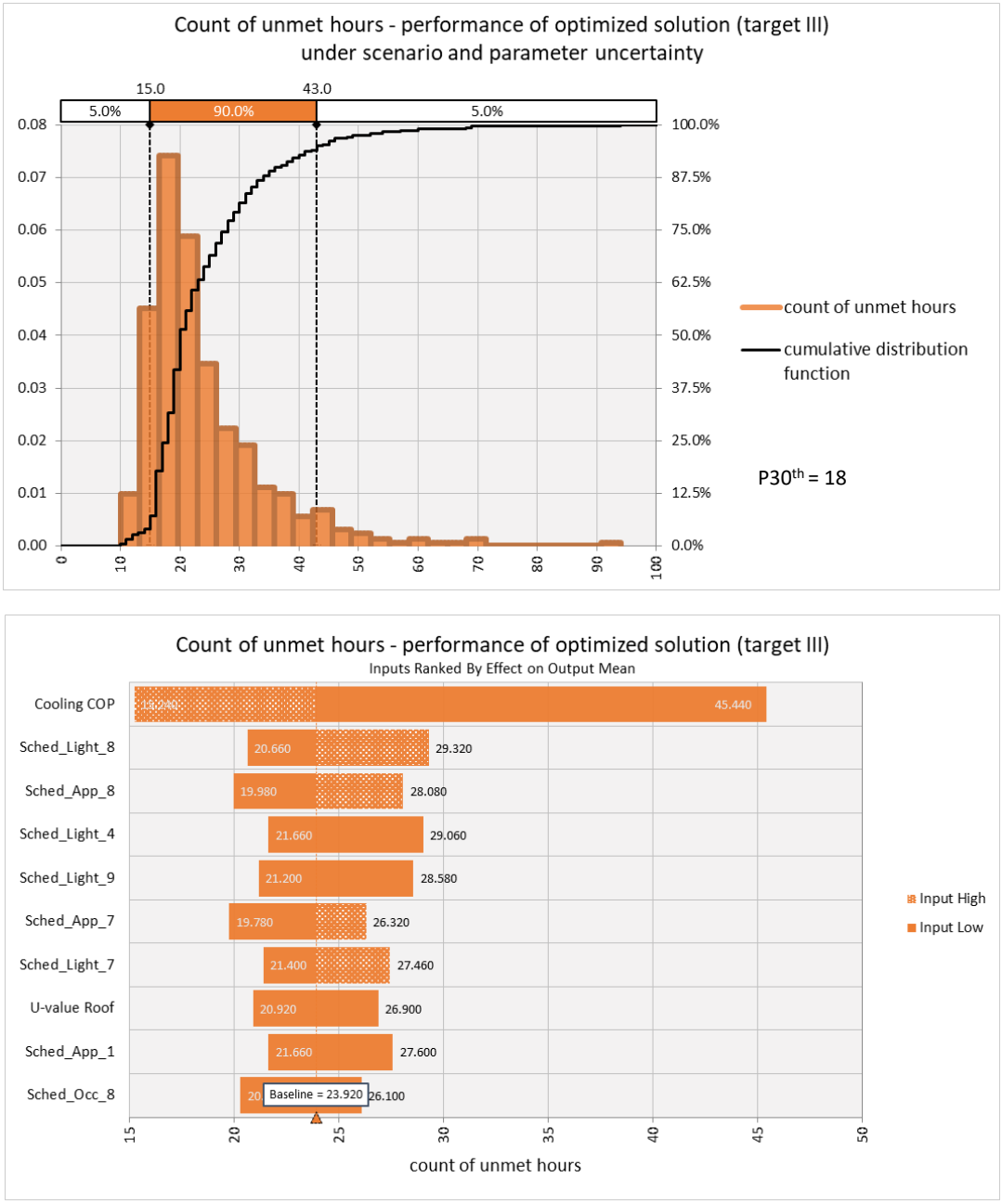

Figure 79 – Performance of optimized solution for TARGET III under scenario and parameter uncertainty (top: density distribution; bottom: sensitivity analysis)

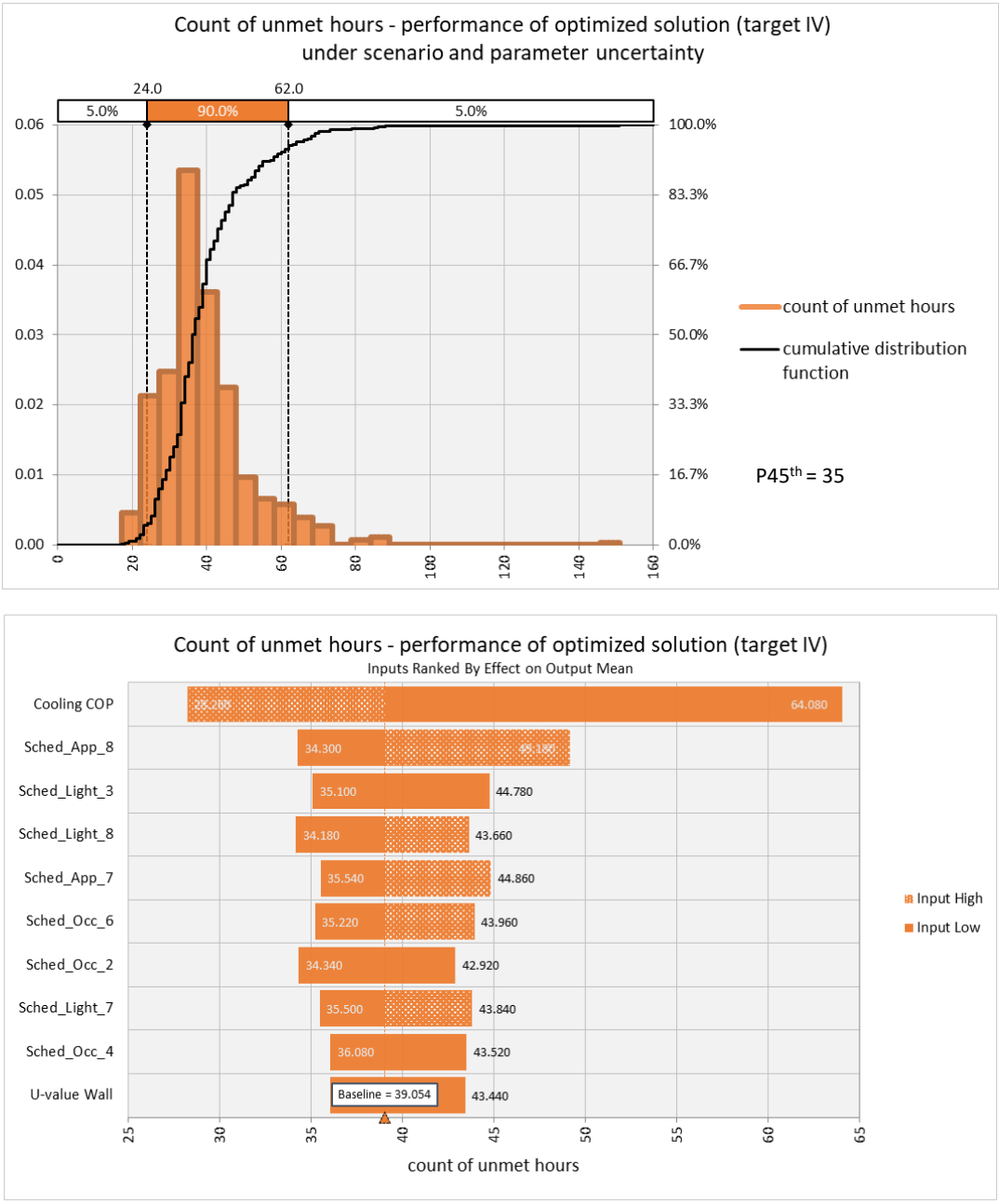

Figure 80 – Performance of optimized solution for TARGET IV under scenario and parameter uncertainty (top: density distribution; bottom: sensitivity analysis)

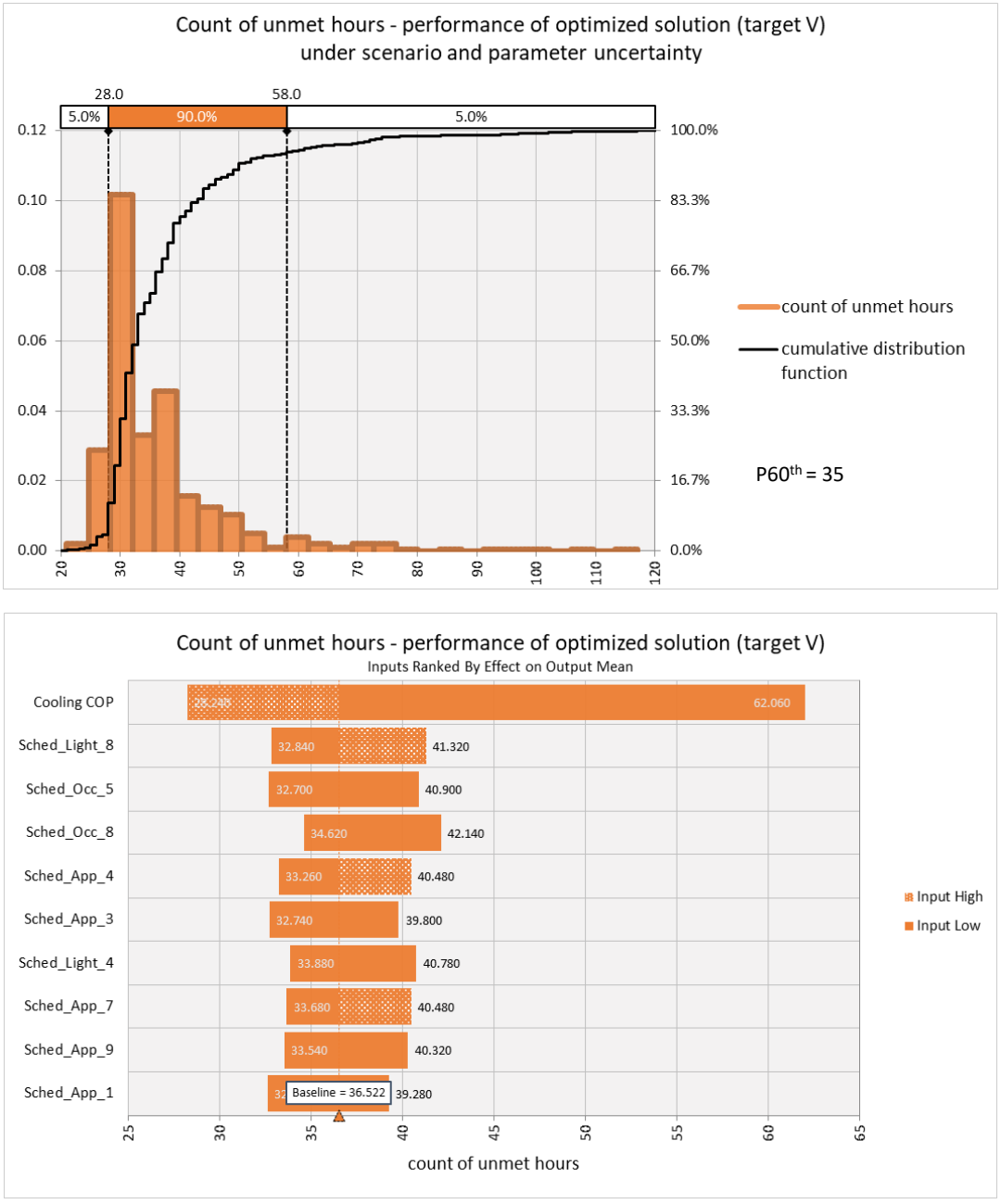

Figure 81 – Performance of optimized solution for TARGET V under scenario and parameter uncertainty (top: density distribution; bottom: sensitivity analysis)

4.4.3 Stochastic Optimization

In this section, we use stochastic optimization techniques to find solutions that are less likely to fail the system constraints in face of random variations in the inputs. This approach can potentially overcome the limitations of the deterministic optimization in terms of revealing underperformance risks of the proposed solution. In a stochastic optimization, we can specify our tolerances and the related risks of failure.

We select targets I, III, and V to test this approach, using the scenario and parameter uncertain inputs of the previous section as random inputs. In each stochastic optimization, we carry out 200 generations of potential solutions. In each generation, a population of candidates is tested through 50 random input samples. The goal is to find a solution with minimum percentile 95% for *PI*_2 (number of unmet hours). NPC_{tot} is thus constrained to 1.05 times the NPC_{tot} of the correspondent deterministic solution found in section 4.4.1. In other words, at every generation, the algorithm looks for the best fit solutions that yield the lower values of *PI*_2 within 95% of the input samples. At the end of the process, the best fit solution is selected.

It is important to note that this implies 10,000 trials (200 x 50) in which a small population of potential solutions is tested. In summary, this stochastic optimization requires several thousand simulations of the community energy model. It took on average around 19 hours to be completed with a computer with an intel i7 processor @2.70GHz and 12 GB of RAM.

Needless to say that this would be nearly impossible to be carried out with a high dimensionality model, which would result from the use of higher order building models. This would require huge computational power and/or days of simulation time.

When testing the obtained energy-storage solutions with an increased sample of 500 sets of random inputs, it is found that, for all three targets, the implementation of the proposed solutions yields a value of $P95^{th}$ for *PI*_2 that is lower than the maximum tolerable number of unmet hours. Next section shows how these solutions compare to their counterparts previously derived through deterministic optimization.

4.4.4 Comparison of Results

Table 15 and Figure 82 show the comparison of results for the solutions found from both deterministic and stochastic optimization approaches, where $P95^{th}$ represents the number of unmet hours that would be guaranteed by each solution in 95% of the possible situations

We observe that the solution derived from stochastic optimization results in a $P95^{th}$ well below the limit for Target I without implying significant additional cost.

Table 15 – Performance Comparison - Solutions for Target I (P95th ≤ 7).

Optimization approach	Solution (capacity ; discharge hours)	NPC_{tot} [US$]	Percentile 95th for *PI*_2 (500 samples)
Deterministic	Group A: 7kWh ; 17, 18, 20 Group B: 7kWh ; 17, 20 Group C: 7kWh ; 19, 20	$241,680	22
Stochastic	Group A: 7kWh ; 18, 19, 20 Group B: 7kWh ; 18, 20 Group C: 9kWh ; 19, 20	$244,440	1

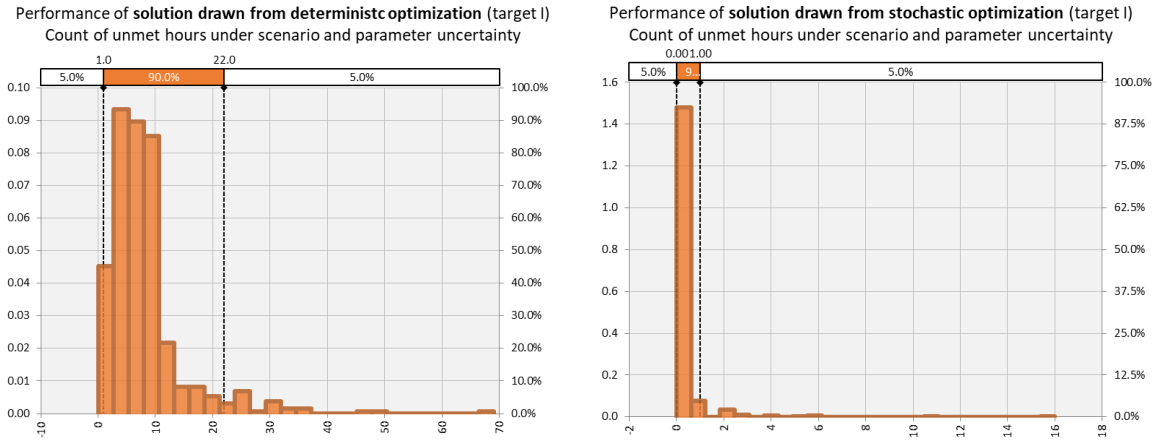

Figure 82 – Performance of solutions for TARGET I under scenario and parameter uncertainty (left: deterministic optimization; right: stochastic optimization)

Solutions for Target III are presented in Table 16 and Figure 83. Once again, the stochastic optimization finds a solution with better performance than its counterpart. It guarantees a P95th for *PI*_2 below the tolerable value of 18, with a relatively small cost addition.

Table 16 – Performance Comparison - Solutions for Target III (P95th ≤ 18).

Optimization approach	Solution (capacity ; discharge hours)	NPC_{tot} [US$]	Percentile 95th for *PI*_2 (500 samples)
Deterministic	Group A: 7kWh ; 19, 20 Group B: 8kWh ; 18, 19, 20 Group C: 8kWh ; 18, 20	$244,080	43
Stochastic	Group A: 7kWh ; 19, 20 Group B: 10kWh ; 18, 19, 20 Group C: 10kWh ; 18, 20	$251,920	17

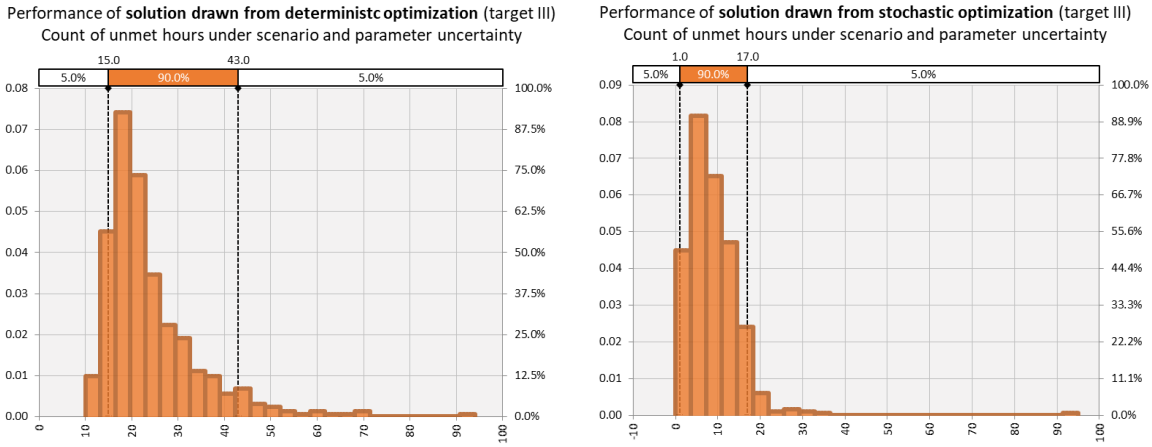

Figure 83 – Performance of solutions for TARGET III under scenario and parameter uncertainty (left: deterministic optimization; right: stochastic optimization)

Finally, Table 17 and Figure 84 present the comparison of solutions defined for Target V. As before, the stochastic optimization proves to be able to find a significantly better solution within the same cost range.

Table 17 – Performance Comparison - Solutions for Target V (P95th ≤ 35).

Optimization approach	Solution (capacity ; discharge hours)	NPC_{tot} [US$]	Percentile 95th for *PI*_2 (500 samples)
Deterministic	Group A: 11kWh ; 17, 18, 19, 20 Group B: 8kWh ; 18, 20 Group C: 10kWh ; 19, 20	$316,270	58
Stochastic	Group A: 11kWh ; 17, 18, 20 Group B: 11kWh ; 18, 19, 20 Group C: 10kWh ; 19, 20	$322,060	28

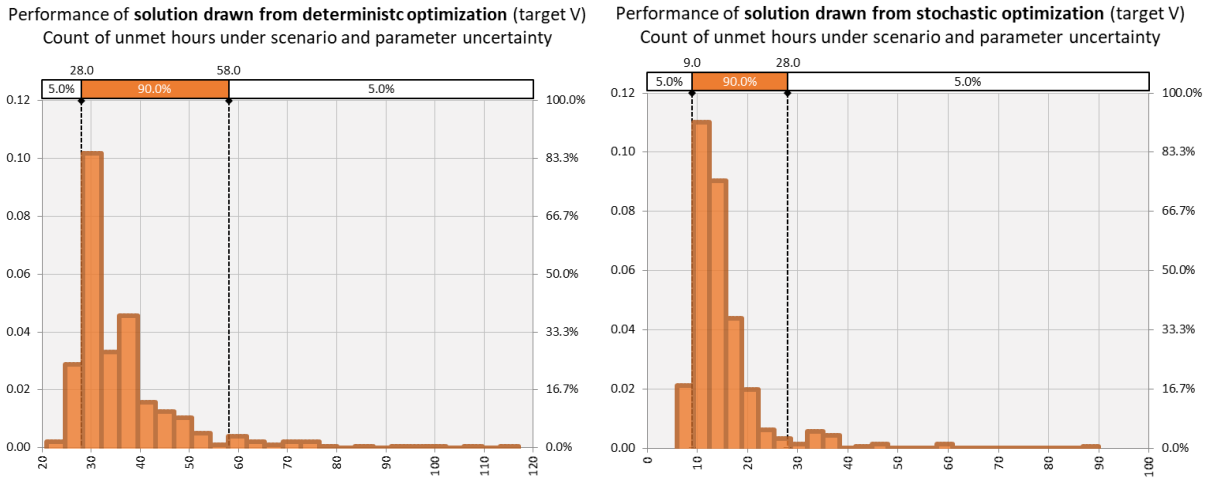

Figure 84 – Performance of solutions for TARGET V under scenario and parameter uncertainty (left: deterministic optimization; right: stochastic optimization)

4.5 Conclusions

This chapter demonstrates how the proposed reduced order approach can be used to model communities with practicality and reliability. With only scarce and general data, it proves possible to formulate and calibrate a community energy model that shows good fit with the outcomes of a real community in terms of hourly energy needs.

This gives us the capacity to explore different DER solutions and arrangements that could not be tested in the respective real scale pilot project.

The convenience of having a unique and comprehensive simulation platform enables us to apply and test different optimization techniques and uncertainty analyses that are rather unfeasible to be carried out with current mainstream modeling tools. This can be of great value for providing means for better and more informed decisions related to energy consumption and energy flexibility at the community scale.

CHAPTER 5. RELEVANT MEASURES OF ENERGY PERFORMANCE AT THE NEIGHBORHOOD SCALE

The previous chapters compared the applicability of the proposed reduced order modeling approach with detailed modeling and real-scale experiments. In this chapter, we take advantage of the unique modeling flexibility of the validated reduced order method to help define and test relevant measures of energy performance of multiple buildings and DER at the neighborhood scale. This directly addresses research question 3, as defined in section 1.3, rendering the EPC_NHood modeling framework a particularly helpful tool for designing and optimizing DER solutions for future communities.

5.1 Introduction

High expectations and great advocacy has been placed on the benefits of the integration of buildings and distributed energy resources in urban settings for improved energy efficiency, reliability, and resilience. Nevertheless, it is rare to find the appropriate means and methods to evaluate and quantify the performance of those integrations of buildings and energy resources.

Our proposed modeling approach is used in this chapter to support the evaluation of rational measures to verify the energy performance of a neighborhood with DER under uncertainty. More specifically, we propose the means to quantify and measure “community energy resilience”, and how to use it to evaluate the performance of different DER options in an integrated community.

With this investigative path, we address the third main research objective, in which we want to know whether our proposed modeling approach can be used to construct and test the means for quantifying key measures of energy performance at the neighborhood scale.

5.2 Community Energy Resilience

There is a growing interest in understanding and applying concepts of resilience to our urban spaces, usually motivated by external threats, such as natural disasters or terrorism, or by internal deficiencies related to population and energy demand growth along with decaying infrastructure. Nevertheless, the pursuit for local energy resilience often suffers from lack of appropriate knowledge and from the inability to adequately frame the problem and to engineer solutions.

More recently we have observed a crescent number of contributions that try to address those gaps, ranging from industry publications (Arup, 2015, Willis and Loa, 2015), white papers and reports (Ribeiro et al. 2015, Ribeiro and Bailey, 2017) and contributions from academia (Cutter et al., 2010, Molyneaux et al., 2014), only to cite a few. However, the definitions, indicators, and measures presented in those studies are in most part subjective or rather generalist. This lack of clarity and objectivity hinders us from properly formulating design problems in which we want to create energy resilient communities.

In face of the above-mentioned research deficiencies, this thesis intends to bring a valuable contribution for defining and measuring community energy resilience. In this

context, we are specifically interested in investigating the capabilities that physically connected buildings and DER can provide for sustaining power to a neighborhood during outages. The evaluated scenarios can range from short-term operational outages (lasting a few hours) to natural disasters and major events (lasting a few days).

For this case, we are calling "community energy resilience" as the main performance measure to be pursued, which is calculated as a function of the number of self-sustained hours of power supply during an outage and their respective convenience levels.

The Miami community energy model developed in section 3.3 is used in this application. The DER solutions that were previously used for peak-load reduction are now tested with regards to community energy resilience. For simplicity, we assume that the community is provided with hardware capability to be islanded during an outage event.

Using the flexibility of our simulation platform, the building models belonging to the community respond to the occurrence of an outage by reducing load demand by adjusting the use of lighting, appliances, and by changing thermostat settings. Energy generation and storage are also deployed to maximize the number of self-sustained hours. As the outage continues and the resources deplete, the buildings can self-adjust their loads to less demanding (hence less comfortable/convenient) usage patterns. These patterns are predefined and labeled into different convenience levels.

In a first step, this experiment allows the testing of control algorithms for building demand response and the formulation of problems aimed at maximizing battery charge/discharge operation. In the following step, different combinations of DER –

including PV size, battery size, and demand response – are simulated and the number of sustained hours and the corresponding convenience levels are computed in a rational formula that yields an energy resilience measure for each case.

In order to compare alternatives for improving power resilience, the premium cost of the implemented microgrid system with DER is considered. With these two PIs (power resilience and premium cost), informed decisions can be made in relation to which technological options to choose to improve the resilience of the neighborhood under cost constraints.

5.2.1 Modeling and Measuring Resilience

As a rational way to quantify community energy resilience, we propose a performance indicator (PI_3) that is calculated through Equation 29. With this measure, we can attribute different weights for each possible convenience level of building usage to be experienced during the outage.

$$PI\_3 = \frac{(1 \times \sum Hr1) + (0.75 \times \sum Hr2) + (0.5 \times \sum Hr3) + (0 \times \sum Hr4)}{Tot\ Hr} \quad (29)$$

Where:

$\Sigma\ Hr\ \boldsymbol{i}$ = number of sustained hours with convenience level $\boldsymbol{i}$ (for $i = 1, \ldots, 4$);

$Tot\ Hr$ = total number of hours during the outage.

The convenience levels are defined according to Table 18, where the adjusted building usage patterns are indicated. The best possible outcome is $PI\_3 = 1$, where all hours are sustained at level 1. On the other end, $PI\_3 = 0$ represents the worst performance, where level 4 is maintained in all outage hours, which means that there is no self-supplied energy at any time.

It is worth mentioning that those adjustments are intentionally generalized, with the sole objective of providing the desired scenarios for the simulations. It is out of the scope of this research to propose the appropriate convenience levels for each building type and location. We are mainly interested in developing the appropriate modeling tool and means of quantification that can be later used, among other applications, to refine the adequate patterns of building usage for each level.

Table 18 – Convenience levels and respective building usage patterns.

Types of adjustments (compared to the default schedules)	Level 1	Level 2	Level 3	Level 4
Thermostat temperature delta adjustment (– for heating setpoint; + for cooling setpoint) [ºC]	1	2	3.5	No heating No cooling
Level of usage of lighting	50%	30%	15%	0%
Level of usage of appliances	50%	30%	15%	0%
Level of usage of DHW	50%	30%	15%	0%

5.2.2 Performance of the Miami Community Model DER Solution

The transition between levels during the outage takes place in our community model at every hour based on intelligent controls that are embedded in the modeling platform. These controls look for the previous patterns of energy consumption for those typical days, as well as the expected availability of DER for that actual day. As existing (battery storage) and expected (solar PV) energy resources diminish, the pattern of building usage for the current hour is adjusted to an appropriate level. As there are more resources available, and the usage level is very low, the controls adjust back the patterns of usage to more convenient levels.

The algorithm tries to optimize the usage of the available resources by raising the level of usage during high solar production, thus saving the stored energy. During times of low or no PV production, the algorithm allows a low pattern of building usage, to be sustained from the batteries, trying to avoid their quick depletion. In some situations, there is energy use from both PV and batteries. The decision-making intelligence embedded in the community energy model creates a peculiar situation in which iterative calculations take place within the building model simulation.

To test this modeling formulation, we use the DER solution described in Table 7, which was initially developed for peak-load reduction. Now we want to check how this DER implementation performs in providing community energy resilience under three outage situations: 4-hour; 24-hour; and 48-hours outages. This is repeated for both typical winter day and typical summer day.

For this analysis, we assume that the batteries are fully charged before the outage, and are used to provide energy to the community and to absorb any energy excess from solar PV.

Figure 85 to Figure 87 present the results obtained in these simulations. The gray curve represents what would be the typical pattern of energy consumption without outage. The green is the realized energy consumption with the DER resources. The dotted blue line refers to the right axis and represents the changes in convenience levels during the outage. The yellow and blue bars represent the sources of energy provided for the adjusted building usage during the outage.

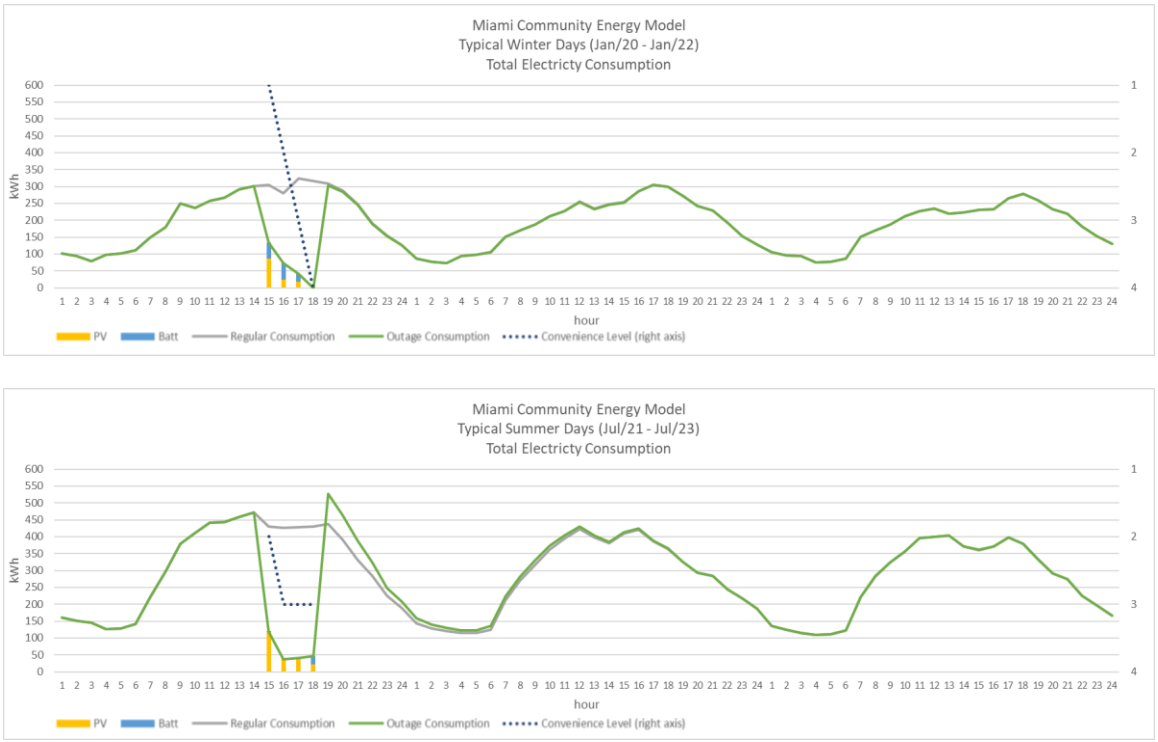

Figure 85 – Performance DER solution for providing "community energy resilience": 4-hour outage

(top: typical winter day [*PI*_3 = 0.56]; bottom typical summer day [*PI*_3 = 0.56])

From Figure 85, we observe that different choices of convenience levels are made in the two cases. For the typical winter day, the battery resource is totally explored as the community has low solar generation. The level of convenience is continually changed from 1 to 4, still allowing for *PI*_3 = 0.56.

In the typical summer day, both the higher demand for cooling and the higher solar generation allow for mid-range choices for convenience levels during the outage, thus sustaining a relatively high overall *PI*_3 (also equal to 0.56) without depleting the battery.

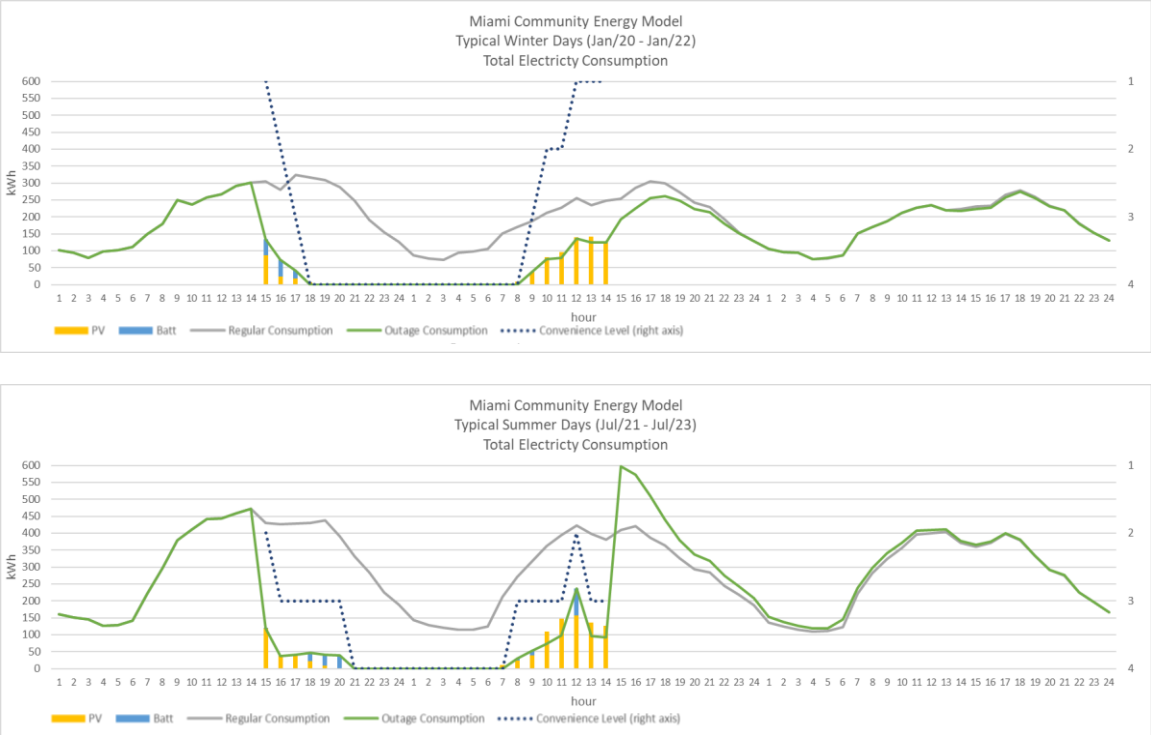

Figure 86 – Performance DER solution for providing "community energy resilience": 24-hour outage

(top: typical winter day [*PI*_3 = 0.30]; bottom typical summer day [*PI*_3 = 0.29])

In the 24-hour outage illustrated in Figure 86, similar values of *PI*_3 are achieved in the winter (0.30) and summer (0.29) cases. In the first situation, the resilient system quickly recovers in the first daylight hours of the second half of the outage, allowing crescent levels of convenience without depending on the battery, which is already depleted.

The summer case maintains mid-range choices for convenience levels in the second half of the outage, optimizing the use of both solar and storage resources. It is interesting to note that the battery alternates charging and discharging operations in the second part of the outage, helping to maintain a good balance of building usage throughout the crisis.

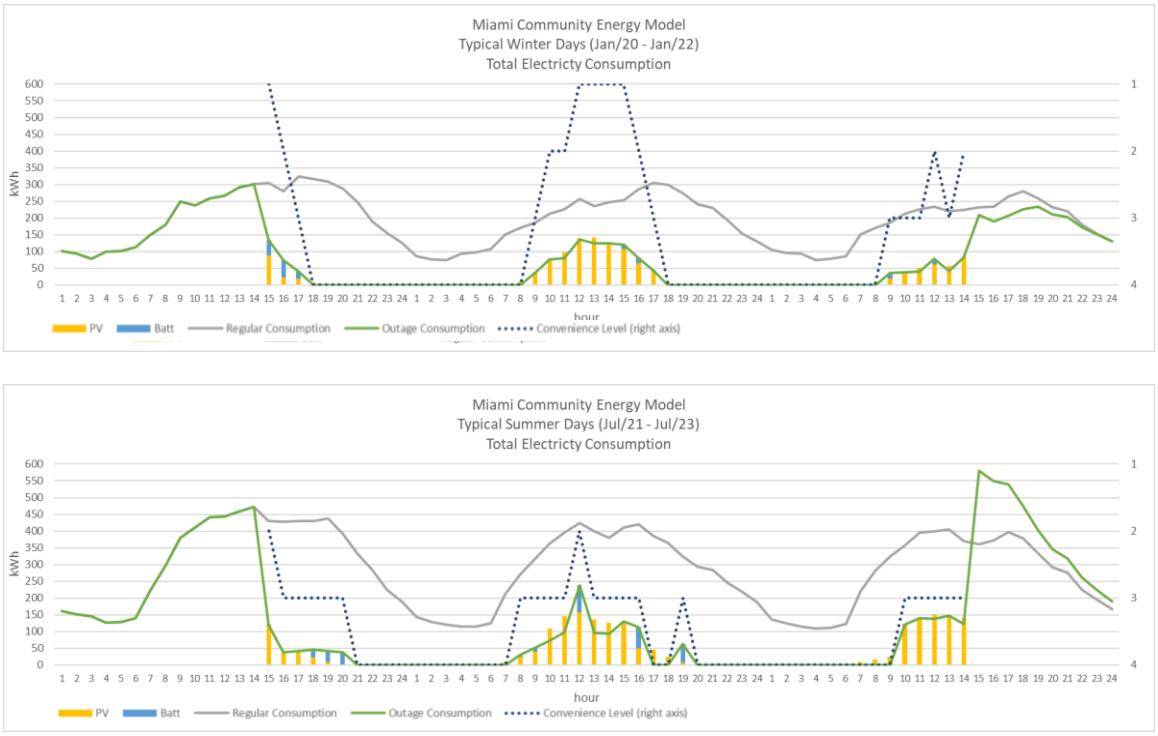

Figure 87 – Performance DER solution for providing "community energy resilience": 48-hour outage

(top: typical winter day [*PI*_3 = 0.27]; bottom typical summer day [*PI*_3 = 0.23])

Finally, the 48-hour outage as depicted in Figure 87 is relatively well managed by the DER system in both winter and summer examples, with a slightly higher value of $PI\_3 = 0.27$ in the first case, compared to $PI\_3 = 0.23$ in the latter.

Higher convenience levels are sustained in the mid-part of the winter outage due to favorable conditions of fair solar generation and lower cooling demands.

For the typical summer day, we see that the storage resource provides an efficient complementation of the solar generation resource, thus boosting the level of building usage in key hours, especially in the mid-part of the outage.

5.2.3 Stochastic Optimization for Improved Resilience

In this section, we want to test the EPC_NHood model using a more sophisticated and yet manageable approach to find a DER solution that is specifically designed to improve the community energy resilience (PI_3). For such exercise, we use a stochastic optimization that searches for the appropriate combination of solar and storage resources to achieve a predefined lower limit of PI_3 at minimum cost.

To set up the stage for this optimization, we define the acceptable lower limit of community energy resilience as $PI\_3 \geq 0.20$ for a summer outage of 48 hours. This means that at least an equivalent of roughly 20 hours are sustained at convenience level 3. Within the stochastic optimization, we want to find a solution that complies with the desired minimum PI_3 at least in 80% of the samples.

The possible DER implementation choices range around a virtually unlimited number of combinations of battery units and PV panels. The measure of cost is the same used in 3.3.4, which refers to the net present cost (NPC) of the selected DER combination.

Using cloud cover variation as our key uncertain input, we add a stochastic ingredient to the optimization problem. This variation directly affects the amount of direct solar radiation on the solar panels, which we are calling “solar radiation uncertainty”.

To define the probabilistic density function for solar radiation uncertainty, we first look at the observed pattern of variation for this input for that location and for that season. Figure 88 shows the curves of minimum, average, and maximum hourly values for solar radiation incidence over a south-oriented surface with 30º tilt. These values are drawn from the TMY3 climate data concerning the months of June, July, and August. The dashed lines are the resulting maximum and minimum values obtained through a function derived from the product of the average data values and a multiplier.

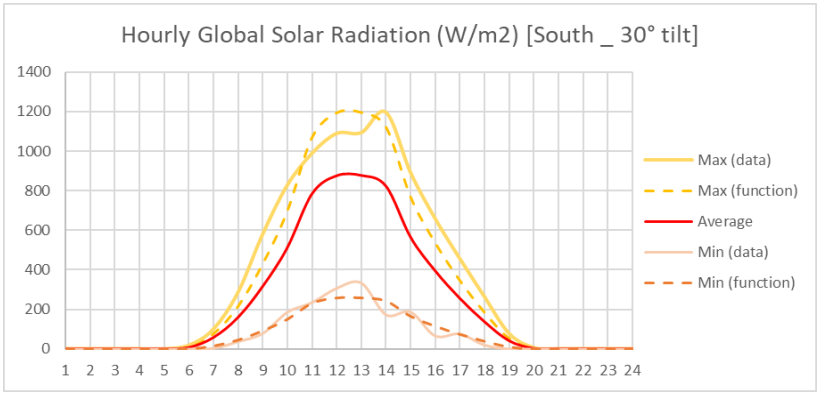

Figure 88 – Hourly global solar radiation onto PV panels facing south with 30º tilt, during summer days and under the influence of cloud cover uncertainty

As random simulation inputs, the sets of hourly values for solar radiation vary at each simulation within the max and min boundaries showed in Figure 88. This random variation follows the probability density function defined in Figure 89.

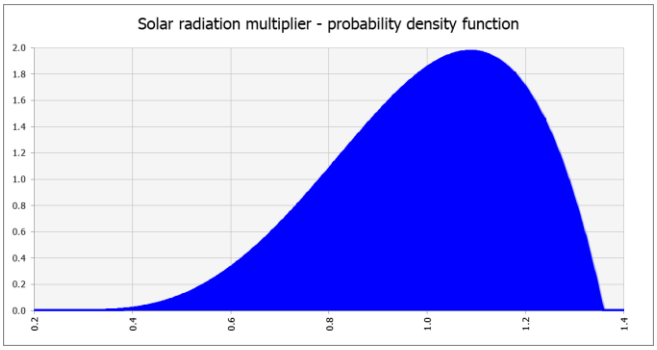

Figure 89 – Probability density function for the solar radiation multiplier

For this stochastic optimization, a best fit solution is found within 70 generations, as illustrated in Figure 90. At every generation, a small population of potential solutions is tested against 30 samples of solar radiation inputs. In each one of these thousands of EPC_NHood simulations, an iterative process takes place within the simulation platform in order to mimic the decision-making process of convenience level choices necessary to calculate *PI*_3. All of this with a total runtime of approximately 15 hours, using the same processing power as before (intel i7 processor @2.70GHz and 12 GB of RAM).

The optimized solution consists of a combination of 1,752 m^2 of solar PV panels, and 97 kWh of gross battery capacity. This amounts to NPC = US$ 863,180, which is only slightly more expensive than the previous solution, which was tailored for *PI*_1 at US$ 851,290 (see Table 7).

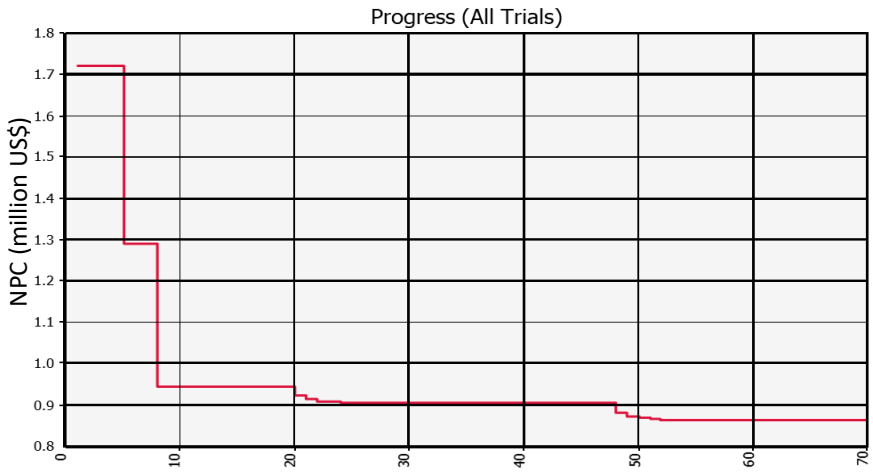

Figure 90 – Evolutionary progress of DER alternatives during the stochastic optimization

To test the reliability of this DER solution, a broader set of simulations under solar radiation uncertainty is carried out with 500 input samples. The results are presented in Figure 91, and they confirm that the solution complies with $PI\_3 > 0.20$ at least in 80% of the samples.

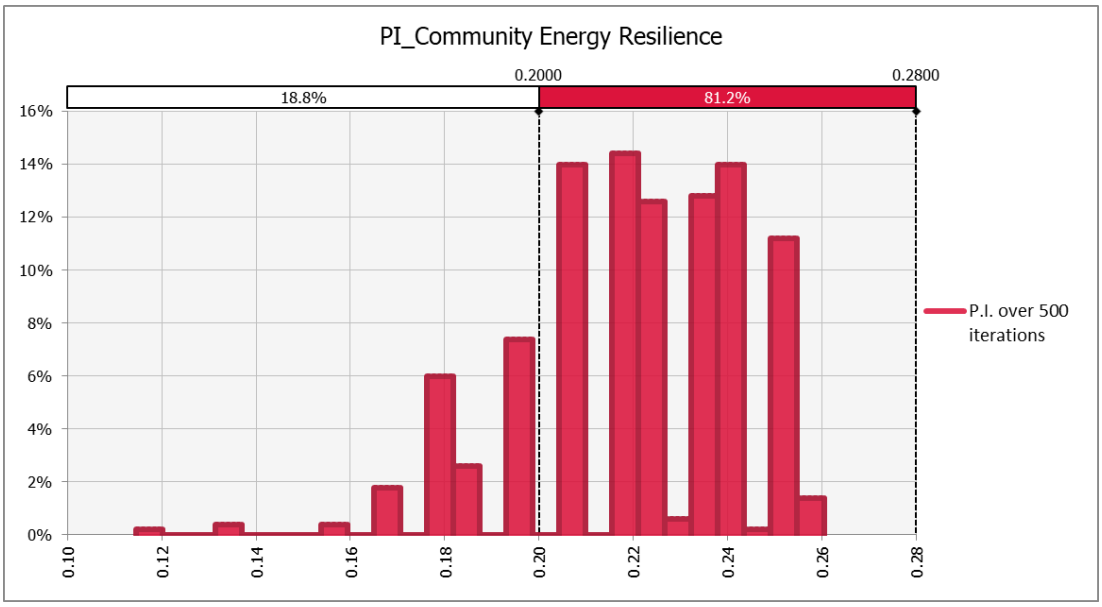

Figure 91 – Performance of optimized DER solution under solar radiation uncertainty

Finally, we examine the performance of the optimized DER solution in a typical summer day 48-hour outage. From Figure 92, we observe that the smaller storage capacity still provides a fair support to the much larger PV array, allowing for convenience level 2 to be achieved a few times. For this typical day, *PI*_3 equals 0.24.

Figure 93 gives us a sense of the impacts of the outage on the indoor temperatures. Calculated for the residential building during the outage, these curves enable the comparison between the indoor temperature without any system (gray line) and the temperature with the resilient system. We note that the resilient system implementation can hold the interior temperatures to levels fairly below the ones observed in the unsupported condition. The resilient system guarantees an indoor temperature below 27.4º C during the times when the outside temperature is higher than 30º C. This would not be possible without the optimized resilient solution, where the indoor temperatures (gray line) reach values above 28º C during more than half of the outage hours. This is an important question of public safety that, when not properly addressed, can subject vulnerable people indoors to unbearable temperatures during longer outages.

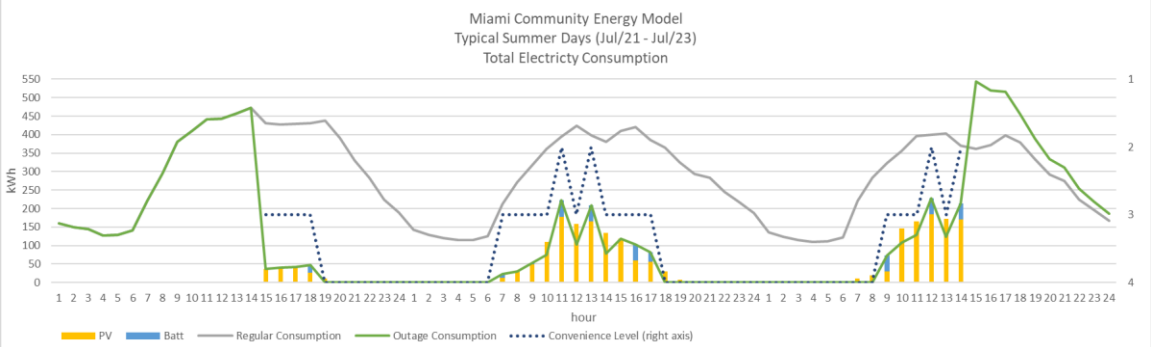

Figure 92 – Performance of optimized DER in a typical summer day 48-hour outage

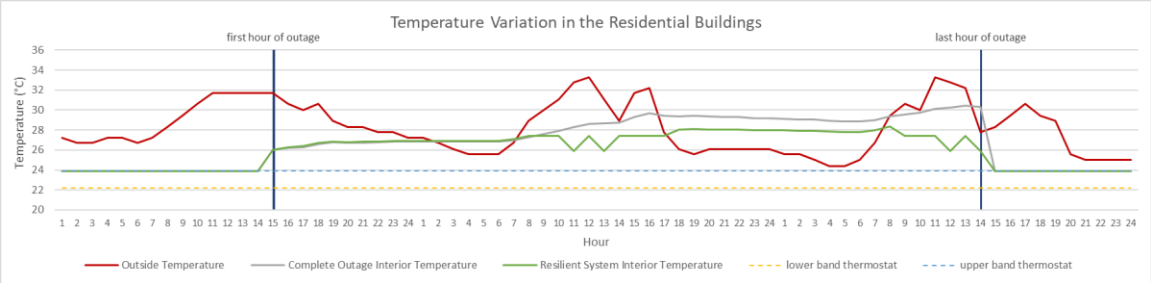

Figure 93 – Temperature variation in the residential buildings in a 48-hour outage

5.2.4 Conclusions

The assessment presented in this chapter gives us a clear demonstration of how the EPC_NHood platform can support the definition and quantification of novel indicators of performance at the community scale. In this context, we present the "community energy resilience" as a key measure for implementing energy-resilient solutions in our built environment. Our proposed quantification approach for community energy resilience can be further explored to provide more customized convenience level thresholds for different locations and building types.

This modeling platform can also be used to carry out more comprehensive optimization analyses where we can target varied sorts of performance indicators, as well as handle uncertain inputs with great transparency.

Finally, in the wake of recent natural disasters that struck the southeast portion of the United States, the Miami case study becomes especially important. With our experiment, we demonstrate that our modeling tool can be used to analyze conditions and find solutions related to unbearable indoor temperature conditions during and after natural disasters.

5.3 Community Energy Flexibility

As stated before, we understand "energy flexibility" as the building's ability to temporarily modify its pattern of energy demand to meet specific targets by deploying different demand-side strategies and resources. Due to the associated demand shaping capabilities, energy flexibility can potentially leverage several benefits in terms of energy usage in neighborhoods. In a prosumer context, this flexibility can be used either for reducing the local peak consumption or for deploying a virtual power plant to the main grid.

Though regarded as a relevant strategy to match building energy consumption with energy generation, there is lack of comprehensive knowledge about the magnitude and the behavior of the energy flexibility that buildings can provide (Jensen et al., 2017). An ongoing project was launched in 2014 by the Energy in Buildings and Communities Programme International Energy Agency (IEA-EBC) specifically tailored to address and demonstrate how energy flexibility in buildings can provide generation capacity for energy grids, which is known as "EBC Annex 67: Energy Flexible Buildings" (IEA, 2017b).

A few studies have proposed methodologies for defining and quantifying the energy flexibility of buildings, as presented in Bode et al. (2017) and Lopes et al. (2016). More recently, Zhang (2017) assessed the optimal management of energy flexibility in commercial buildings for reducing demand charges. Such studies are mainly focused on building thermal storage and electric load operation shifting as means for enabling energy flexibility in building.

There is a void in the current literature with regards to the integration of buildings and distributed energy resources for providing energy flexibility at larger scales. This understanding is fundamental to properly evaluate the potential of energy flexibility for providing services to the electric grid. This section provides a path for addressing this knowledge gap at the community scale. With this aim, we carry out a case study over the Anatolia model previously developed in CHAPTER 4.

In this study, we demonstrate the applicability of our reduced order modeling approach for modeling and testing the integration of buildings and diverse DER options for achieving the desired community energy flexibility at minimum cost.

5.3.1 Modeling and Monetizing Energy Flexibility

The Anatolia solar smart residential community was already designed with a combination of features related to energy conservation and efficiency, such as solar generation, efficient envelope and systems, efficient lighting and appliances. Nevertheless, the average occupancy profile in the neighborhood results in peak demand at later hours, particularly after 5pm when the solar generation is not significant anymore. As observed in CHAPTER 4, home-battery solutions were tested to address this issue by alleviating the community demand during “super-peak” hours. The costs associated with the implementation of home-batteries are still high, which makes such technological alternative not attractive in many instances, at least not yet at the current battery costs.

In this section, we combine different DER strategies for providing the desired energy flexibility to reshape the load profile of the Anatolia community. This study takes the utility's side, which wants to find the minimum-cost solution for achieving the targeted energy flexibility.

Besides home-batteries, we are considering building demand response (DR), and the use of the available stored energy in EV batteries for feeding back electricity to their homes via vehicle-to-home interaction (V2H).

The DER options in the community model in this assessment are set up as follows:

(i) each home can deploy separately a DR operation mode during the super-peak hours by reducing appliances and lighting usage;

(ii) individual home-batteries can be applied to groups of five homes;

(iii) individual V2H operation can be applied to groups of five homes. In this case, we are assuming that only 10 out of the fifteen homes have EVs available for V2H.

With this configuration, each home can be used separately for DR with its own level of resulting usage reduction. However, we assume that the implementation of individual home-batteries and V2H operations can only happen in groups of five homes. This constraint is to provide a lower freedom of customization when finding the optimized solutions, since one might face similar limitations in real scale programs driven by a utility company.

The DR scheme is co-simulated in each building model belonging to the EPC_NHood. It is triggered whenever a "signal" is sent to that building model, thus causing the reduction of lighting and appliance usage in critical days.

The home-battery is charged during off-peak hours and then used for local discharge during the super-peak hours when a DR signal is sent. It alleviates the energy consumption of the respective building, after the DR intervention. The optimal discharge hours for each group of five homes are defined according to the more stringent stochastic optimization case simulated in 4.4.3 (see Table 17).

After the deployment of DR and home-batteries, the vehicle-to-home scheme takes place. V2H is available for only ten homes in the community, as to represent a more limited scenario for this technology in a near future. The share of EV battery capacity available for V2H is assumed to be 8.4 kWh. The discharge hours, which depend on the presence of the EV at each home during the super-peak hours, vary according to Table 19. These assumptions for V2H operation in the ten homes are based on the study carried out by Kono et al. (2017).

As a rational way to quantify community energy flexibility, we use a performance indicator (PI_4) that is calculated through Equation 30. It monetizes the combined implementation of several possible modes of energy flexibility solutions.

$$PI\_4 = NPC_{HB} + NPC_{V2H} + NPC_{DR} \quad (30)$$

Where:

NPC_{HB} = net present cost of home-battery solution (implementation cost for a 5-yr life cycle);

NPC_{V2H} = net present cost of reimbursement for EV battery usage as V2H (valued at 1/5 the battery replacement cost);

NPC_{DR} = net present cost of assigned DR credits (valued at 3x the avoided electricity consumption, before DER, during the super-peak hours in a 5-yr period).

*PI*_4 is calculated for a cycle of five years. The specifications and cost per kWh of the home-battery solution are the same as assumed in 4.4.1.

For the V2H scheme, we assume a cost for the utility company equal to 20% of the total cost of a regular EV battery replacement (estimated at US$ 6,000). This is to reimburse the EV owner for the additional cycles of battery operation during the 5-year V2H program.

Finally, the DR program assigns credits to the household participating in the program. As an incentive for participation, these credits are calculated as three times the tariff value of the avoided energy consumption during the super-peak hours with relation to the expected demand for those hours. The avoided load is calculated before the intervention of the batteries, so that the credits are only related to the inconvenience placed on the household with regards to appliance and lighting usage.

Table 19 – DER options for Energy Flexibility and related costs.

DER Options	Deployment	Specification	NPC [US$]
Home-battery	Group A Homes: 1, 3, 4, 8, 9 7 kWh each	Discharge hours: 17, 18, 20	**15,750**
	Group B Homes: 5, 11, 12, 13 ,15 7 kWh each	Discharge hours: 18, 19, 20	**15,750**
	Group C Homes: 2, 6, 7, 10, 14 7 kWh each	Discharge hours: 19, 20	**15,750**
EV – Vehicle to Home (V2H)	Group A Homes: 1, 3, 4, 8, 9 8.4 kWh for V2H each	(1): Discharge hours: 19, 20 (3): Discharge hours: 19, 20 (4): Discharge hours: 17, 18, 19, 20 (8): Discharge hours: 17, 18, 19, 20 (9): Discharge hours: 19, 20	**5,660**
	Group B Homes: 5, 11, 12, 13 ,15 8.4 kWh for V2H each	(5): Discharge hours: 20 (11): Discharge hours: 19, 20 (12): Discharge hours: 18, 19, 20 (13): Discharge hours: 19, 20 (15): Discharge hours: 19, 20	**5,660**
Building Demand Response (DR)	Home 1	Usage reduction: App. = 46%; Light = 31%	**470**
	Home 2	Usage reduction: App. = 32%; Light = 13%	**270**
	Home 3	Usage reduction: App. = 46%; Light = 31%	**470**
	Home 4	Usage reduction: App. = 36%; Light = 15%	**360**
	Home 5	Usage reduction: App. = 24%; Light = 35%	**280**
	Home 6	Usage reduction: App. = 25%; Light = 29%	**330**
	Home 7	Usage reduction: App. = 25%; Light = 29%	**330**
	Home 8	Usage reduction: App. = 32%; Light = 13%	**210**
	Home 9	Usage reduction: App. = 48%; Light = 19%	**570**
	Home 10	Usage reduction: App. = 41%; Light = 15%	**310**
	Home 11	Usage reduction: App. = 27%; Light = 12%	**180**
	Home 12	Usage reduction: App. = 27%; Light = 17%	**180**
	Home 13	Usage reduction: App. = 27%; Light = 12%	**180**
	Home 14	Usage reduction: App. = 25%; Light = 29%	**330**
	Home 15	Usage reduction: App. = 29%; Light = 24%	**250**

5.3.2 Optimized (Combined) DER Solutions for the Anatolia Community Model

With *PI*_4 and the DER options presented in Table 19, an assessment is carried out to find the minimum cost solution, from the utility company's perspective, for the desired energy flexibility scenarios.

In each design scenario, a community load threshold is established, which must not be surpassed during the super-peak hours. For these targets, a deterministic optimization shuffles through the available DER options to find the minimum-cost combination of energy flexibility measures.

Table 20 and Figure 94 to Figure 96 show the results of the optimization assessment. The graphs depicted in these figures show the maximum and the mean consumption values for every hour within the super-peak season (comprising all week-days from June 1st to September 30th, as defined in section 4.4)

Table 20 – Optimized (combined) DER solutions for different energy flexibility targets.

Energy Flexibility (load management during super-peak hours)	DR	Home-Battery	V2H	*PI*_4 [US$]
Target I: threshold of 50 kWh/hr	Homes: 1, 2, 3, 5, 9, 10, 12	-	Groups A, B	**13,860**
Target III: threshold of 40 kWh/hr	Homes: 2, 15	Group B	Groups A, B	**27,590**
Target V: threshold of 30 kWh/hr	Homes: 4, 6, 7, 9, 11, 13, 14	Groups A, B	Groups A, B	**45,080**

For target I (with the community load threshold of 50 kWh/hr), we observe that it is possible to reshape the community load curve with only DR and V2H strategies at a very

low implementation cost. From Figure 94, we see the relative importance of the V2H intervention for peak shaving, especially during the days of maximum peak loads (as seen on the top graph).

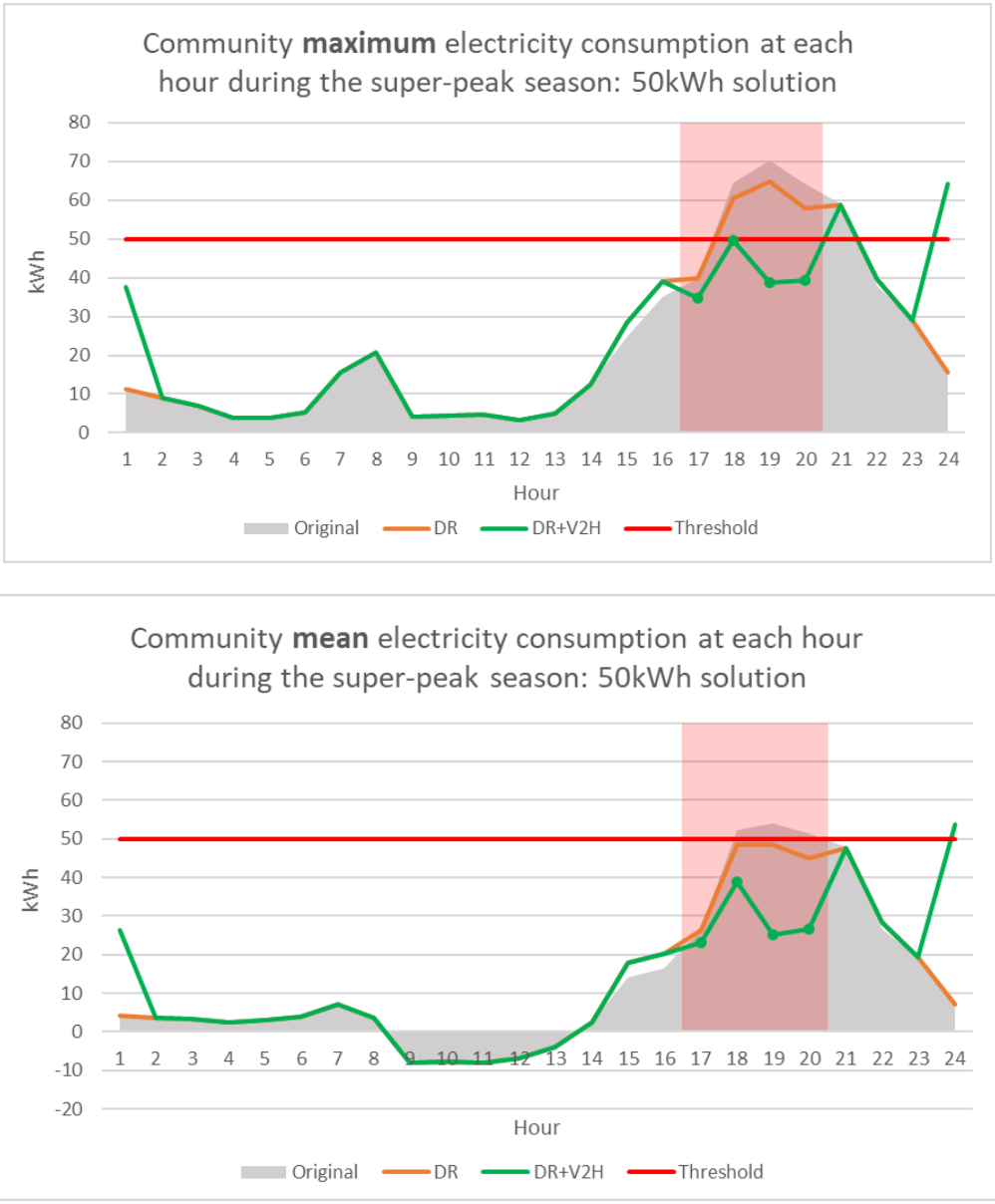

Figure 94 – Performance of combined DER solution for providing "community energy flexibility" to comply with the 50 kWh/hr load threshold

(top: hourly maximum consumption; bottom: hourly mean consumption)

For target II (threshold of 40 kWh/hr), all three strategies are selected in the optimized solution. However, as observed in Figure 95, the DR program has a rather insignificant effect when compared to the other strategies. The operation of home-battery in five homes compensates the absence of EVs during hours 17 and 18.

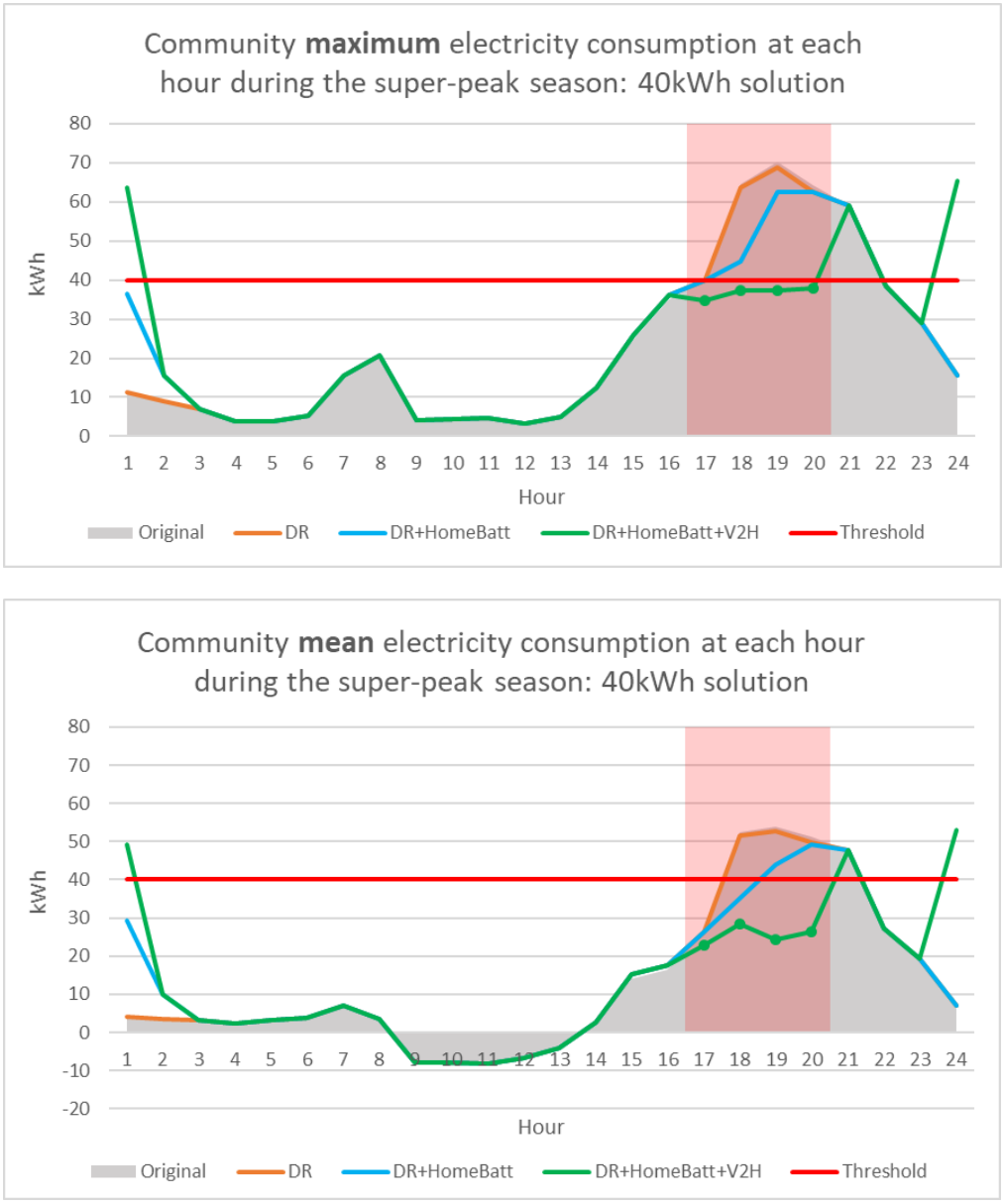

Figure 95 – Performance of combined DER solution for providing "community energy flexibility" to comply with the 40 kWh/hr load threshold

(top: hourly maximum consumption; bottom: hourly mean consumption)

Finally, the more stringent load threshold (30 kWh/hr) requires a more comprehensive solution. In this case, home-battery and V2H strategies are applied to ten homes, while DR is operated in seven homes.

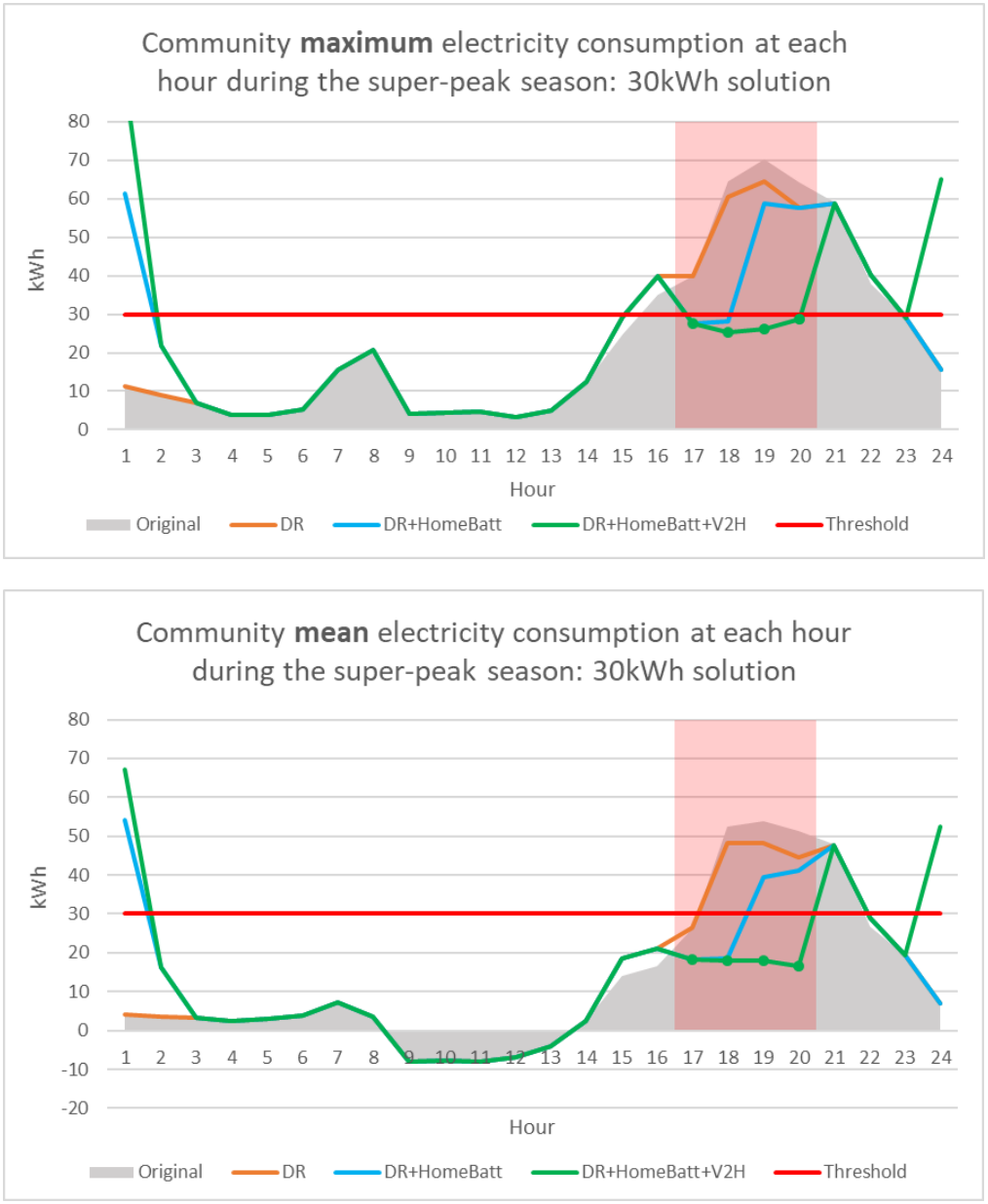

Figure 96 – Performance of combined DER solution for providing "community energy flexibility" to comply with the 30 kWh/hr load threshold

(top: hourly maximum consumption; bottom: hourly mean consumption)

5.3.3 Conclusions

The assessment presented in this section demonstrates the versatility that the EPC_NHood platform provides for quantifying and testing energy flexibility at the neighborhood scale. The case study carried out bundles different technologies and diverse strategies that are likely to be more frequent in the modern building-to-grid relationship.

The co-simulation approach of EPC_NHood allows the investigation of diversity within the community, both in terms of building occupation and DER options, and the related impacts to their overall energy flexibility. This is crucial for a more comprehensive and accurate assessment, which other modeling approaches fail to achieve.

This model can be further used for stochastic optimization, where occupant behavior, EV-V2H availability, and uncertain parameters can be considered for more robust decision making, similar to what was performed in 4.4.3.

CHAPTER 6. CLOSURE

This thesis identifies the need for more functional methodologies for modeling the integration of multiple buildings and distributed energy resources (DER) at the neighborhood scale. A reduced order modeling approach is developed to address this issue, culminating in EPC_NHood.

The EPC_NHood modeling framework is validated in a virtual community test bed, where its hourly energy consumption data are compared against the outputs of a high-fidelity energy model. The experiment uses data related to the annual "load duration curve" to construct the performance indicator *PI*_1. Using different DER alternatives to improve *PI*_1, the analyses show that the uncertainties related to model form reduction are rather insignificant when compared to other sources of uncertainties, such as scenario and building parameters.

In an application to an existing solar community, we demonstrate the possibility of calibrating EPC_NHood, with statistical reliability, using only general and scarce data, such as histograms of total energy supplied and consumed by the neighborhood and histograms of times of day when peak power occurs. The calibrated EPC_NHood model offers a unique opportunity to explore alternatives for implementing DER into a community for achieving specific energy consumption targets. Using a performance indicator, *PI*_2, related to the number of hours on unwanted super-peak loads, it is possible to design and optimize energy-storage solutions aimed at minimizing *PI*_2 under cost constraints and with risk consciousness.

EPC_NHood also proves to be adequate for supporting the definition and testing of novel performance indicators for integrated assessments of communities with DER. In this direction, the “community energy resilience”, measured in the form of *PI*_3, provides a rational way to test DER alternatives for improving energy resilience in connected neighborhoods. Similarly, “community energy flexibility”, monetized in the form of *PI*_4, creates an opportunity to develop and test various strategies for shaping the neighborhood load profile.

Relatively short runtimes and low computational overhead makes the proposed approach especially appealing to various applications. The possibility to embed advanced optimization algorithms that run in the same modeling environment is also a significant advantage of the proposed EPC_NHood framework. This enables more comprehensive assessments in a timely and manageable fashion, which may support more informed engineering and design decisions.

CHAPTER 7. FUTURE WORK

This thesis makes an important contribution in providing means for developing community energy models with a good balance between modeling practicality and representation accuracy. Nevertheless, additional research is necessary to cover other aspects and other paths of investigation that are out of the scope of this thesis.

The effects of scalability need further study. It is still unclear and underexplored in the literature how scalability relates to input uncertainty, to building parameter representation, and to model order reduction. Is there a scale threshold for which such aspects are averaged out and, thus, are irrelevant to the model outcomes?

On another aspect, when we assume that the calibration of lower order building parameters subsumes some of the behavior that is not represented in the model, we should acknowledge that the resulting model will be unfit to be used for assessing detailed building behavior. However, it might be hard to identify the level of output granularity to which we can assign acceptable reliability. This is also influenced by the questions for what the model is being used to answer.

Community model with different building types and in other locations should be investigated more thoroughly to find out whether there are specific cases for which model form uncertainty might be more impactful to the modeled outcomes.

The measure of "community energy resilience" needs to be consolidated for different convenience necessities related to various building types and occupant profiles.

The quantification and monetization of "community energy flexibility" needs to be further investigated with respect to stochastic behavior of building occupants and to uncertain building parameters.

Uncertainty due to climate change and the resulting patterns of temperature and cloud cover should be explored in the optimization assessments, especially those involving solar generation solutions, in a manner to enhance the related risk analyses.

REFERENCES

Allegrini, J., Orehounig, K., Mavromatidis, G., Ruesch, F., Dorer, V., and Evins, R. (2015). A review of modelling approaches and tools for the simulation of district-scale energy systems. *Renewable and Sustainable Energy Reviews*, 52, pp. 1391-1404

Arup (Arup International Development). (2015). City Resilience Framework. New York: Rockefeller Foundation. <www.rockefellerfoundation.org/report/city-resilience-framework/> accessed on 2016/03/31.

Augenbroe, G. (2004). Trends in building simulation. Chapter 1. In: Malkawi and Augenbroe (eds.), *Advanced Building Simulation*, Spon Press

Augenbroe, G. (2011). The role of simulation in performance-based building. In: Hensen and Lamberts (eds.), *Building Performance Simulation for Design and Operation*, Spon Press

Augenbroe, G., Carneiro, G. A., Kim, J. H., and Lee, S. H. (2017). EPC – *Energy Performance Calculator – hourly version 2.0*. High Performance Building Group, College of Architecture, Georgia Institute of Technology.

Bacher, P., and Madsen, H. (2011). Identifying suitable models for the heat dynamics of buildings. *Energy and Buildings*, 43 (7), pp. 1511-1522

Berger, J., Mendes, N., Guernouti, S., Woloszyn, M., and Chinesta, F. (2016). Review of Reduced Order Models for Heat and Moisture Transfer in Building Physics with Emphasis in PGD Approaches. *Archives of Computational Methods in Engineering*, pp. 1-13, DOI: 10.1007/s11831-016-9184-1

Berthou, T., Duplessis, B., Rivière, P., Stabat, P., Casetta, D., and Marchio, D. (2015). Smart-e: A tool for energy demand simulation and optimization at the city scale, In: *Proc. BS2015: 14th Conference of International Building Performance Simulation Association*, Hyderabad, India, Dec. 7-9, 2015

Berthou, T., Stabat, P., Salvazet, R., and Marchio, D. (2014). Development and validation of a gray box model to predict thermal behavior of occupied office buildings. *Energy and Buildings*, 74, pp. 91-100

Best, R. E., Flager, F., and Lepech, M. D. (2015). Modeling and optimization of building mix and energy supply technology for urban districts. *Applied Energy*, 159, pp. 161-177

Bode, G., Behrendt, S., Fütterer, J., and Müller, D. (2017). Identification and utilization of flexibility in non-residential buildings. *Energy Procedia*, 122, pp. 997-1002

Bonvini, M., and Leva, A. (2011). Object-oriented sub-zonal modelling for efficient energy-related building simulation, *Mathematical and Computer Modelling of Dynamical Systems*, 17:6, 543-559, DOI: 10.1080/13873954.2011.592143

Box, G. E. P. (1976). Science and Statistics. *Journal of the American Statistical Association*, 71, (356), pp. 791-799

Chassin, D. P., Fuller, J. C., and Djilali, N. (2014). GridLAB-D: An agent-based simulation framework for smart grids. Journal of Applied Mathematics, 2014, Article ID 492320, 12p, http://dx.doi.org/10.1155/2014/492320

City Energy Analyst. (2017a). Databases: Archetypes. <http://city-energy-analyst.readthedocs.io/en/latest/archetypes.html> accessed on 2017/04/10

City Energy Analyst. (2017b). Overview: Roadmap. <https://cityenergyanalyst.com/overview/#Roadmap> accessed on 2017/04/10

City of Rancho Cordova. (2005). *Anatolia IV – Mitigated Negative Declaration*

Coakley, D., Raftery, P., and Keane, M. (2014). A review of methods to match building energy simulation models to measured data. *Renewable and Sustainable Energy Reviews*, 37, pp. 123-141

Cui, C. (2016). Building Energy Modeling: A Data-Driven Approach. *Ph.D. Thesis*, Arizona State University

Cutter, S., Burton, C., and Emrich. C. (2010). Disaster Resilience Indicators for Benchmarking Baseline Conditions. *Journal of Homeland Security and Emergency Management*, 7 (1) pp. 1–22

Davila, C. C., Reinhart, C. F., and Bemis, J. L. (2016). Modeling Boston: A workflow for the efficient generation and maintenance of urban building energy models from existing geospatial datasets. *Energy*, 117, pp. 237-250

Del Barrio, E. P., Lefebvre, G., Behar, P., and Bailly, N. (2000). Using model size reduction techniques for thermal control applications in buildings. *Energy and Buildings*, 33 (1), pp. 1-14

Dobos, A. P. (2014). *PVWatts Version 5 Manual*, Technical Report – NREL/TP-6A20-62641

Energy Storage Association – ESA. (2017). Energy Storage Technologies. <http://energystorage.org/energy-storage/energy-storage-technologies> accessed on 2017/04/10

Fonseca, J. A., Nguyen, T.-A., Schlueter, A., and Marechal, F. (2016). City Energy Analyst (CEA): Integrated framework for analysis and optimization of building energy systems in neighborhoods and city districts, *Energy and Buildings*, 113, pp. 202–226

Fonseca, J.A., and Schlueter, A. (2015). Integrated model for characterization of spatiotemporal building energy consumption patterns in neighborhoods and city districts. *Applied Energy*, 142, pp. 247-265

Foucquier, A., Robert, S., Suard, F., Stéphan, L., and Jay, A. (2013). State of the art in building modelling and energy performances prediction: A review. *Renewable and Sustainable Energy Reviews*, 23, pp. 272-288

Fumo, N. (2014). A review on the basics of building energy estimation. *Renewable and Sustainable Energy Reviews*, 31, pp. 53-60

Gilman, P. (2015). *SAM Photovoltaic Model: Technical Reference*, Technical Report – NREL/TP-6A20-64102

Good, N., Zhang, L., Navarro-Espinosa, A., and Mancarella, P. (2015). High resolution modelling of multi-energy domestic demand profiles. *Applied Energy*, 137, pp. 193-210

Gorrino, A. (2012). Sviluppo e validazione di modelli di calcolo della prestazione energetica dell'edificio: ponti termici e componenti speciali di involucro *Ph.D. Thesis,* Politecnico di Torino

Graven, R. M., and Hirsch, P. R. (1977). *Cal-ERDA: Users Manual*, Argonne National Laboratory, Report ANL/ENG-77-03

GridLAB-D. (2017). GridLAB-D. <http://www.gridlabd.org/> accessed on 2017/03/20, 2017

Harish, V. S. K. V., and Kumar, A. (2016a). A review on modeling and simulation of building energy systems. *Renewable and Sustainable Energy Reviews*, 56, pp. 1272-1292

Harish, V. S. K. V., and Kumar, A. (2016b). Reduced order modeling and parameter identification of a building energy system model through an optimization routine. *Applied Energy*, 162, pp. 1010-1023

He, M., Lee, T., Taylor, S., Firth, S. K., and Lomas, K. (2015). Coupling a stochastic occupancy model to EnergyPlus to predict hourly thermal demand of a neighbourhood, In: *Proc. BS2015: 14th Conference of International Building Performance Simulation Association*, Hyderabad, India, Dec. 7-9, 2015

HOMER Energy. (2017). HOMER Pro. <http://www.homerenergy.com/HOMER_pro.html> accessed on 2017/03/20, 2017

International Building Performance Simulation Association – IBPSA-USA. (2017). BEST-D: Building Energy Simulation Tools web directory, <http://www.buildingenergysoftwaretools.com> accessed on 2017/03/15

International Code Council – ICC. (2017). I-Codes, <https://codes.iccsafe.org/public/collections/I-Codes> accessed on 2017/03/15

International Energy Agency – IEA. (1980). *Annex I – Computer modeling of building energy performance: Results and analyses of Avonbank building simulation*, IEA/Energy Conservation in Buildings and Community Systems Programme

International Energy Agency – IEA. (2017a). EBC Annex 67 – Energy Flexible Buildings. <http://www.iea-ebc.org/projects/ongoing-projects/ebc-annex-67> accessed on 2017/07/20

International Energy Agency – IEA. (2017a). Energy in Buildings and Communities Programme – IEA-EBC: Projects. <http://www.iea-ebc.org/projects/> accessed on 2017/03/20

International Organization for Standardization – ISO. (2008). *ISO 13790:2008 - Energy performance of buildings - Calculation of energy use for space heating and cooling*, International Standard, 162 p.

Jensen, S. Ø., Marszal-Pomianowska, A., Lollini, R., Pasut, W., Knotzer, A., Engelmann, P., Stafford, A., and Reynders, G. (2017). IEA EBC Annex 67 Energy Flexible Buildings. *Energy and Buildings*, 155, pp. 25-34

Kavgic, M., Mavrogianni, A., Mumovic, D., Summerfield, A., Stevanovic, Z., and Djurovic-Petrovic, M. (2010) A review of bottom-up building stock models for energy consumption in the residential sector. *Building and Environment*, 45 (7) pp. 1683-1697

Keirstead, J., Samsatli, N., and Shah, N. (2009). SynCity: An integrated tool kit for urban energy systems modelling. In: *Proc. Fifth Urban Research Symposium – Cities and Climate Change: Responding to the Urgent Agenda*, Marseille, France, Jun. 28-30, 2009

Koirala, B. P., Chaves Ávila, J. P., Gómez, T., Hakvoort, R. A., and Herder, P. M. (2016). Local Alternative for Energy Supply: Performance Assessment of Integrated Community Energy Systems. *Energies*, 2016, 9, 981

Kono, J., Carneiro, G. A., Bras, B., and Augenbroe, G. (2017). "Potential of shared electrical resources in residential communities". In: *Energy Expo 2017 – Georgia Tech*, Atlanta, GA, Feb 9-10, 2017

Kośny, J. (2015). Thermal and Energy Modeling of PCM-Enhanced Building Envelopes. Chapter 6. In: Kośny, *PCM-Enhanced Building Components*. Springer International Publishing. pp. 167‑234

Kramer, R., Schijndel, J. van., and Schellen, H. (2012). Simplified thermal and hygric building models: A literature review. *Frontiers of Architectural Research*, 1 (4), pp. 318-325

Lauster, M., Brüntjen, M. A., Leppmann, H., Fuchs, M., Teichmann, J., Streblow, R., Treeck, C. van., and Müller, D. (2014). Improving a low order building model for urban scale applications. In: *Proc. Fifth German-Austrian IBPSA Conference – BauSIM 2014*, Aachen University, Germany, Sep. 22-24, 2014

Lawrence Berkeley National Laboratory – LBL. (2017). DER-CAM. <https://building-microgrid.lbl.gov/projects/der-cam> accessed on 2017/03/20

Lee, S. H. (2012). Management of building energy consumption and energy supply network on campus scale. *Ph.D. Thesis*, Georgia Institute of Technology

Lee, S. H., Hong, T., and Piette, M. A. (2014). *Review of existing energy retrofit tools*, Lawrence Berkeley National Laboratory, July 2014. LBNL-6774E

Lee, S. H., Hong, T., Piette, M. A., and Taylor-Lange, S. C. (2015). Energy retrofit analysis toolkits for commercial buildings: A review. *Energy*, 89, pp. 1087-1100

Lee, S. H., Zhao, F., and Augenbroe, G. (2013). The use of normative energy calculation beyond building performance rating. *Journal of Building Performance Simulation*, 6 (4), pp. 282-292

Lennar. (2017). Lennar new homes: Rancho Cordova, CA, <https://www.lennar.com/new-homes/california/sacramento/rancho-cordova> accessed on 2017/05/07

Li, X., and Wen, J. (2014). Review of building energy modeling for control and operation. *Renewable and Sustainable Energy Reviews*, 37, pp. 517-537

Lim, T. K., Ignatius, M., Miguel, M., Wong, N. H., and Juang, H-M. H. (2017). Multi-scale Urban System Modeling for Sustainable Planning and Design, *Energy and Buildings*, http://dx.doi.org/10.1016/j.enbuild.2017.02.024

Loonen, R. C. G. M., Favoino, F., Hensen, J. L. M, and Overend, M. (2017) Review of current status, requirements and opportunities for building performance

simulation of adaptive facades. *Journal of Building Performance Simulation*, 10 (2), pp. 205-223, DOI: 10.1080/19401493.2016.1152303

Lopes, R. A., Chambel, A., Neves, J., Aelenei, D., and Martins, J. (2016). A literature review of methodologies used to assess the energy flexibility of buildings. *Energy Procedia*, 91, pp. 1053-1058

Malkawi, A. M., and Augenbroe, G. (2004). Introduction and overview of field. Prologue. In: Malkawi and Augenbroe (eds.), *Advanced Building Simulation*, Spon Press

McKenna, E., and Thomson, M. (2016). High-resolution stochastic integrated thermal–electrical domestic demand model. *Applied Energy*, 165, pp. 445-461

Molina, M. (2014). *The Best Value for America's Energy Dollar: A National Review of the Cost of Utility Energy Efficiency Programs,* Report Number U1402, ACEEE

Molyneaux, L., Brown, C., Wagner, L., and Foster, J. (2014). *Measuring Resilience in Energy Systems: Insights from a Range of Disciplines*. Brisbane: University of Queensland.

National Association of Regulatory Utility Commissioners – NARUC. (2016). *NARUC Manual on Distributed Energy Resources Rate Design and Compensation*, Washington, D.C., USA

National Renewable Energy Laboratory – NREL. (2017). *Best Research-Cell Efficiencies*, available at < https://www.nrel.gov/pv/assets/images/efficiency-chart.png> accessed on 2017/01/10

Navigant Consulting Inc. – Navigant. (2012). *Monitoring and Testing Plan* – Presented to SMUD – Final Report

Nelder, C., Newcomb, J., Fitzgerald, G. (2016). *Electric Vehicles as Distributed Energy Resources*, Rocky Mountain Institute/Electricity Innovation Lab

Nielsen, T. R. (2005). Simple tool to evaluate energy demand and indoor environment in the early stages of building design. *Solar Energy*, 78 (1), pp. 73-83

Orehounig, K., Mavromatidis, G., Evins, R., Dorer, V., and Carmeliet, J. (2014). Towards an energy sustainable community: An energy system analysis for a village in Switzerland. *Energy and Buildings*, 84 , pp. 277-286

Otter, M., and Elmqvist, H. (2001). *Modelica Language, Libraries, Tools, Workshop and EU-Project RealSim*, available at <https://www.modelica.org/documents/ModelicaOverview14.pdf> accessed on 2017/03/23

Panão, M. J. N. O., Santos, C. A. P., Mateus, N. M., and Graça, G. C. da. (2016). Validation of a lumped RC model for thermal simulation of a double skin natural and mechanical ventilated test cell. *Energy and Buildings*, 121, pp. 92-103

Patteeuw, D., Bruninx, K., Delarue, E., Helsen, L., D'haeseleer, W. (2014). *Short-term demand response of flexible electric heating systems: an integrated model*, KU Leuven Energy Institute Working Paper, WP2014-28, available at <http://www.mech.kuleuven.be/en/tme/research/energy_environment/Pdf/wpen2014-28.pdf> accessed on 2017/03/30

Patteeuw, D., Bruninx, K., Arteconi, A., Delarue, E., D'haeseleer, W., and Helsen, L. (2015). Integrated modeling of active demand response with electric heating systems coupled to thermal energy storage, *Applied Energy*, 151, pp. 306-319

PECO Energy Company - PECO. (2016). *PECO Microgrid Integrated Technology Pilot*, Petition, May 18, 2106

Quan, S. J., Li, Q., Augenbroe, G., Brown, J., and Yang, P. P. J. (2015). Urban Data and Building Energy Modeling: A GIS-Based Urban Building Energy Modeling System Using the Urban-EPC Engine. Chapter 24. In: Geertman et al. (eds.), *Planning Support Systems and Smart Cities, Lecture Notes in Geoinformation and Cartography*, DOI: 10.1007/978-3-319-18368-8_24

Rawson, M. (PI). (2013). *Sacramento Municipal Utility District PV and Smart Grid Pilot at Anatolia*, SMUD, Final Report

Reinhart, C. F., Davila, C. C. (2016). Urban building energy modeling – A review of a nascent field. *Building and Environment*, 97, pp. 196-202

Reinhart, C. F., Dogan, T., Jakubiec, J. A., Rakha, T., and Sang, A. (2013). UMI - An urban simulation environment for building energy use, daylighting, and walkability. In:

Proc. BS2013: 13th Conference of International Building Performance Simulation Association, Chambéry, France, Aug. 26-28, 2013

Ribeiro, D., and Bailey, T. (2017). *Indicators for Local Energy Resilience*, White Paper, Washington, DC, ACEEE

Ribeiro, D., Mackres, E., Baatz, B., Cluett, R., Jarrett, M., Kelly, M., and Vaidyanathan, S. (2015). *Enhancing Community Resilience through Energy Efficiency*, Research Report U1508, Washington, DC, ACEEE

Robinson, D., Haldi, F., Kämpf, J., and Perez, D. (2011). Building Modelling. Chapter 5. In: Robinson, D. (ed.), *Computer Modelling for Sustainable Urban Design: Physical Principles, Methods & Applications*, Earthscan, London

Robinson, D., Haldi, F., Kämpf, J., Leroux, P., Perez, D., Rasheed, A., and Wilke, U. (2009). CITYSIM: Comprehensive micro-simulation of resource flows for sustainable urban planning, In: *Proc. Building Simulation 2009: 11th International IBPSA Conference*, Glasgow, Scotland, July 27-30, 2009

Sacramento Municipal Utility District – SMUD. (2015). *Photovoltaic and Smart Grid Pilot at Anatolia*, Energy Research and Development Division, Final Project Report

Sandia National Laboratories – SANDIA. (2014). *The Advanced Microgrid: Integration and Interoperability*, SANDIA Report – SAND2014-1535

Schijndel, A. W. M. van. (2007). Integrated heat air and moisture modeling and simulation. *Ph.D. thesis*, Eindhoven University of Technology, 200p

Schmidt, O., Hawkes, A., Gambhir, A., and Staffell, I. (2017). The future cost of electrical energy storage based on experience rate, *Nature Energy*, 2, 17110 (2017)

Solar Energy Laboratory. (2017). General TRNSYS Questions. <http://sel.me.wisc.edu/trnsys/faq/faq.htm#General> accessed on 2017/03/23

Song, Z., Murray, B. T., and Sammakia, B. (2013). A Compact Thermal Model for Data Center Analysis using the Zonal Method. *Numerical Heat Transfer, Part A: Applications*, 64 (5), pp. 361-377, DOI: 10.1080/10407782.2013.784138

Swan, L. G., and Ugursal, V. I. (2009). Modeling of end-use energy consumption in the residential sector: A review of modeling techniques. *Renewable and Sustainable Energy Reviews*, 13 (8), pp. 1819-1835

Taylor, Z. T., Gowri, K., and Katipamula, S. (2008). *GridLAB-D Technical Support Document: Residential End-Use Module Version 1.0*, Report, PNNL-17694

U.S. Department of Energy – DOE. (2016a). *EnergyPlus™ Version 8.6 Documentation: Engineering Reference*, DOE.

U.S. Department of Energy – DOE. (2016b). *2015 Wind Technologies Market Report*, DOE/Energy Efficiency & Renewable Energy

U.S. Department of Energy – DOE. (2017a). EnergyPlus. <https://www.energy.gov/eere/buildings/downloads/energyplus-0> accessed on 2017/03/23

U.S. Department of Energy – DOE. (2017b). Building Energy Codes Program. <https://www.energycodes.gov/development> accessed on 2017/02/10

U.S. Department of Energy – DOE. (2017c). EnergyPlus: Latest Release. <https://energyplus.net/downloads> accessed on 2017/04/08

U.S. Energy Information Administration – EIA. (2017). *Electric Power Monthly: January 2017*, EIA/Independent Statistics & Analysis

U.S. Environmental Protection Agency – EPA. (2015). *Catalog of CHP Technologies*, EPA/Combined Heat and Power Partnership.

U.S. National Aeronautics and Space Administration – NASA. (2016). NASA Surface meteorology and Solar Energy: A renewable energy resource web site. <https://eosweb.larc.nasa.gov/cgi-bin/sse/sse.cgi?> accessed on 2016/03/31

Vela Solaris. (2017). Polysun simulation software. <http://www.velasolaris.com/english/home.html> accessed on 2017/03/15

Viot, H., Sempey, A., Mora, L., and Batsale, J. C. (2015). Fast on-site measurement campaigns and simple building models identification for heating control. *Energy Procedia*, 78, pp. 812-817

Walter, E., and Kämpf, J. H. (2015). A verification of CitySim results using the BESTEST and monitored consumption values. In: *Proc. Building Simulation Applications: BSA 2015 – 2nd IBPSA-Italy Conference*, Bozen-Bolzano, Italy, Feb. 4-6, 2015

Wetter, M. (2009). Modelica-Based Modelling and Simulation to Support Research and Development in Building Energy and Control Systems. *Journal of Building Performance Simulation*, 2 (2), pp. 143-161, DOI: 10.1080/19401490902818259

Wetter, M., and Haves, P. (2008). A modular building controls virtual test bed for the integration of heterogeneous systems. In: *Proc. Third National Conference of IBPSA-USA*, Berkeley, CA, Jul. 30 – Aug. 1, 2008

Williams, T., Wang, D., Crawford, C., and Djilali, N. (2013). Integrating renewable energy using a smart distribution system: Potential of self-regulating demand response. *Renewable Energy*, 52, pp. 46-56

Willis, H., and Loa. K. (2015). *Measuring the Resilience of Energy Distribution Systems*. Santa Monica, CA: RAND Corporation. <www.rand.org/content/dam/rand/pubs/research_reports/RR800/RR883/RAND_RR883.pdf> accessed on 2016/03/31.

Wilson, E., Christensen, C., Horowitz, S., and Horsey, H. (2016). A high-granularity approach to modeling energy consumption and savings potential in the U.S. residential building stock. In: *Proc. ASHRAE and IBPSA-USA SimBuild 2016: Building Performance Modeling Conference*, Salt Lake City, UT, Aug. 8-12, 2016

Wilson, E., Metzger, C. E., Horowitz, S., and Hendron, R. (2014). *2014 Building America House Simulation Protocols*, Technical Report – NREL/TP-5500-60988

Wit, M. H. de. (2006). *HAMBase, Heat, Air and Moisture Model for Building and Systems Evaluation*, Bouwstenen (100), ISBN 90-6814-601-7, Eindhoven University of Technology

Woloszyn, M., and Rode, C. (2008). Tools for Performance Simulation of Heat, Air and Moisture Conditions of Whole Buildings. *Building Simulation*, 1 (1) pp. 5-24, DOI: 10.1007/s12273-008-8106-z

Wu, R., Mavromatidis, G., Orehounig, K., and Carmeliet, J. (2017). Multiobjective optimisation of energy systems and building envelope retrofit in a residential community, *Applied Energy*, 190, pp. 634-649

Yeonsook, H. (2011). Bayesian calibration of building energy models for energy retrofit decision-making under uncertainty. *Ph.D. Thesis*, Georgia Institute of Technology

Yildiz, B., Bilbao, J. I., and Sproul, A. B. (2017). A review and analysis of regression and machine learning models on commercial building electricity load forecasting. *Renewable and Sustainable Energy Reviews*, 73, pp. 1104-1122

Zhang, Y. (2017). Optimal strategies for demand charge reduction by commercial building owners. *Ph.D. Thesis*, Georgia Institute of Technology

Zhao, F. (2012). Agent-based modeling of commercial buildings stocks for energy policy and demand response analysis. *Ph.D. Thesis*, Georgia Institute of Technology